Modeling Tuberous Sclerosis Complex Using Patient-Derived Cells

By

Laura Craig Armstrong

Dissertation

Submitted to the Faculty of the

Graduate School of Vanderbilt University

in partial fulfillment of the requirement

for the degree of

DOCTOR OF PHILOSOPHY

in

Cell and Developmental Biology

September 30, 2017

Nashville, Tennessee

Approved:

Kevin C. Ess, M.D., Ph.D.

David M. Miller, III, Ph.D.

Aaron B. Bowman, Ph.D.

Charles C. Hong, M.D., Ph.D.

Andrea Page-McCaw, Ph.D.

ACKNOWLEDGEMENTS

This work was supported by the National Institute of Neurological Disorders and Stroke (RO1 NS078289 to KCE) and Public Health Service award T32 GM07347 from the National Institute of General Medical Studies for the Vanderbilt Medical Scientist Training Program.

First, I want to thank my mentor, Kevin Ess, for his guidance and support throughout the twists and turns of this project. Thank you to Cary Fu and Rob Carson for their advice and time spent teaching me the techniques necessary for my project, from western blots to caffeine extraction. To all the past and present members of the Ess, Fu and Carson labs: thank you for your company, keeping my cells alive when I was gone, and always being there to help me solve any problem I encountered.

To my committee, thank you for your insights and encouraging me to follow the unexpected results. The Vanderbilt MSTP has been a wonderful community to be a part of and always inspires my curiosity no matter what phase of the training I am in.

To my friends, family, and husband: thank you for the laughter, encouragement and love.

TABLE OF CONTENTS

Page

ACKNOWLEDGEMENTS……..iii

LIST OF TABLES…….....vi

LIST OF FIGURES……. vii

LIST OF ABBREVIATIONS…….viii

Introduction……...……1

Chapter

I. Clinical Presentation of Tuberous Sclerosis Complex and Molecular Function of TSC1 and TSC2….. 2
Tuberous Sclerosis Complex……...2
Neuropathology……... 3
Genetics of TSC……...4
Hamartin and Tuberin Protein Function……..6
mTOR complex 1 and mtor complex 2……... 7
mTOR in stem cells……9
Crosstalk between p53 and TSC/mTOR……10
Mouse and Rat Models of TSC……. 12
Summary……....13

II. Heterozygous loss of TSC2 alters p53 signaling and human stem cell reprogramming……14
Abstract……..14
Introduction……... 14
Results……..... 15
Discussion……..30
Materials and Methods……...32

III. Stem Cell Dynamics and Signaling in Plasmid-Integrated TSC2+/- iPSCs……...35
Abstract……..35
Introduction……35
Results……36
Discussion……..43
Materials and Methods……...45

IV. Homozygous loss of TSC2 causes impaired mTOR regulation during neurodevelopment……...46
Abstract……..46
Introduction……46
Results……47
Discussion……..55
Materials and Methods…….. 56

V. Pathogenesis and Treatment of TSC……... 58
Mechanisms of Cortical Dysfunction in TSC……58
Treatment of TSC…….. 60

Summary……61

Appendix……..62

REFERENCES…….65

LIST OF TABLES

Page

1.1 Diagnostic Criteria of Tuberous Sclerosis (2 major or 1 major and 2 minor) 2
1.2. TSC Patient Clinical History, Biopsy Information, and Genotyping……15

LIST OF FIGURES

Page

1.1 TSC Pathway 7
1.2 p53 and mTOR crosstalk 11
2.1 Heterozygous nonsense mutations in *TSC2* result in reduced *TSC2* mRNA and tuberin protein levels. 16
2.2 Induced pluripotent stem cell validation. 17
2.3 Increased integration of reprogramming plasmids in TSP iPSC lines. 19
2.4 TSC patient fibroblasts display increased p53 in response to UV light. 21
2.5 Changes in nuclear and cytoplasmic protein levels in TSC patient fibroblasts. 22
2.6 Impaired reprogramming and increased apoptosis in TSC patient fibroblasts. 24
2.7 Stability, mRNA and translation of p53 in *TSC2*+/- fibroblasts. 26
2.8 Increased p53 in heterozygous and homozygous *TSC2* mutant stem cells. 28
2.9 Stability, translation and DNA damage response in isogenic *TSC2*-/- stem cells. 29
3.1 Heterozygous nonsense mutations in *TSC2* result in reduced *TSC2* mRNA and tuberin protein levels in plasmid-reprogrammed iPSCs. 37
3.2 p53 protein expression in integrated TSP iPSCs 38
3.3 Heterozygous nonsense mutations in *TSC2* result in reduced tuberin protein in Sendai-reprogrammed iPSCs. 38
3.4 Decreased pluripotent stability in integrated TSP iPSC lines. 39
3.5 Abnormal spontaneous differentiation in TSP iPSCs 41
3.6 Integrated *TSC2*+/- iPSCs have increased cell survival and proliferation 42
3.7 Increased MEK1/2 signaling in integrated *TSC2*+/- iPSCs 43
4.1 TSC2 mRNA and protein expression in TSP16-8 47
4.2 Impaired formation of neural progenitors in integrated TSC iPSC line TSP16-11 48
4.3 Impaired formation of neural progenitors in integrated TSC iPSC line TSP16-11 is mTORC1-independent 49
4.4 mTORC1 activity decreases and mTORC2 activity increases during neural differentiation of plasmid-reprogrammed iPSCs 50
4.5 Impaired formation of neural progenitors from *TSC2*-/- iPSCs 51
4.6 Expression of neural progenitor marker Pax6 during directed differentiation 52
4.7 Changes in mTORC1 and mTORC2 signaling during neural differentiation of iPSCs 53
4.8 mTORC1 signaling during neural differentiation of iPSCs 54
4.9 Impaired early neural differentiation of *TSC2*-/- iPSCs is mTORC1-independent 54
5.1 Immunoblot of fibroblast time course response to UV challenge 62
5.2 mRNA, translation and stability of p53 in fibroblasts 63
5.3 Immunoblot of *TSC2* heterozygous and homozygous stem cells 64

LIST OF ABBREVIATIONS

4E-BP1, Eukaryotic initiation factor 4E-binding protein 1

AML, Angiomyolipoma

AMPK, AMP-activated protein kinase

eIF4E, Eukaryotic initiation factor 4E

ESC, Embryonic stem cell

FKBP12, FK506-binding protein of 12 kDa

GAP, GTPase activating protein

iPSC, Induced pluripotent stem cell

KLF4, Kruppel-like factor 4

LAM, lymphangioleiomyomatosis

mTOR, Mechanistic target of rapamycin

mTORC1, Mechanistic target of rapamycin complex 1

mTORC2, Mechanistic target of rapamycin complex 2

Oct4, Octamer-binding transcription factor 4

p53, tumor suppressor protein p53

RHEB, Ras homologue enriched in brain

Sox2, Sex determining region Y-box 2

S6K1, p70-S6 Kinase 1

S6K2, p70-S6 Kinase 2

S6, ribosomal protein S6

TSC, Tuberous sclerosis complex

INTRODUCTION

Tuberous sclerosis complex (TSC) is an autosomal dominant genetic disease of pediatric onset affecting multiple organ systems, including the kidney, brain, retina, heart, skin, and lungs (Northrup and Krueger 2013). It is estimated to affect at least 1/10,000 births (O'Callaghan et al 1998, Sampson et al 1989). TSC is characterized by hamartomas or benign tumor growths in the affected organs. The most debilitating symptoms in TSC are a consequence of brain involvement, including a high rate of epilepsy, autism spectrum disorder, and learning disabilities (Sahin et al 2016). TSC is caused by mutations in either the *TSC1* or *TSC2* genes, which encode the proteins hamartin and tuberin, respectively (1993, van Slegtenhorst et al 1997). Hamartin and Tuberin bind together to negatively regulate mechanistic target of rapamycin complex 1 (mTORC1). Genetic loss of *TSC1* or *TSC2* leads to elevated and constitutively active mTORC1 signaling that impacts multiple processes, including cell growth and protein translation.

Hamartomas in TSC are generally thought to arise from a “second-hit” somatic mutation in the other allele of *TSC1* or *TSC2*, resulting in unhindered growth but leaving the surrounding heterozygous tissue functionally normal. While this model is supported by existing data in kidney and lung samples, molecular analyses of cortical hamartomas in the brain (“tubers”) demonstrate few cells with loss of heterozygosity (Henske et al 1996, Martin et al 2017, Niida et al 2001, Qin et al 2010). Furthermore, imaging and pathologic data indicate abnormalities also exist in non-hamartomatous regions including decreased grey matter volume, abnormal white matter tracts, focal dyslamination, and dysplastic neurons (Chandra et al 2007, Lewis et al 2013, Marcotte et al 2012, Peters et al 2012, Ridler et al 2001). Developmental brain abnormalities have also been detected in TSC patients as early as 20 weeks of gestation (Muhler et al 2007, Park et al 1997, Prabowo et al 2013, Tsai et al 2014). These results indicate an important role for mutations of *TSC1* and *TSC2* genes contributing to abnormal neural development.

To better understand the impact of *TSC2* loss on development, we generated induced pluripotent stem cells (iPSCs) using human dermal fibroblasts obtained from TSC patients and control volunteers. In addition to these heterozygous *TSC2* lines, we generated homozygous *TSC2* iPSCs using CRISPR-Cas9 technology to edit the genome. The following chapters detail what we have learned from human fibroblast, stem cell, and neural progenitor models of *TSC2* mutations. Chapter I will describe the clinical presentation of TSC and the current understanding of the molecular functions of *TSC1*, *TSC2*, and mTOR. Chapter II provides evidence for an unexpected finding of heterozygous *TSC2* mutations hindering the reprograming process and discusses what can be learned from heterozygous patient fibroblasts. Chapter III explores how heterozygous TSC mutations or integration of the OCT4/shp53 plasmid may alter stem cell biology. Chapter IV focuses on neural differentiation of TSC stem cells and how heterozygous or homozygous mutations in *TSC2* affect formation of neural progenitors. Finally, Chapter V places these results in a broader context and considers what questions remain.

CHAPTER I

CLINICAL PRESENTATION OF TUBEROUS SCLEROSIS COMPLEX AND MOLECULAR FUNCTION OF *TSC1* AND *TSC2*

Tuberous Sclerosis Complex

The first descriptions of tuberous sclerosis complex may have been as early as 1835 when dermatologists described a papule eruption over the nose and cheeks in a butterfly pattern (Rayer 1835). It was not until 1862-1908 that a more complete clinical description included the pathological findings of cardiac rhabdomyomas and cortical tubers/scleromas in patients with intellectual disability and epilepsy (Bourneville 1880, Hartdegen 1881, Vogt 1908, Von Recklinghausen 1862). Bourneville named the disease "Tuberous sclerosis of cerebral convolutions" after the hard (sclerotic) cortical tubers (Bourneville 1880). Later, Vogt established the first diagnostic criteria for TSC: intellectual disability, epilepsy, and facial angiofibromas (Vogt 1908). Following this initial triad of symptoms, the range of clinical presentations and variable expressivity of the disease became evident. The diagnostic criteria, updated in 2013, now include genetic testing as well as dermatologic, cortical, renal, retinal, cardiac, and pulmonary manifestations (Table 1.1) (Northrup and Krueger 2013).

	Diagnostic Criteria	**Prevalence in TSC**	**Onset**
Major	Hypomelanotic macules (3, at least 5mm)	90%	birth
Major	Angiofibromas (3) or fibrous cephalic plaque	75%/25%	childhood
Major	Ungual fibromas (2)	20%	>10 years
Major	Shagreen patch	50%	<10 years
Major	Multiple retinal hamartomas	30-50%	
Major	Tubers or white matter radial migration lines	90%/40%	prenatal
Major	Subependymal nodules	80%	prenatal
Major	Subependymal giant cell astrocytoma	5-15%	birth to adolescence
Major	Cardiac rhabdomyoma	50%	prenatal
Major	Lymphangioleiomyomatosis	30-40% (female)	>18 years
Major	Angiomyolipomas (2)	80%	<10 years
Minor	"Confetti" skin lesions	3-58%	<10 years
Minor	Dental enamel pits (>3)	100%	increase with age
Minor	Intraoral fibromas (>2)	20-50%	increase with age
Minor	Retinal achromic patch	39%	
Minor	Multiple-renal cysts		
Minor	Non-renal hamartomas		

Table 1.1 Diagnostic Criteria of Tuberous Sclerosis (2 major or 1 major and 2 minor)

Cardiac rhabdomyomas can be detected by prenatal ultrasound and have a 75-80% positive predictive value (Hinton et al 2014, Northrup and Krueger 2013). This allows for early identification of patients and, potentially, early treatment. Interestingly, the onset and potential for continued growth varies between hamartomas. For example, cardiac rhabdomyomas have an exclusively prenatal onset and frequently regress postnatally. Cortical tubers appear prenatally and appear to be static in number and

size; however, there is evidence for increasing calcification of tubers throughout life. Even within the same organ, lesions may have different patterns of growth; in contrast to tubers, subependymal nodules (SEN) in the brain can continue to grow until adolescence and in some cases progress to subependymal giant cell astrocytomas (SEGA). Angiomyolipomas (AML) and facial angiofibromas have a later onset in childhood and may continue to progress throughout life. Pulmonary lymphangioleiomyomatosis (LAM), meanwhile, almost only appears in female patients after puberty. This suggests that there may be different molecular mechanisms for hamartoma development depending on the targeted organ.

The phenotype-genotype correlation in TSC patients is poor; patients with the same or similar mutations even within the same family can present with drastically different disease burdens. Most patients with TSC have a near normal life expectancy; however, the mortality in patients with TSC differs significantly between patients with more or less severe disease manifestations. In the most recent study examining causes of death in TSC, 284 patients were divided into two groups based on the presence or absence of learning disabilities (Amin et al 2016). Mortality was significantly more common in TSC patients with learning disabilities; however, no patients in the study died before 16 years of age, regardless of which group they were in. The most common causes of death related to TSC were complications of renal pathology (50%, chronic kidney disease, polycystic kidney disease, hemorrhage, renal cell carcinoma). Next was sudden unexplained death in epilepsy (25%), followed by pulmonary complications (heart failure, hemorrhage), hydrocephalus and metastatic pancreatic disease (Amin et al 2016). The *TSC2* gene is located upstream of the polycystic kidney disease gene, *PKD1*, and large deletions affecting both genes can occur, leading to more severe kidney disease.

The most debilitating symptoms are a consequence of the brain involvement in TSC. The most common symptoms are epilepsy (75%), intellectual disability (50%), and other behavioral problems, including autism and ADHD (40%) (Jones et al 1999). Epilepsy in TSC usually presents in the first year and is frequently refractory to anti-seizure medications (Chu-Shore et al 2010). Treatments for refractory epilepsy include surgery or possibly TSC signaling specific agents (mTORC1 inhibitors) (Feliciano et al 2013).

Reports of cases of TSC in families led to the conclusion that TSC was caused by an inherited genetic mutation and, further, it was inherited in an autosomal dominant manner (Fuhs 1925, Gunther and Penrose 1935). However, the causative genes were not identified until 1993 and 1997 (1993, van Slegtenhorst et al 1997). The known genetic cause makes TSC a tractable model for understanding the pathogenesis of less genetically defined disorders like autism or epilepsy.

Neuropathology

The most common neuropathological features of TSC are cortical tubers, subependymal nodules (SEN), or subependymal giant cell astrocytomas (SEGA). Other findings include dysplastic neurons throughout the brain, radial glial lines, and white matter tract abnormalities. Tubers can be found in any lobe of the cortex, subcortical white matter, or cerebellum. They vary widely in distribution and size, even within an individual patient. There is some evidence of a correlation between neurological symptoms and tuber number, size, and/or location. Tuber burden (number and total volume) correlates with intellectual disability (Goodman et al 1997, Jansen et al 2008b). Tubers located in the cerebellum or the temporal lobe correlate with autism spectrum disorder (Bolton et al 2002, Eluvathingal et al 2006, Jambaque et al 1991).

Histologically, tubers and SEGAs display a mix of glial and neuronal markers and morphology. Tubers have disorganized cortical lamination with marked gliosis and inflammation with infiltration of T

cells and microglial activation (Muhlebner et al 2016). Giant cells in the tubers stain positive for neural progenitor or astrocyte markers and phospho-S6, suggesting abnormal differentiation and activation of mTORC1. There is some evidence for decreased myelin within tubers and decreased numbers of oligodendrocytes (Muhlebner et al 2016, Scholl et al 2016). Tubers have been identified as early as 20 weeks gestation; the number and size of tubers do not change postnatally. This suggests that tubers may form during normal cortical proliferation and development when neural progenitors are most active. However, that does not mean the cortical tubers are completely static, as they can become calcified over time (Altman et al 1988, Koh et al 2000, Muhlebner et al 2016). Subependymal nodules (SEN) are localized along the ventricle wall, especially near the foramen of Monro. Subependymal giant cell astrocytomas (SEGA) are thought to progress from SENs, although it is not currently possible to predict which SENs will progress to SEGAs. SEGAs also contain enlarged neurons and multinucleated cells which stain positively for neural progenitor or astrocyte markers (Buccoliero et al 2009, Ess et al 2005, Hirose et al 1995, Lopes et al 1996). The precise cellular progenitors of tubers and SEGAs are unclear, but the continued expression of neural progenitor and astrocyte markers suggest abnormal neural differentiation contributes to the pathology.

There is also evidence for neuropathological abnormalities outside of the hamartomatous growths in the brain. Diffusion tensor imaging of TSC patients reveals white matter abnormalities even in apparently “normal” areas of the brain. Patients have increased apparent diffusion coefficient values (reflecting total diffusion), decreased fractional anisotropy (reflecting directional diffusion), and increased radial diffusivity (reflecting diffusion out of the main axis, orthogonal to the axon) (Arulrajah et al 2009, Garaci et al 2004, Krishnan et al 2010, Makki et al 2007, Simao et al 2010, Widjaja et al 2010). All three of these measurements together suggest decreased white matter integrity and impaired neuronal connectivity in TSC.

Genetics of TSC

The causative genes in TSC, named *TSC1* and *TSC2*, were identified in 1997 and 1993, respectively (1993, van Slegtenhorst et al 1997). Subsequently, it was shown that the *TSC1* gene product, hamartin, and the *TSC2* gene product, tuberin, form a complex along with TBC1D7 which inhibits mTORC1 via Rheb (ras homolog enriched in brain). Tuberin contains a GTPase activating (GAP) domain which converts Rheb-GTP to Rheb-GDP while hamartin is thought to function primarily as a scaffolding protein.

TSC1 is located on chromosome 9 and is transcribed into a 23 exon 8.6kb transcript. The protein, hamartin, is 1164 amino acids and 130kDa. Human hamartin protein is 20% identical to Drosophila, 49%/41% identical to zebrafish *tsc1a/tsc1b*, 87% identical to mouse, 86% identical to rat, and 99% identical to chimpanzee orthologues (ensembl). *TSC2* is located on chromosome 16 which is transcribed into a 42 exon 5.5kb transcript. By convention, the exons of *TSC2* are numbered 1-41 with the untranslated leader exon designated as 1a. The protein, tuberin, is 1807 amino acids and 200kDa. Human *TSC2* protein is 31% identical to Drosophila, 56% identical to zebrafish, 88% identical to mouse, 91% identical to rat, and 98% identical to chimpanzee orthologues (ensembl).

There is evidence to support two alternative transcripts of *TSC2* missing exon 25 and/or exon 31 that are expressed in both adult and fetal tissue in humans, as well as other species (Ekong et al 2016, Kobayashi et al 1995, Maheshwar et al 1996, Xu et al 1995). Exon 31 is less well-conserved than the other exons of *TSC2*. Furthermore, no pathogenic mutations have been identified in either exon 25 or 31. This suggests that any functions of these exons are dispensable for the pathogenesis of TSC (Ekong et al 2016).

Mutations are identifiable in 80-90% of patients with TSC, and, given the marked improvements in sequencing technology, there is growing evidence that the majority of remaining patients have causative mutations that were initially undetected because they were mosaic or localized to introns (Jones et al 1999, Tyburczy et al 2015). In TSC patients, mutations in *TSC2* are ~3-4x more common than mutations in *TSC1* (Jones et al 1999, Niida et al 2001, Sancak et al 2005). TSC is inherited in families in an autosomal dominant manner one third of the time, with the remaining cases being *de novo* (Jones et al 1999). In contrast to the overall pattern of *TSC2* versus *TSC1* mutations, in cases of familial inheritance approximately half are linked to mutations in *TSC1* (Niida et al 2001, Povey et al 1994). Although TBC1D7 binds to the tuberin/hamartin complex and loss-of-function results in increased mTORC1 signaling, mutations in the *TBC1D7* gene do not cause tuberous sclerosis complex (Dibble et al 2012).

The types of mutations seen in patients in *TSC1* versus *TSC2* also hint at the differences in function. Consistent with the role of hamartin as a scaffolding protein, missense mutations are not commonly pathogenic (1%). Instead, nonsense, frameshift, or splice-site mutations account for almost all the pathogenic mutations identified; these would be expected to significantly alter protein sequence or decrease protein levels (Jones et al 1999, Sancak et al 2005). In contrast, the mutations identified in *TSC2* display a much wider variety. Although the majority of mutations (72-75%) show larger changes (nonsense, frameshift, large rearrangements, splice site), there are a significant number of missense mutations and in-frame indels (insertion/deletions). Unsurprisingly, many missense mutations occurred in the GAP domain (exon 34-38), presumably impairing regulation of Rheb (Jones et al 1999, Niida et al 2001, Sancak et al 2005). However, the highest mutation rate is found in exons 16 and 40, which are not part of any particular domain in the tuberin protein (Jones et al 1999, Kwiatkowski et al 2011, Sancak et al 2005). It is unclear why these two exons are disproportionately affected in *TSC2* mutations. The difference in mutation types seen in *TSC1* versus *TSC2* suggest that *TSC2* is more sensitive to genetic alterations; this may partially explain why more patients are identified with mutations in *TSC2*. Mutations in *TSC1* or *TSC2* do not predispose for increasing rates of somatic mutations, which is consistent with the normal rate of carcinomas in TSC patients (Martin et al 2017).

Attempts to correlate the phenotype and genotype have led to the conclusion that mutations in TSC are highly penetrant but with variable expressivity, such that even identical mutations in twins present with different symptoms (Humphrey et al 2004). Mutations in *TSC2* correlate with increased severity of disease including intellectual disability and tuber burden (Sancak et al 2005). This is consistent with the increased rate of *TSC2* mutations in sporadic cases (increased likelihood of presentation with more severe disease) and the increased rate of *TSC1* mutations in familial cases (increased likelihood of reproduction with less severe disease).

A major hypothesis in this field is that the hamartomatous growths in TSC occur following a second-hit or loss-of-heterozygosity (LOH) in the other allele, consistent with a tumor suppressor pathway. This helps explain the variability in patient presentations: the occurrence of somatic second-hits occurs randomly and, depending on when and where during development they occur, resulting signs and symptoms could be dissimilar. This hypothesis has been confirmed in renal angiomyolipomas, hypopigmented macule melanocytes, facial angiofibromas, cephalic fibrous plaques, and subependymal giant cell astrocytomas (Cao et al 2017, Li et al 2011, Martin et al 2017, Tyburczy et al 2014). Interestingly, the types of second-hit mutations found in angiofibromas were consistent with UV-induced damage, suggesting that sun exposure contributes to second-hits and explaining why the appearance and number of angiofibromas increase with age (Tyburczy et al 2014). In contrast, molecular analyses of cortical tubers demonstrate few cells with loss of heterozygosity (Henske et al 1996, Martin et al 2017, Niida et al 2001, Qin et al 2010). Furthermore, the giant cells seen in cortical tubers are electrically silent, suggesting that if they do contribute to seizure activity, it is not as the primary electrical source (Cepeda, Andre, Vinters et al. 2005; Cepeda, Andre, Flores-Hernandez et al. 2005).

Hamartin and Tuberin Protein Function

TSC1 and *TSC2* have been shown to encode the proteins hamartin and tuberin respectively. Initial insights into the function of tuberin came after *Tsc2* was identified as the causative mutation in the Eker rat, a model of hereditary renal cell carcinoma first described in 1954 (Eker 1954, Yeung et al 1994). Following identification of the human *TSC2* gene, similarities between the protein sequence of *TSC2* in exon 37 and the GTPase-activating protein GAP3 led authors to hypothesize that tuberin may have GAP activity (1993). GAPs inhibit G proteins by binding and enhancing conversion of GTP to GDP, thus shifting the G protein to its inactive state. Tuberin was later confirmed to bind to Rheb and inhibit its activity (Inoki et al 2003a, Tee et al 2003).

Other domains identified in tuberin include the hydrophobic potential leucine zipper domain (exons 3-4), and two coiled-coil domains (exons 10-11 and exon 26). The hydrophobic/leucine zipper domain and the first coiled-coil domain of tuberin were identified as the hamartin binding domains (van Slegtenhorst et al 1998). Hamartin protein contains a coiled-coil domain in exon 17-23 which corresponds to the tuberin binding domain (van Slegtenhorst et al 1998). Hamartin also contains a transmembrane domain in the N-terminal region of the protein. The two proteins form a complex along with TBC1D7 which localizes to the lysosome, perinuclear region, Golgi apparatus, and cytoplasmic vesicles. Tuberin and hamartin are constitutively expressed in all cells, supporting their fundamental role in regulating cell growth and differentiation (1993). Homozygous knockouts of *TSC1* or *TSC2* result in embryonic lethality in mice.

Hamartin and tuberin act upstream to inhibit mTORC1 (Figure 1.1). The TSC complex regulates mTORC1 by localizing to the lysosomal surface where tuberin binds to Rheb GTPase and inhibits the protein by promoting switching from the active GTP-bound state to the inactive GDP-bound state (Inoki et al 2003a, Menon et al 2014, Tee et al 2003). Rheb activates mTORC1 by phosphorylating mTOR. There is crosstalk between several proteins important for transmitting growth factor signals (Akt, ERK, Wnt) and mTORC1 in order to coordinate cell growth and proliferation. Akt, ERK, and Wnt activate mTORC1 by phosphorylating tuberin to disrupt TSC complex binding and localization, releasing mTORC1 from TSC complex inhibition (Inoki et al 2002, Inoki et al 2006, Ma et al 2005, Manning et al 2002, Potter et al 2002, Roux et al 2004). Additionally, Akt can phosphorylate PRAS40 independently of TSC1/TSC2 to relieve inhibition of mTORC1(Kovacina et al 2003, Sancak et al 2007, Vander Haar et al 2007). Signals of stress, when the cell needs to slow down proliferation and anabolic processes, activate TSC2 or TSC1 to inhibit mTORC1. Low energy via AMPK, hypoxia via REDD1, or DNA damage via p53 activate or increase expression of tuberin or hamartin in order to inhibit mTORC1 driven growth (Brugarolas et al 2004, Budanov and Karin 2008, DeYoung et al 2008, Feng et al 2005, Feng et al 2007, Inoki et al 2003b). Homozygous loss of tuberin or hamartin disrupts this important regulatory node resulting in constitutively active mTORC1 signaling regardless of the inhibitory or stimulatory signals.

TBC1D7 binds to TSC1 to stabilize the hamartin-tuberin complex. Knockdown of TBC1D7 decreases hamartin-tuberin binding, leading to growth-factor independent activation of mTORC1 similar to loss of hamartin or tuberin (Dibble et al 2012, Nakashima et al 2007). Although mutations in TBC1D7 in patients cause elevated mTORC1 signaling, they do not cause TSC; instead, homozygous mutations cause autosomal recessive macrocephaly (Alfaiz et al 2014, Capo-Chichi et al 2013).

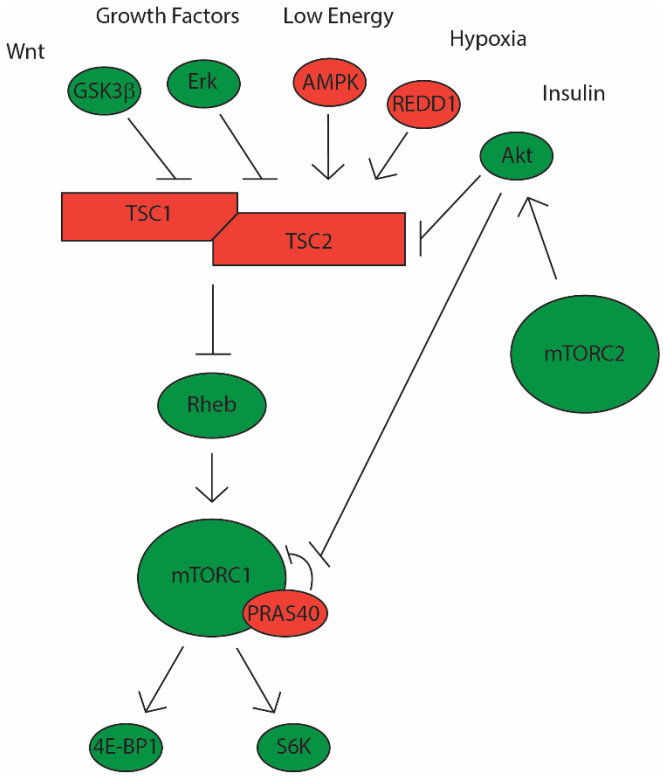

Figure 1.1 TSC Pathway

mTOR complex 1and mTOR complex 2

Mechanistic target of rapamycin (mTOR) is a 289-kDa serine/threonine kinase, which forms two complexes called mTORC1 and mTORC2. mTORC1 is composed of the proteins mTOR, raptor, pras40, deptor, mLST8 and Tti1/Tel2. Raptor (regulatory-associated protein of mammalian target of rapamycin) is a scaffolding protein which regulates mTORC1 localization and substrate binding. The Tt1/Tel2 complex is a scaffold regulating mTORC1 stability. Proline-rich Akt substrate 40kDa (PRAS40) and DEP domain containing mTOR-interacting protein (DEPTOR) are mTORC1 inhibitors. Mammalian lethal with sec-13 protein 8 (mLST8) has unknown functions. mTORC2 also shares mTOR, DEPTOR, mLST8, and Tti1/Tel2, but has the unique protein components rictor (rapamycin-insensitive companion of mTOR), mSin1 (mammalian stress-activated map kinase interacting protein 1), and protor 1/2 (protein observed with rictor 1 and 2) (Laplante and Sabatini 2012).

Rapamycin is a macrolide antifungal produced by *Streptomyces Hygroscopius* discovered on the island of Rapa Nui (Easter Island). Its anti-proliferative effects are mediated by inhibition of mTOR. Rapamycin binds to FKBP12 (12-kDa FK506-binding protein) and the complex inhibits mTORC1 (Brown et al 1994, Sabatini et al 1994). Rapamycin primarily targets mTORC1 although mTORC2 can be affected following long exposures, presumably due to sequestration of mTOR during complex turnover (Sarbassov et al 2005).

mTORC1 localizes to the lysosomal membrane in response to amino acids. Amino acids activate Rag GTPases which interact with raptor to bring the mTORC1 to the lysosomal membrane (Sancak et al

2008). At the lysosomal surface mTORC1 is exposed to and can be activated by Rheb. Thus, the presence of amino acids is required before any other upstream signal can activate mTORC1.

The effects of mTORC1 activity can be generally categorized as promoting anabolic processes (cell growth, energy consumption) and inhibiting catabolic processes (molecular breakdown, energy production). mTORC1 stimulates protein translation primarily through eukaryotic initiation factor 4E binding protein 1 (4E-BP1) and cell size through regulation of ribosomal protein S6 (S6). mTORC1 also regulates cholesterol synthesis by activating sterol regulatory-element binding proteins 1 and 2 (SREBP1 and SREBP2) which increase expression of genes involved in cholesterol and other sterol synthesis or regulation.

mTORC1 increases cap-dependent protein translation through phosphorylation of 4E-BP1. Initiation faction eIF4E is a component of the complex which recruits the 40S ribosome to the 5'-cap of an mRNA in order to begin translation. 4E-BP1 binds to and inhibits eIF4E until it is phosphorylated by mTORC1. Following phosphorylation 4E-BP1dissociates from eIF4E and translation can proceed. 4E-BP1 is phosphorylated in an ordered manner: first at Thr37 and Thr46, then at Thr70, and finally at Ser65. Ser65 and Thr70 are the only sites phosphorylated by mTORC1 (Gingras et al 2001). Either inhibiting the pathway through Rapamycin treatment or activating mTORC1 via TSC mutations does not cause global changes in protein synthesis; instead, changes in a subset of transcripts occurs (Bilanges et al 2007, Thoreen et al 2009, Yu et al 2009).

Eukaryotic ribosomes consist of two subunits: the small 40S subunit and the large 60S subunit; S6 is part of the small 40S subunit. Ribosome biosynthesis begins in the nucleolus where the ribosomal RNAs are synthesized. Many of the ribosomal proteins, including S6, are imported from the cytoplasm to associate with the newly formed ribosomal RNAs in the nucleolus (Reviewed in (Meyuhas 2015)). The pre-40S ribosomal complex is then exported out of the nucleus. There has been intense interest in S6 because it was one of the first and still one of the few ribosomal proteins known to be regulated by phosphorylation (Gressner and Wool 1974, Kabat 1970). mTORC1 increases S6 phosphorylation by activating S6 kinase 1 (S6K1) and S6 kinase 2 (S6K2). In response to growth factors, ribosomal protein S6 is phosphorylated in five locations in an ordered manner. S6 is first phosphorylated at Ser236 then Ser235 by multiple kinases, including S6 kinase (S6K) activated by mTORC1, but also 90kDa ribosomal S6 kinases (RSK), downstream of ERK1/2. S6 is next phosphorylated at Ser240 and Ser244 by S6K, downstream of mTORC1, and lastly at Ser247 (Martin-Perez and Thomas 1983).

Knock-out of S6K in Drosophila is semi-lethal and causes a reduction in size (Montagne et al 1999). This phenotype is consistent with findings from *TSC2* or *TSC1* knock-out Drosophila, where loss of the negative regulators hamartin or tuberin results in enlarged cells (Tapon et al 2001). However, unlike Drosophila, two homologues of S6K exist in mammals: S6K1 and S6K2. S6K1 has two isoforms: p70 S6K1, which is cytoplasmic, and p85 S6K1, which is nuclear. Both isoforms of S6K2 are primarily nuclear. Originally S6K1 and S6K2 were thought to be redundant because in S6K-/- mice, S6K2 expression is upregulated and S6 is still phosphorylated, suggesting compensation (Shima et al 1998). Surprisingly, loss of S6K1 and S6K2 have opposite effects on mouse body size; S6K1-/- mice are smaller while S6K2-/- mice are similar in size or even slightly larger. Double knock-out mice are pre- or postnatally lethal (Pende et al 2004). Interestingly, S6 mutant mice do not display prenatal lethality or smaller birth size, suggesting there are other S6K1 and S6K2 targets regulating prenatal development. S6 also regulates glucose homeostasis, such that loss of S6K1 or mutations in S6 in mice display glucose intolerance similar to malnutrition during prenatal development (reviewed in (Meyuhas 2015)). Despite the fact that S6 is a critical component of the 40S ribosomal subunit, loss of phosphorylation of S6 does not alter global protein synthesis (Chauvin et al 2014, Garelick et al 2013, Mieulet et al 2007, Ruvinsky et al 2005). S6 is one of the essential early proteins involved in assembly of the pre-18S-rRNA prior to nuclear export and phosphorylation of S6 is critical to this process (Ferreira-Cerca et al 2005, Kruger et al 2007, Zhang et al 2016). Rapamycin, inhibits S6 phosphorylation and causes accumulation of the pre-18s-

rRNA in the nucleus, but it is not clear how over-activation of S6 would alter ribosomal assembly (Zhang et al 2016).

mTORC1 inhibits catabolic processes by regulating autophagy. mTORC1 phosphorylates ULK1 and Atg13 which suppresses ULK1-Atg13-FIP200 complex activity, an early step in autophagosome formation (Ganley et al 2009, Hosokawa et al 2009, Jung et al 2009). The second mechanism connecting mTORC1 to autophagy regulation is through the transcription factor EB (TFEB). TFEB is the master controller activating autophagy genes, and it is regulated by its phosphorylation status. Phosphorylated TFEB localizes to the cytoplasm, unable to activate the autophagy gene network. Dephosphorylation of TFEB allows it to translocate to the nucleus (Sardiello et al 2009). mTORC1 phosphorylates TFEB, preventing activation of autophagy genes and lysosomal biogenesis (Martina et al 2012, Settembre et al 2012). In this way mTORC1, localized to the lysosomal surface, connects lysosome content and nutrient status to lysosome biogenesis.

The regulation and downstream effects of mTORC2 are not as well studied as mTORC1. One of the main effects of mTORC2 activation is phosphorylation of Akt1 at Ser^{473}, which then enhances Akt phosphorylation at Thr^{308} by PDK1 (Sarbassov et al 2005). Phosphorylated and activated Akt can phosphorylate and inhibit tuberin, activating mTORC1.

To complicate the pathway, mTORC1 also participates in several inhibitory feedback loops. S6K1 inhibits PI3K/Akt signaling by phosphorylating and inhibiting IRS1, preventing its association with PI3K. Decreased signaling through PI3K and phospho-Akt^{Thr308} then inhibits mTORC1 activity (Harrington et al 2004). S6 kinase can inhibit mTORC2 activity by phosphorylating rictor, leading to decreased phospho-Akt^{Ser473} (Julien et al 2010). The signaling changes usually seen in *TSC2* or *TSC1* knock-out models are increased mTORC1 activity and decreased mTORC2 activity.

mTOR in stem cells

Given the essential function of mTOR in regulating cell metabolism and growth, it is not surprising that mTOR signaling impacts stem cell reprogramming and growth. mTOR protein as well as phospho-Akt and phospho-S6 protein levels drop during the first two days of reprogramming before returning to baseline levels at Day 3 (He et al 2012, Wang et al 2013). Overexpression of mTOR or inhibition of mTORC1 activity throughout reprogramming impairs reprogramming (He et al 2012, Wang et al 2013). Further, knock-out or knock-down of *TSC2* inhibits reprogramming efficiency (He et al 2012). The four reprogramming factors inhibit mTORC1 leading to elevated autophagy which enhances reprogramming (Wang et al 2013, Wu et al 2015). This highlights the strict regulation of mTOR during reprogramming.

mTOR activity is crucial to stem cell maintenance and development. Loss of mTOR in mice causes E5.5-E6.5 lethality due to defects in cell proliferation and mTOR knock-out embryonic stem cells are unable to grow *in vitro* (Gangloff et al 2004, Murakami et al 2004). Excess mTOR activity in murine hematopoietic and germline stem cells leads to abnormal proliferation, differentiation, and exhaustion of the stem cell pool (Chen et al 2008, Magri and Galli 2013, Sun et al 2010, Zhou et al 2009). Mouse and Drosophila models further support a role for hamartin and tuberin in neural stem cell maintenance and precocious neuronal differentiation (Bateman and McNeill 2004, Feliciano et al 2013, Magri et al 2011, Magri and Galli 2013, Way et al 2009).

Studies are just beginning to address the role of hamartin/tuberin and excess mTOR signaling in the human neural stem cell population. Human embryonic stem cells with homozygous or heterozygous

mutations in *TSC2* have impaired formation of post-mitotic neurons from neural progenitors (Costa et al 2016). However, this is not correctable with rapamycin treatment, pointing to a need for an improved understanding of the mechanisms and timing of neurodevelopmental abnormalities.

Crosstalk between p53 and TSC/mTOR

Tumor suppressor protein p53 is a transcription factor important in the regulation of apoptosis, senescence and cell cycle progression in response to various stressors. At baseline, p53 has a short half-life and overall levels in the cell are low, but following stress signals, such as DNA damage, nucleoside depletion and hypoxia, p53 protein is rapidly stabilized to control the cellular response (reviewed in (Marine et al 2006)). The primary mechanism for p53 stabilization is through inhibition of its primary inhibitor, MDM2. MDM2 is an E3 ligase which ubiquitinates p53, targeting it for degradation, and also binds to the transcriptional activation domain to block p53 function (Haupt et al 1997, Kubbutat et al 1997). Upon stabilization, p53 is then able to translocate to the nucleus to activate its transcriptional program. The various stress signals modify p53 by phosphorylation, sumoylation, acetylation and methylation to activate specific transcriptional responses. Further, p53 negatively regulates its own response by increasing MDM2 transcription. In this way p53 controls the cellular response to stress signals, pushing the cell towards cell cycle arrest if the cell can be repaired or towards apoptosis if the cell cannot survive the stress.

Given its role in protecting the genomic integrity of the cell, p53 has important functions in stem cell biology and stem cell reprogramming. Overexpression of p53 in MDM2 mutant mice causes embryonic lethality between implantation and E7.5 (Kubbutat et al 1997). In 2006, Shinya Yamanaka identified four factors sufficient for reprogramming adult human fibroblasts to induced pluripotent stem cells, although the efficiency of reprogramming was low (Takahashi and Yamanaka 2006). Shortly thereafter four papers published in *Nature* in 2009 identified p53 as a potential barrier to reprograming. Knocking-down, knocking-out, or inhibiting p53 through genetic or pharmacologic means was found to enhance reprograming (Hong et al 2009, Kawamura et al 2009, Li et al 2009, Marion et al 2009, Utikal et al 2009). On the flip side, elevated p53 levels were found to impair reprograming (Li et al 2009). Knocking down p53 during the reprogramming process enhances reprogramming by overcoming stress signals from DNA damage, however, permanent ablation of p53 allows reprogramming at the expense of genomic integrity (Li et al 2009, Marion et al 2009). When MDM4, a negative regulator of p53, is knocked out in neural progenitors the mice have cell cycle abnormalities in the neural progenitors and increased apoptosis in the post-mitotic neurons (Francoz et al 2006).

Throughout development cells must carefully balance cell growth and proliferation with senescence or apoptosis. p53 acts as a hub for sensing cell stress including DNA damage, nucleoside depletion, and reactive oxygen species. mTOR is an important pathway for sensing nutrient and growth factor status. In order to efficiently coordinate all of these inputs to appropriately regulate cell cycle progression and proliferation, crosstalk exists between these two important pathways. The same upstream regulator, AMPK, activates p53 and inhibits mTORC1 in order to pause cell proliferation and growth (Figure 1.2). AMPK senses AMP/ATP ratios or low energy levels and programs the cell to conserve energy including activating autophagy and decreasing protein translation, notably through inhibition of mTORC1 via tuberin. AMPK activates p53 by acetylation and inhibition of the inhibitor MDM4 (He et al 2014, Lee et al 2012). Additionally, p53 may participate in a positive feedback loop by increasing phosphorylation of AMPK to further activate the kinase (Feng et al 2005).

Ribosomal proteins are translocated to the nucleus where they localize to the nucleolus for assembly with rRNAs. Ribosomal stress, due to DNA damage or transcriptional inhibition, causes

disruption of the nucleolus and inhibition of further ribosomal protein nuclear import leading to increased ribosomal protein levels in the nucleoplasm or cytoplasm (Boisvert and Lamond 2010). Binding of ribosomal proteins to MDM2 leads to inhibition of MDM2 and stabilization of p53 protein (Boulon et al 2010). Fourteen ribosomal proteins have been shown to bind to and inhibit MDM2 to increase p53 (Kim et al 2014). Mutant phosphorylation-resistant S6 mice harboring an oncogenic KRAS mutation show increased stability of p53 protein in the nucleus, but it is not clear what effect increased phosphorylation of S6 would have on p53 levels (Khalaileh et al 2013).

DNA damage and genotoxic stress can inhibit mTORC1 signaling through multiple regulators, many of which converge on the tuberin/hamartin complex. DNA damage inhibits mTORC1 activity in a p53-dependent manner (Budanov and Karin 2008, Feng et al 2005, Horton et al 2002). One pathway connecting p53 to mTORC1 is through expression of the proteins Sestrin1 and Sestrin2, which increase phosphorylation and activation of AMPK. Increased activation of AMPK, in turn, increases phosphorylation and activation of tuberin and inhibits mTORC1 (Budanov and Karin 2008, Feng et al 2005). Further, *TSC2* mRNA and protein levels increase in response to DNA damage in a p53-dependent manner (Feng et al 2005, Feng et al 2007). These results support a p53-dependent inhibition of mTORC1 in response to DNA damage via a rapid (minutes-hours) activation of AMPK along with a slower (12-24 hours) induction of *TSC2* mRNA and protein. However, Akt and MAPK can also inhibit phospho-S6 following DNA damage in an mTORC1-, p53-, and AMPK- independent manner (Cam et al 2014).

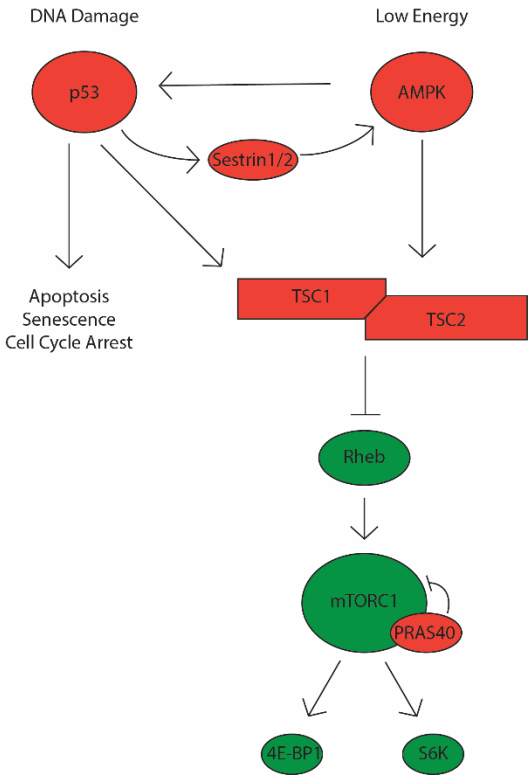

Figure 1.2 p53 and mTOR crosstalk

Existing studies using cells with loss of *TSC1* or *TSC2*, including TSC patient AML samples, found mTORC1 activation of p53 with increased apoptosis or senescence, but the mechanism connecting p53 to mTORC1 was unclear (Habib et al 2011, Lee et al 2007, Miceli et al 2012, Pai et al 2016, Wataya-Kaneda et al 2001, Zhang et al 2003) While attempting to generate MEFs to model TSC, Zhang et al. observed that *TSC2*-/- MEFs did not grow well unless the cells were immortalized by also knocking-out p53 (Zhang et al 2003). This was the first evidence that there may be interactions between TSC and p53. Renal angiomyolipomas from TSC patients have elevated p53 levels compared to kidney tissue from control patients. This is in marked contrast to the renal cell carcinomas of the TSC-model Eker rat, pointing to species-specific differences and a potential explanation for why TSC patients do not develop carcinomas like the rat model (Habib et al 2011). Homozygous *TSC1* mutant MEFs are more sensitive to cell death following glucose starvation and genotoxic agents and have marked elevation of p53 (Lee et al 2007, Pai et al 2016). This increased sensitivity to genotoxic cell death may be secondary to elevated AMPK activity with decreased ATP stores. The cell death phenotype can be partially inhibited by knocking-down p53 (Lee et al 2007). However, the mTORC1-inhibitor rapamycin, despite inhibiting p53 and phospho-p53 levels, has shown mixed results in its ability to inhibit cell death (Lee et al 2007, Pai et al 2016). Rapamycin decreases p53 transcript association with polysomes, suggesting that mTORC1 regulates p53 through increased translation of p53 protein (Lee et al 2007). Another potential mechanism connecting mTORC1 to p53 is through the p53 positive regulator ARF. ARF binds and sequesters MDM2 to stabilize and increase p53 protein levels. Knocking-down or knocking-out *TSC1* in MEFs increases ARF protein levels through increased translation, which then increases p53 protein levels; this is correctable with rapamycin treatment (Miceli et al 2012). All of these studies are in homozygous *TSC* mutant cells, but heterozygous skin tissue from TSC patients have increased rates of apoptosis, suggesting that at least some of these same pathways may be altered in heterozygous mutant cells as well (Wataya-Kaneda et al 2001).

Mouse and Rat Models of TSC

The Eker rat was unknowingly the first animal model of TSC. It was initially used as a model of hereditary renal cell carcinoma before the causative mutation in *Tsc2* and connection to TSC was identified (Eker 1954, Yeung et al 1994). Evidence from the Eker rat supported the model of TSC as a tumor suppressor pathway; the Eker rat has a germline heterozygous mutation in *Tsc2* and tumor formation is consistent with loss-of-heterozygosity or Knudson's two-hit hypothesis. However, the Eker rat is predisposed to renal cell carcinoma as well as pituitary, splenic, and uterine tumors, while human TSC patients rarely develop cancer or even hamartomatous growths in the pituitary or spleen. Comparing the *Tsc2*-null renal cell carcinoma tissue in the Eker rat to the *TSC2*-null renal angiomyolipoma tissue in TSC patients reveals divergent signaling pathways. While renal cell carcinomas in the Eker rat have decreased levels of PTEN and p53, tissue samples from patient angiomyolipomas have increased expression of p53 and PTEN (Habib et al 2011). This highlights the differences between the Eker rat renal cell carcinoma and human renal hamartoma pathogenesis. Further, it suggests that additional mutations in cancer driving pathways may be necessary for carcinoma formation in TSC patients.

Heterozygous *Tsc2* Eker rats have impaired novel object exploration and social behavior but have improved episodic memory for the Morris water maze or radial maze (Waltereit et al 2006, Waltereit et al 2011). Germline homozygous *Tsc2* Eker mutant rats are embryonic lethal midgestation due to defects in neural tube closure (Rennebeck et al 1998). Germline homozygous *TSC2* mutant mice are embryonic lethal at E9.5-12.5 due to hepatic hypoplasia or neural tube defects (Kobayashi et al 1999, Onda et al 1999). Heterozygous loss of *Tsc2* or *Tsc1* in mice causes a subtle neurological phenotype with impaired spatial and fear learning, abnormal mother-pup interactions, decreased spine density and impaired axonal guidance (Ehninger et al 2008, Goorden et al 2007, Nie et al 2010, Tavazoie et al 2005).

Summary

TSC is a pediatric disorder which causes epilepsy and intellectual disability. Mutations in *TSC1* or *TSC2* cause benign growths in multiple organs but the onset of hamartomas varies from prenatally (cortical tubers) to post-puberty (lung LAM). The differences in the timing of onset (and regression or lack thereof) point to differences in the tissue specific pathogenesis of TSC lesions. Evidence from human samples and clinical trials supports the critical role of increased mTORC1 activity in the symptoms of TSC. While mTORC1 inhibitors have been shown to be effective in treating some aspects of the disease (e.g. SEGA, AML, and LAM), reversal of growth is usually static and is restricted to the treatment period, pointing to the need for a better understanding of mechanisms controlling cell growth and differentiation (Bissler et al 2008, Cardamone et al 2014, Franz et al 2006, Franz 2013, Krueger et al 2013, McCormack et al 2011, Sasongko et al 2016). This limitation could be potentially overcome by treatment targeting the specific cell types relevant to the disease process at the initial onset of dysfunction and thereby provide lasting protection against developmental abnormalities. Although the current model in the field centers on excess mTORC1 activity as the critical mediator of the neurologic symptoms, it is unknown how increased mTORC1 activity alters neurodevelopment to induce cortical malformations.

Furthermore, while some lesions have evidence of loss of heterozygosity (kidney AML, facial angiofibromas, SEGAs), the cortical tubers have little evidence of second mutations. This, along with evidence of abnormalities in the heterozygous “normal” cortical regions in patients, led the field to consider alternative hypotheses. First, haploinsufficiency could be contributing to the neurological phenotype. Differences in tissue sensitivity to loss of tuberin could render neurons, oligodendrocytes, or astrocytes more sensitive to loss of tuberin or hamartin, such that loss of only one copy is sufficient to alter neural dynamics. Second, non-cell autonomous mechanisms could be causing formation of tubers and disrupting neurodevelopment. Small numbers of cells with loss of heterozygosity (e.g. the giant cells within the tubers) could be secreting factors which disrupt neighboring neurodevelopment. Possibly, it is a combination of mechanisms. Heterozygous mutations in *TSC1* or *TSC2* may cause subtle (by pathological standards) but widespread changes in neuron, oligodendrocyte, and astrocyte function. In the setting of this background process, then loss-of-heterozygosity causes non-cell autonomous localized disruption of neural development leading to tuber formation.

To explore how gene dosage alters signaling and cellular dynamics in TSC, we have used fibroblasts, stem cells, and neural progenitors harboring heterozygous and homozygous mutations in *TSC2*. Chapter II presents evidence for heterozygous loss of *TSC2* altering p53 protein response in fibroblasts and stem cells, providing a potential explanation for the lack of cancer development in TSC patients. Chapter III explores how heterozygous *TSC* mutations alter stem cell behavior. Chapter IV uses heterozygous and homozygous *TSC2* mutant iPSCs to model early neural development in TSC. Our results support a model of haploinsufficiency in TSC but do not exclude non-cell autonomous mechanisms.

CHAPTER II

HETEROZYGOUS LOSS OF *TSC2* ALTERS P53 SIGNALING AND HUMAN STEM CELL REPROGRAMMING

Parts of this work were published under the same title in Human Molecular Genetics by Oxford University Press (Armstrong, Westlake, Snow, Cawthon, Armour, Bowman, Ess, 2017).

Abstract

Tuberous Sclerosis Complex (TSC) is a pediatric disorder of dysregulated growth and differentiation caused by loss of function mutations in either the *TSC1* or *TSC2* genes, which regulate mTOR kinase activity. *We generated induced pluripotent stem cells using dermal fibroblasts obtained from patients with TSC to test the hypothesis that heterozygous loss of TSC2 alters neurodevelopment.* During validation, we found that stem cells generated from TSC patients had a very high rate of integration of the reprograming plasmid containing an shRNA against *TP53*. Here we showed loss of one allele of *TSC2* in human fibroblasts is sufficient to increase p53 levels and impair stem cell reprogramming. Increased p53 was also observed in *TSC2* heterozygous and homozygous mutant human stem cells, suggesting that the interactions between *TSC2* and p53 are consistent across cell types and gene dosage. These results support the contributions of *TSC2* heterozygous mutant cells to the pathogenesis of TSC and the important role of p53 during reprogramming.

Introduction

As described in Chapter I, Tuberous Sclerosis Complex (TSC, OMIM #613254) is a genetic disorder of pediatric onset characterized by benign tumor growths (hamartomas) in multiple organ systems including the brain, kidney, heart, skin, and lungs (Sahin et al 2016). The most debilitating symptoms in TSC are a consequence of brain involvement, including a high rate of epilepsy, autism spectrum disorder, and learning disabilities (Sahin et al 2016). Emerging evidence discussed in Chapter I suggests that heterozygous mutations may contribute to the neural pathogenesis of TSC. We hypothesized that heterozygous loss of *TSC2* would be sufficient to alter neural development *in vitro* in a stem cell model of TSC. However, in the process of generating stem cells to address these questions, we found a surprising role for heterozygous mutations in *TSC2* in the regulation of p53 and the reprogramming process.

We generated induced pluripotent stem cells (iPSCs) using human dermal fibroblasts obtained from TSC patients and control volunteers. We reprogrammed primary fibroblasts using established episomal methods employing three plasmids expressing *OCT4*, *KLF4*, *SOX2*, *L-MYC*, *LIN28*, and a shRNA knockdown targeted to *TP53* (Okita et al 2011). Inhibiting mTORC1 or knocking out *TSC2* impairs reprogramming efficiency, suggesting that mTORC1 activity is tightly regulated during reprogramming (He et al 2012, Wang et al 2013). Knocking down p53 enhances reprogramming efficiency and survival; however, the mTOR pathway is also known to interact with p53. p53 inhibits mTORC1 signaling, notably upregulating *TSC2*, but the role of mTORC1 in the regulation of p53 is less clear (Budanov and Karin 2008, Cam et al 2014, Feng et al 2005, Feng et al 2007, Horton et al 2002, Stambolic et al 2001). Existing studies using cells with loss of *TSC1* or *TSC2*, including TSC patient AML samples, found mTORC1 activation of p53 with increased apoptosis or senescence (Habib et al 2011, Lee et al 2007, Miceli et al 2012, Pai et al 2016, Wataya-Kaneda et al 2001, Zhang et al 2003). As

most studies were done in the context of homozygous loss of *TSC1* or *TSC2*, it is unclear how heterozygous loss of *TSC2* in patient fibroblasts might affect p53 and stem cell reprogramming. We now show that loss of one copy of *TSC2* is sufficient to increase p53 levels and inhibit reprogramming to iPSCs. These results indicate critical interactions between hamartin/tuberin, mTOR, and p53 to regulate stem cell reprogramming, cell maintenance, and cell death.

Results

TSC patient fibroblasts harbor heterozygous mutations leading to nonsense mediated decay of *TSC2*.

To develop a human *in vitro* model of TSC, we derived primary dermal fibroblast cultures from multiple patients with TSC. The diagnosis of TSC was based on clinical presentation, genetic testing, and imaging studies (Table 1.2). Fibroblasts were isolated from patients' normal-appearing skin or from TSC associated skin lesions Shagreen patches or hypopigmented macules, (also known as "Ash leaf spots"). The original intent, consistent with the two-hit hypothesis, was to acquire fibroblasts with either heterozygous or homozygous genetic mutations in *TSC1* or *TSC2*; the reasoning being that normal appearing skin had a germline heterozygous mutation whereas TSC associated skin lesions also had a second somatic mutation. These Tuberous Sclerosis Patient (TSP) cells were later sequenced using highly redundant exome sequencing to identify pathogenic mutations in either *TSC1* or *TSC2*. For all TSP lines, we identified only heterozygous mutations of either *TSC1* or *TSC2* regardless of whether the fibroblasts were obtained from normal appearing skin or skin lesions (E. Armour Dissertation, Vanderbilt University). Thirty-three percent of the tested lines contained no identifiable mutation in *TSC1* or *TSC2*, broadly consistent with clinical testing for patients with TSC (Rosset et al 2017). As mutations in *TSC2* are more common than *TSC1* and patients with mutations in *TSC2* tend to have more severe disease (Dabora et al 2001, Devlin et al 2006, Jansen et al 2008a, Kothare et al 2014), we selected three well characterized patient lines with nonsense mutations in *TSC2* (denoted as TSP20, TSP23, TSP31) (Table 1.2). To determine whether the premature stop codon mutations lead to nonsense mediated decay of RNA transcripts, we sequenced mRNA from these patient lines. Only the wild-type mRNA was detectable by sequencing in TSP20, TSP23, and TSP31 fibroblast lines (Figure 2.1A). Consistent with these sequencing results, mRNA levels of *TSC2* and expression of tuberin protein in *TSC2* heterozygous mutant fibroblast lines were both reduced by approximately one-half compared to control fibroblasts (Figure 2.1B-C, $p=0.039$ and $p=0.016$). As tuberin is an important negative regulator of mTORC1 we next measured phospho-S6, a downstream target of mTORC1. We did not observe increased mTORC1 activity in fibroblasts with or without nutrient starvation (Figure 2.1D).

Table 1.2: TSC Patients

Patient	Gene	DNA NG_005895.1	Protein NP_000539.2	Exon	Age of Epilepsy Onset	Autism	Intellect. Disability	Age at dermal biopsy	Biopsy site
TSP20	*TSC2*	g.11900T>A	p.Cys203Ter	6/41	6 months	Y	Y	6 years	Hypopigmented patch
TSP23	*TSC2*	g.34854C>T	p.Arg1032Ter	26/41	6 months	Y	Y	2 years	Hypopigmented patch
TSP31	*TSC2*	g.40172C>T	p.Gln1419Ter	33/41	2 months	Y	Y	12 years	Shagreen Patch

Table 1.2. TSC Patient Clinical History, Biopsy Information, and Genotyping

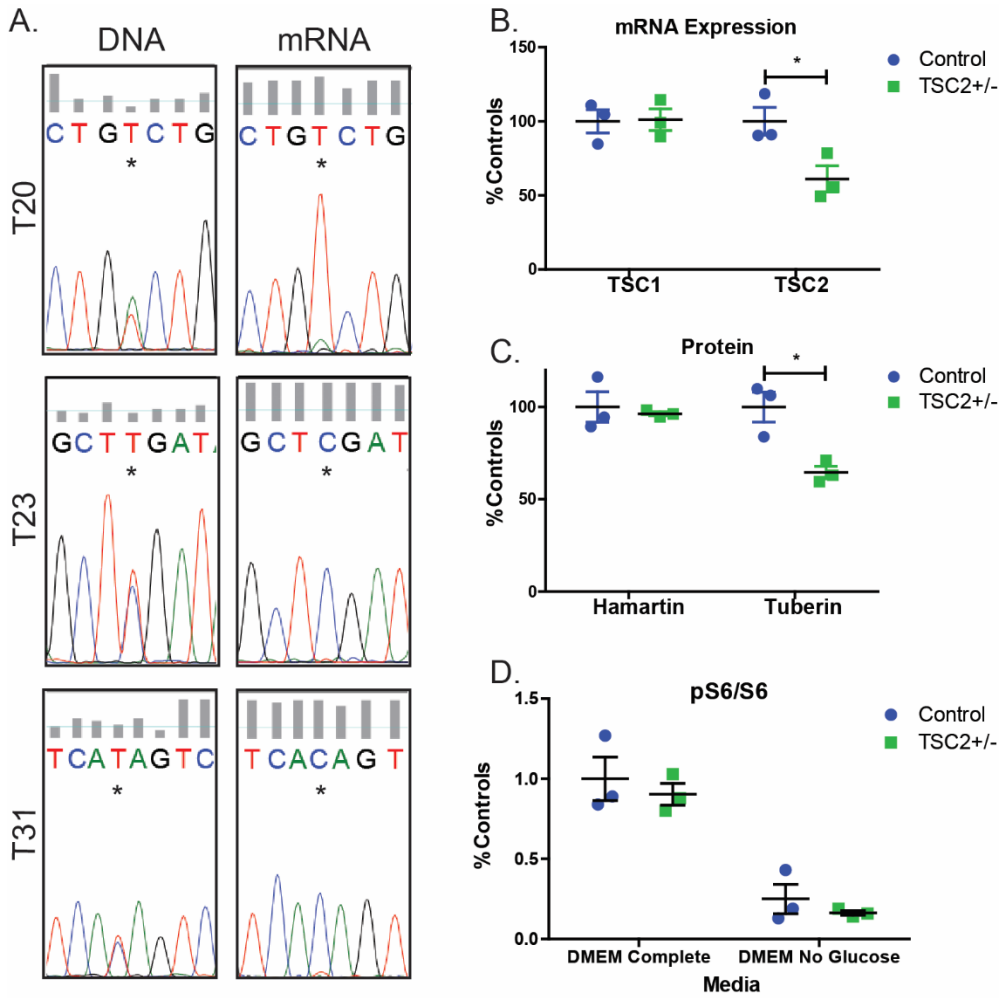

Figure 2.1. Heterozygous nonsense mutations in *TSC2* result in reduced *TSC2* mRNA and tuberin protein levels.

(**A**) Sequencing confirms single nucleotide changes causes premature stop codons in *TSC2*+/- fibroblasts. DNA sequencing reveals wild type and mutant allele but only wild-type allele was detected in mRNA. (**B**) *TSC1* and *TSC2* mRNA quantified by qPCR in control and TSC patient (TSP) fibroblasts (n=3 average of four experimental replicates; p=0.039, t-test). (**C**) Tuberin and hamartin protein quantified by immunoblot (n=3; p=0.016, t-test). (**D**) Control and *TSC2*+/- fibroblasts were grown in DMEM complete or DMEM without glucose for 5hrs. Protein levels of phospho-S6 were quantified by immunoblot (n=3).

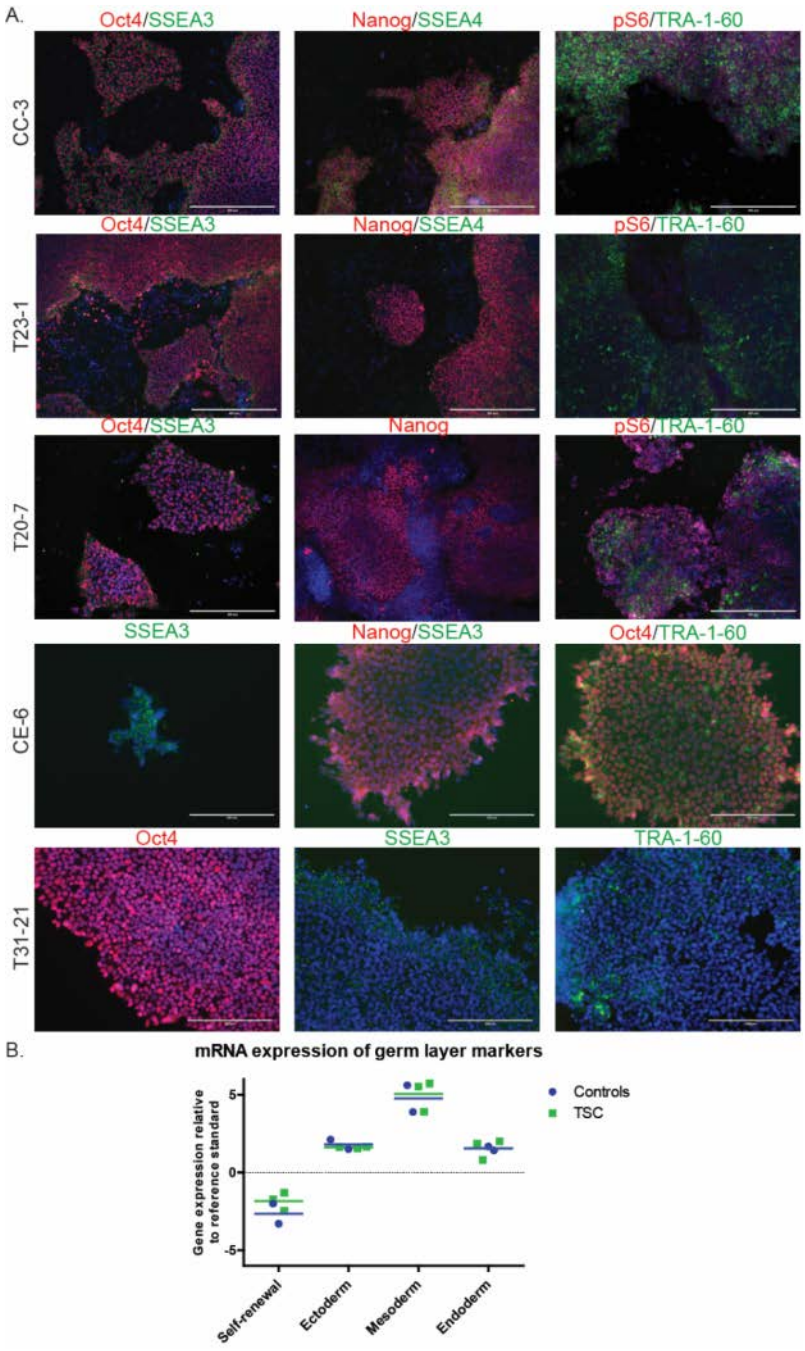

Figure 2.2. Induced pluripotent stem cell validation.

(**A**) Stem cell lines were stained for expression of several pluripotent markers (OCT4, SSEA3, SSEA4, NANOG, TRA-1-60) at 10X (CC-3, T23-1, T20-7) or 20x (CE-6, T31-21) magnification. (**B**) Stem cell lines were differentiated to embryoid bodies to confirm pluripotency with capacity to form all three germ layers (mesoderm, endoderm, and ectoderm) and then analyzed by a panel of qPCR primers directed at mRNA transcripts associated with each germ layer or pluripotency.

Selective retention of reprogramming plasmid with shRNA against *TP53*

We next reprogrammed control (obtained from healthy unrelated volunteers) and TSP fibroblast lines to iPSCs by transfecting episomal plasmids expressing the reprogramming genes *OCT4*, *KLF4*, *SOX2*, *L-MYC*, *LIN28*, as well as a shRNA knockdown targeted to *TP53* (Okita et al 2011). All TSP and control iPSC lines were validated as pluripotent both by expression of established stem cell markers and the ability to differentiate to all three germ layers (Figure 2.2). The reprogramming plasmids used are expected to remain episomal in the cytoplasm and then be lost from emerging iPSCs through the repeated cell division and passaging required for iPSC generation. As the original publication from the Yamanaka laboratory reported occasional genomic integration of the reprogramming plasmids (Okita et al 2011), all iPSC lines were checked for plasmid integration using a PCR assay. Although control lines showed the expected low rate of integration (20%) (Okita et al 2011, Schlaeger et al 2015), TSP lines showed a marked increase in the incidence of integration of one or more of the plasmids (80%, Figure 2.3A $p=0.023$). To determine whether this was consistent across multiple rounds of reprogramming, we also included several additional iPSC lines from controls and patients with TSC that were not as fully characterized. The high rate of plasmid retention was an unexpected finding that has not been observed while reprogramming any of the other genetic disorders modeled with iPSCs in our laboratory or those of collaborators (>100 independent iPSC lines made to date). In TSP lines, this could be explained by an increased tendency to integrate any exogenous DNA or may reflect a requirement for sustained expression from one or more of the plasmid-encoded genes to drive cellular proliferation and survival during the stress of reprogramming. To distinguish these possibilities, we designed PCR primer sequences to unambiguously identify each plasmid used for reprogramming. In the control integrated lines, one of the two integrated control lines integrated only the *OCT4/shTP53* plasmid and the other had integrated more than one plasmid. In contrast, all of the TSP iPSC lines integrated only a single plasmid, the one that expresses both *OCT4* and the shRNA directed against *TP53* (Figure 2.3B).

Studies from our group and others supporting a complex interaction between tuberin, mTOR, and p53 led us to hypothesize that p53 signaling would be altered in cells from patients with TSC (Habib et al 2011, Lee et al 2007, Miceli et al 2012, Pai et al 2016, Wataya-Kaneda et al 2001, Zhang et al 2003). To determine whether the incorporated shRNA to *TP53* was expressed and functioning, we measured p53 protein levels in non-integrated control, integrated control, non-integrated TSP and integrated TSP iPSC lines. For the integrated TSP lines, p53 protein levels were decreased in 5 out 6 of the integrated *TSC2+/-* iPS lines measured (Chapter III Figure 3.1). Furthermore, integrated iPSCs displayed increased proliferation and survival following single-cell suspension, which is consistent with decreased p53 levels (Chapter III Figure 3.6).

Given a recent report showing that human stem cells acquire mutations in p53 in culture, we further sequenced 16 identified “hot spots” in our original fibroblasts as well as several iPSC lines (Merkle et al 2017). We did not identify any mutations in p53 that might explain the increased rate of integration in the TSC patient lines.

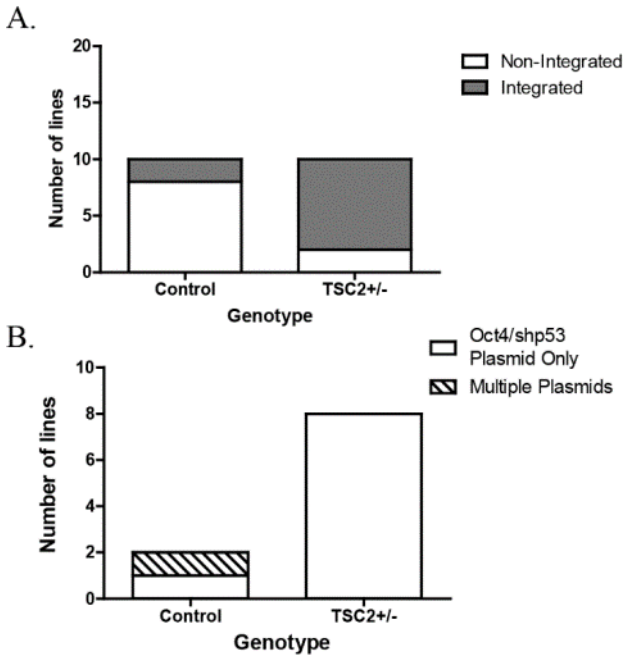

Figure 2.3. Increased integration of reprogramming plasmids in TSP iPSC lines.

(**A**) PCR for continued presence of the reprogramming plasmids at passage ≥10. Multiple iPSC clones generated from five individual patients and five individual controls were analyzed. Plasmid bands were detectable in eight of ten *TSC2* heterozygous mutant clones analyzed and two of ten control clones from control volunteers (p=0.023, Fisher's exact test). (**B**) PCR to distinguish between the three reprogramming plasmids.

Increased levels of p53 in *TSC2* heterozygous mutant fibroblasts

In normally growing "unstressed" cells, p53 is a transcription factor that is rapidly ubiquitinated by MDM2 and degraded. However, following DNA stress, p53 is stabilized in the nucleus where it regulates gene transcription. We examined p53 levels and found expression in both TSP and control fibroblasts were barely detectable by immunoblotting and immunofluorescence. We tested whether p53 activity was increased in TSP fibroblasts after DNA damage. Control and heterozygous TSC patient fibroblasts were exposed to UV light, and twenty-four hours later nuclear p53 was measured by immunofluorescence. The mean fluorescent intensity of p53 was significantly higher in *TSC2* heterozygous mutant fibroblasts compared to controls (Figure 2.4A, $p<0.01$). To test whether the increase in p53 was due to increased mTORC1 activity, we treated fibroblasts with the mTORC1 inhibitor rapamycin beginning 24 hours before and continuing 24 hours after UV challenge. Rapamycin treatment at concentrations near the IC_{50} (0.2 nM) decreased nuclear p53 levels in both control and TSP cells (Figure 2.4A, $p=0.008$). With rapamycin treatment, the p53 signal decreased in both wildtype and TSP cells, and in TSP cells was reduced to the level of untreated control cells (Figure 2.4A). This pattern is consistent with an interaction between *TSC2*, mTORC1 and p53.

To determine the impact of *TSC2* heterozygous mutations on the response to DNA damage, p53 levels in control and TSP fibroblasts were measured at 0, 8, 16, and 24 hours following UV challenge. p53 levels rapidly increased with TSP fibroblasts upregulating p53 significantly more relative to controls (Figure 2.4B, $p=0.035$, interaction). Tuberin protein levels were also significantly increased in response to UV challenge, consistent with previous studies (Figure 2.4B, $p<0.0001$, time) (Feng et al 2005, Feng et al 2007). However, the relative response was similar in both control and TSP fibroblasts, suggesting the wild-type copy of *TSC2* is appropriately upregulated in *TSC2* heterozygous mutant fibroblasts following UV exposure. To further assess p53 activity and function, we measured p21, a cyclin-dependent kinase inhibitor whose levels are regulated by p53. Levels of p21 increased post-UV challenge and TSP lines displayed increased p21 relative to controls (Figure 2.4B, $p=0.01$). mTORC1 signaling, as measured by phospho-S6 levels, showed a small initial increase at 8 hours before normalizing to pre-challenge levels; however, no difference between control and TSP lines was observed (Figure 2.4B). The activity of mTORC2, as measured by $pAkt^{Ser473}$, decreased following UV challenge but there was, again, no difference between control and TSP fibroblasts for genotype (Figure 2.4B). Degradation of p53 protein is tightly regulated by ubiquitination by MDM2, which is activated by phosphorylation at serine residue 166. There were no differences seen in $pMDM2^{Ser166}$ levels and it was appropriately upregulated in response to increased p53 levels in both controls and TSP lines (Figure 2.4B).

Phosphorylation of p53 at Ser15 by ATM, ATR and AMPK increases its stability and its activity (Loughery et al 2014). In order to measure phosphorylation of p53, it was necessary to enrich for nuclear protein extracts. Twenty-four hours post-UV challenge, nuclear and cytoplasmic extracts were isolated from control and heterozygous *TSC2* fibroblasts. Although the results were not significant, the overall pattern of increased p53 protein in the nucleus of *TSC2+/-* fibroblasts was consistent with what was observed by immunofluorescence and whole-cell extract immunoblot (Figure 2.5A, $p=0.247$). There was no significant difference in nuclear phospho-$p53^{Ser15}$ normalized to p53 or nuclear $pMDM2^{Ser166}$ (Figure 2.5B-C). However, each individual line was measured over multiple experimental replicates and the direction of the change in *TSC2+/-* fibroblasts was consistent across all experimental replicates. Interestingly, while there was no difference in phospho-$S6^{Ser240/244}$ in whole cell extracts (Figure 2.4B), there was a significant increase in nuclear phospho-$S6^{Ser240/244}$ following UV challenge in heterozygous *TSC2* fibroblasts (Figure 2.5D, $p<0.05$). However, future studies are necessary to rule out a possible contribution of lysosomes, mitochondria or other organelles which may be segregating with the nuclear extraction

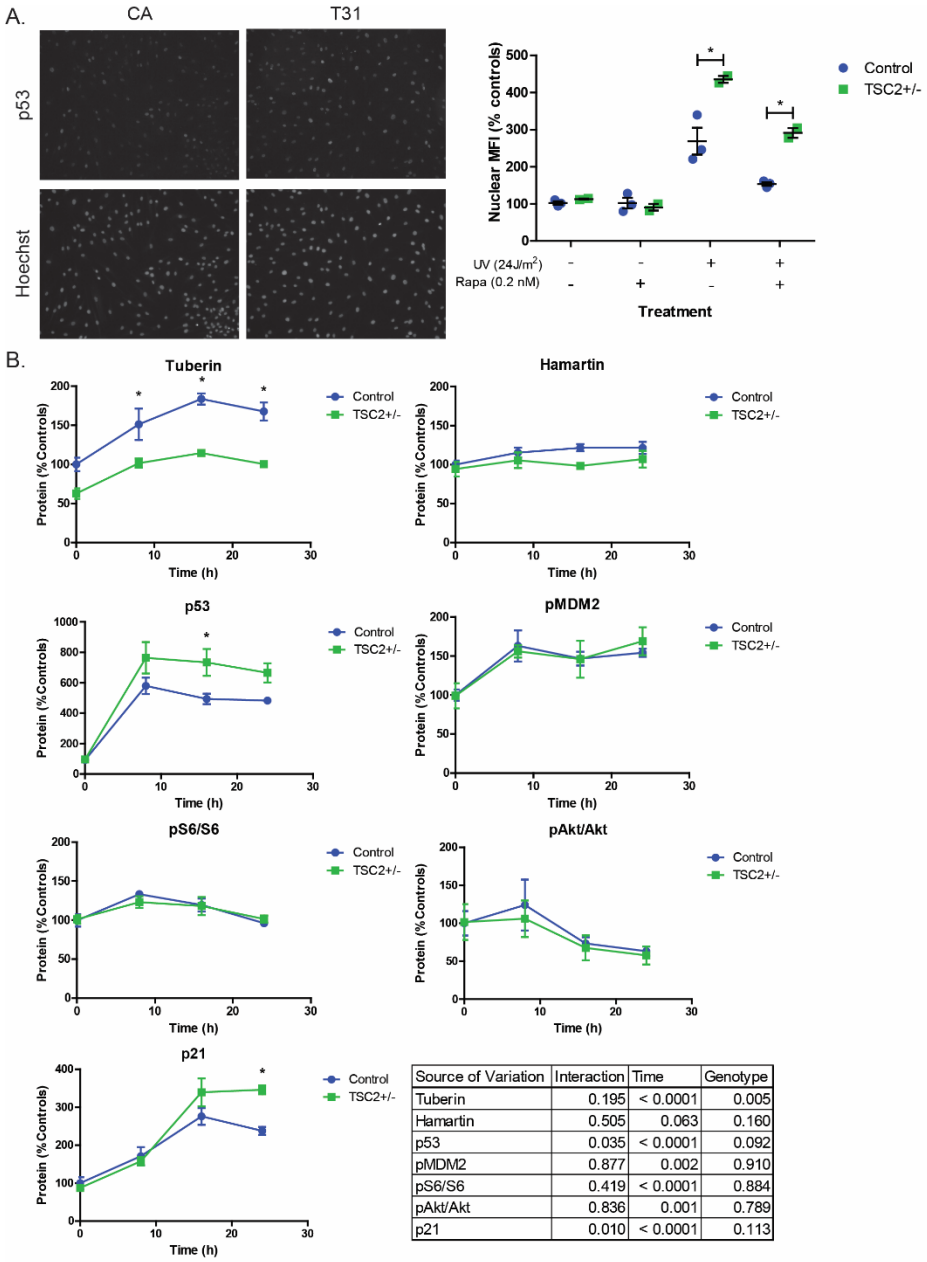

Source of Variation	Interaction	Time	Genotype
Tuberin	0.195	< 0.0001	0.005
Hamartin	0.505	0.063	0.160
p53	0.035	< 0.0001	0.092
pMDM2	0.877	0.002	0.910
pS6/S6	0.419	< 0.0001	0.884
pAkt/Akt	0.836	0.001	0.789
p21	0.010	< 0.0001	0.113

Figure 2.4 TSC patient fibroblasts display increased p53 in response to UV light.

(**A**) Three control and two TSC patient fibroblast lines were challenged with UV light and then immunostained for p53 24 hours later. Cells were treated with 0.2 nM rapamycin for 24 hours before and 24 hours after UV challenge. Mean fluorescent intensity of p53 was quantified in nuclei defined by Hoechst staining. Nuclear p53 was analyzed by two-way ANOVA in UV treated cells (n=2-3; interaction p=0.532, genotype p=0.012, rapamycin treatment p=0.008; Bonferroni post-test control UV vs TSP UV p<0.01). (**B**) Fibroblast lines were exposed to UV light and protein isolated at 0, 8 16, and 24 hours post-exposure was analyzed by immunoblot. (n=3, each patient average of 3-4 experimental replicates; two-way ANOVA values in table). See also Figure 5.1

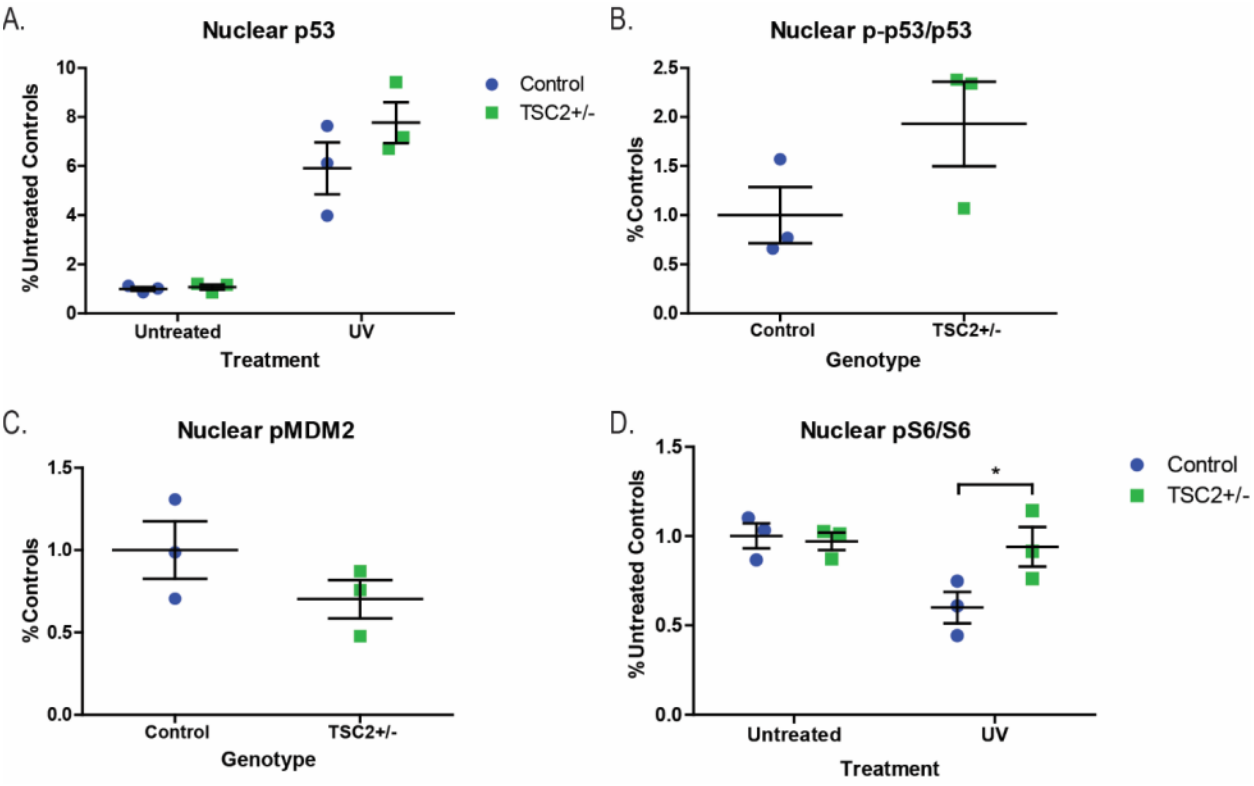

Figure 2.5. Changes in nuclear and cytoplasmic protein levels in TSC patient fibroblasts.

Fibroblasts were challenged with UV light and protein was isolated from nuclear and cytoplasmic compartments 24 hours later. Phospho-p53 ^{Ser15}, phospho-MDM2 ^{Ser166} and phospho-S6 $^{Ser240/244}$ proteins were quantified by immunoblot. (**A**) Total p53 protein normalized to total protein (n=3, average of 3 experimental replicates; interaction p=0.238, UV treatment p=0.001, genotype p=0.247, two-way ANOVA) (**B**) Phospho-p53 protein normalized to total p53 (n=3, average of 2 experimental replicates; p=0.146 t-test) (**C**) Phospho-MDM2 protein normalized to total protein (n=3, average of 2 experimental replicates; p=0.229 t-test) (**D**) Phospho-S6 normalized to total S6 (n=3, average of 2 experimental replicates; interaction p=0.088, UV treatment p=0.060, genotype p=0.135; Bonferroni post-test Control UV vs TSP UV p<0.05)

Impaired reprogramming and cell death in *TSC2* heterozygous mutant cells

p53 has been reported to be increased during cellular reprogramming, likely via the DNA damage pathway, and knocking down p53 enhances reprogramming efficiency (Hong et al 2009, Kawamura et al 2009, Li et al 2009, Marion et al 2009, Okita et al 2011). We hypothesized that the increased p53 levels seen in *TSC2* heterozygous mutant fibroblasts would impair reprogramming efficiency. To test this, we embarked on further rounds of reprograming using two control and three TSP fibroblast lines with either the same three programming plasmids used previously or by using the same genes except omitting the shRNA cassette directed against *TP53*. Three weeks following plasmid reprogramming, we stained the resulting iPSC colonies for alkaline phosphatase (AP) as a marker of pluripotency and quantified the number of positive AP colonies (Figure 2.6A). We expected the largest difference between controls and *TSC2+/-* cells to be in the lines reprogrammed without the sh*TP53* cassette; however, the reprogramming efficiency was too low in both groups to draw conclusions. We hypothesized that the addition of the sh*TP53* cassette would partially rescue the reprogramming efficiency of *TSC2+/-* fibroblasts, with the caveat that *TSC2+/-* lines would need to integrate the sh*TP53* plasmid and integration may be a rare event. Reprogramming efficiency was significantly reduced in *TSC2* heterozygous mutant fibroblasts compared to controls reprogrammed with sh*TP53* (Figure 2.6A, p=0.015). However, there was no significant difference between reprogramming efficiency of *TSC2+/-* fibroblasts with or without the sh*TP53* cassette (Figure 2.6A). We found reprogramming efficiency correlated inversely with the expected p53 levels: the number of AP^+ colonies was highest in control fibroblasts reprogrammed with the sh*TP53* and lowest in *TSC2* heterozygous mutant fibroblasts reprogrammed without the sh*TP53* plasmid. As AP is an early marker of pluripotency, we also picked and expanded several iPSC colonies from each experiment and stained them for the more mature stem cell marker TRA-1-60. We found TRA-1-60 positive colonies from all control and TSP lines reprogrammed with or without sh*TP53*.

Given the known role for p53 in regulating apoptosis, we next hypothesized that increased p53 in our TSP fibroblasts would lead to an increased rate of apoptosis. We first measured apoptosis in fibroblasts by Annexin V staining twenty-four hours after UV challenge. We found a significant increase in the percentage of Annexin V positive apoptotic cells in TSP fibroblast lines (Figure 2.6B, p<0.05). To determine whether mTORC1 signaling contributes to this finding we next treated fibroblasts with rapamycin for a total of 48 hours, starting 24 hours before UV challenge and 24 hours after. There was a significant interaction between rapamycin treatment and genotype (Figure 2.6C, p=0.012). Rapamycin had divergent effects on apoptosis in control and TSP fibroblasts. While rapamycin significantly increased apoptosis in control fibroblasts, there was no change, or perhaps even decreased, apoptosis in TSP fibroblasts (Figure 2.6C, p<0.05).

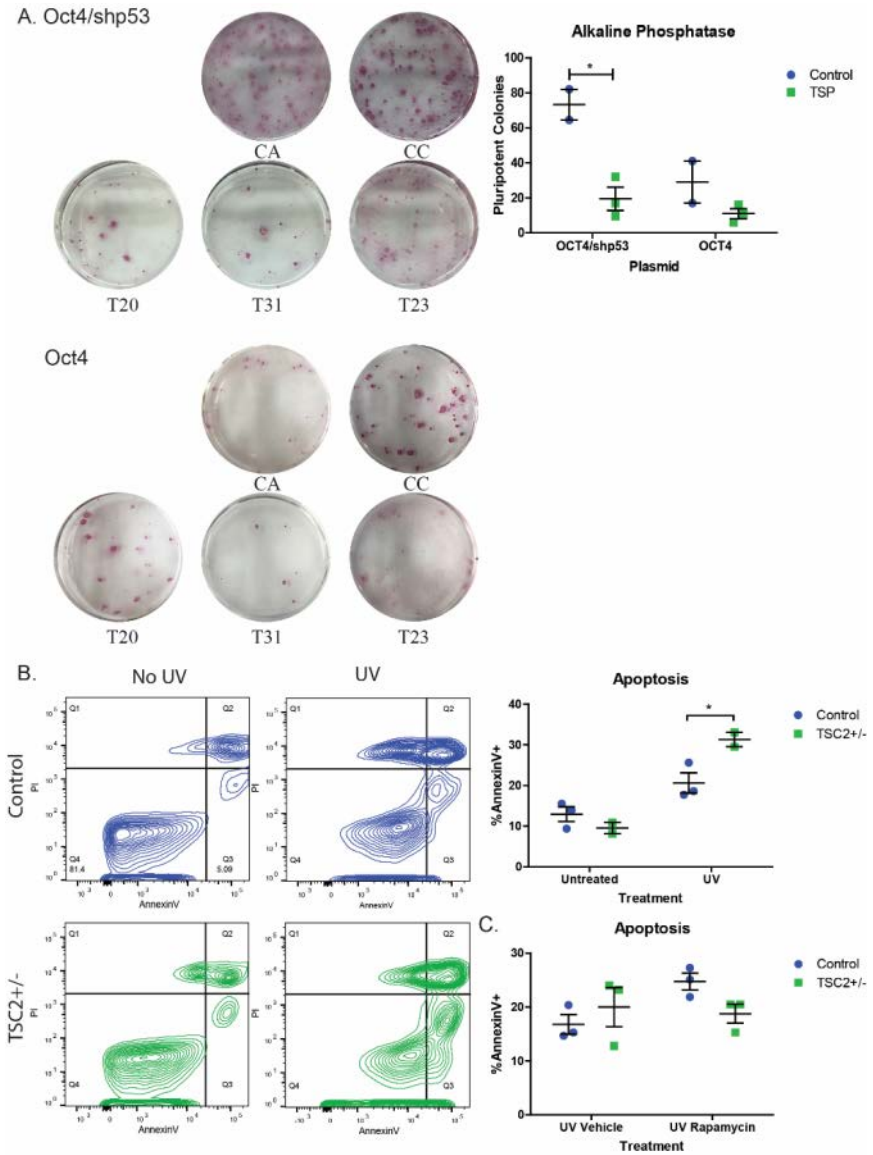

Figure 2.6. Impaired reprogramming and increased apoptosis in TSC patient fibroblasts.

(**A**) Control (CA, CC) and patient (T20, T31, T23) fibroblasts were reprogrammed with the three plasmids including either the Oct4 plasmid containing shRNA to *TP53* or the Oct4 plasmid alone. Pluripotent colonies were stained for alkaline phosphatase. Alkaline phosphatase positive colonies were counted using grey scale images in ImageJ (n=2 controls and 3 patients, average of 1-2 wells per individual; p=0.015, t-test). (**B**) Fibroblast lines were challenged with UV light and apoptosis measured by Annexin V staining by flow cytometry. Annexin V versus propidium iodide is plotted for untreated and UV challenged fibroblasts; control (blue) and TSP (green) samples have been combined for display purposes. (n=3 controls and 2 TSP, average of 2 experimental replicates; interaction p=0.048, genotype p=0.189, UV treatment p=0.007; Bonferroni post-test control UV vs TSP UV p<0.05). (**C**) Fibroblasts were treated with 0.2 nM rapamycin or DMSO for a total of 48 hours, starting 24 hours before UV challenge and ending 24 hours after. Apoptosis was measured by Annexin V staining by flow cytometry. (n=3, average of 2 experimental replicates; interaction p=0.012, genotype p=0.678, rapamycin treatment p=0.032; Bonferroni post-test Control Vehicle vs Rapa p<0.05).

Possible mechanisms of increased levels of p53 in *TSC2* heterozygous mutant cells

We next sought to determine the molecular mechanism of increased p53 protein in *TSC2* heterozygous mutant fibroblasts. We first measured *TP53* mRNA levels and found no increase in *TP53* mRNA at baseline (Figure 2.7A). We instead observed decreased *TP53* mRNA in TSP cells following challenge with UV light (Figure 2.7A, p=0.025). As alternative splicing results in multiple *TP53* isoforms (Marcel et al 2011), we designed primers for both the 3' end (Figure 2.7A) and the 5' end (Appendix Figure 5.2) of the full-length transcript and found similar results. As p53 is important in regulating multiple cell processes (including, DNA repair, apoptosis, cell cycle, and reactive oxygen species), we wondered whether the increase in p53 in the heterozygous *TSC2* fibroblasts represented activation of a specific p53 process. Using the same mRNA samples from UV treated fibroblasts we measured thirteen p53 target genes that were validated in multiple genome-wide data sets (Fischer 2017). Although none were significantly increased or decreased, the transcript that had the largest change in *TSC2+/-* fibroblasts was *GDF15* mRNA, a secreted member of the TGF-β superfamily previously shown to be increased in *TSC2-/-* hESC-derived neurons (Figure 2.7A, p=0.171) (Costa et al 2016). We next tested the stability of p53 protein by treating cells with the translation inhibitor cycloheximide. Fibroblasts were challenged with UV light 24 hours prior to treatment with cycloheximide and protein samples were taken before and after one hour of cycloheximide treatment. There was no difference in the relative protein remaining following treatment supporting a similar degradation rate of p53 protein in control and TSP fibroblasts (Figure 2.7C). Next, we used the protease inhibitor MG132 to inhibit degradation of p53 in order to isolate the contribution of translation to increased p53 protein levels. Control and TSP fibroblasts were treated with MG132 for four or eight hours post-UV challenge. There was no difference in p53 protein levels between patient and control fibroblasts (Figure 2.7D). To test whether p53 transcription/translation was increased at baseline in *TSC2+/-* cells we treated patient and control fibroblasts with MG132 for 6 hours without UV challenge and found no difference (Figure 2.7D). MG132 strongly increases p53 protein and we worried that a ceiling effect may be obscuring any differences between controls and *TSC2+/-*. To test this, we compared p53 protein with MG132 treatment alone to MG132 and UV challenge. The addition of UV challenge should further stimulate p53 activation pathways increasing p53 protein above proteasome inhibition alone. There was a significant increase in p53 protein levels in cells challenged with UV light and MG132 compared to MG132 alone, suggesting that MG132 treatment alone is not leading to a ceiling effect (Figure 2.7D p=0.02). The results of Figure 2.7D imply that the mechanism is increased p53 stability because when both groups are treated with the proteasome inhibitor MG132, there is no difference between the groups. However, at 8 hours post UV challenge the difference between controls and *TSC2+/-* cells was not significant (Figure 2.4B). Further, we cannot rule out the possibility that treatment with MG132 and UV challenge is increasing p53 to maximum levels and a ceiling effect is causing the lack of difference between controls and *TSC2+/-* fibroblasts. Finally, the more direct measurement of p53 stability using cycloheximide treatment did not find increased stability in *TSC2+/-* fibroblasts.

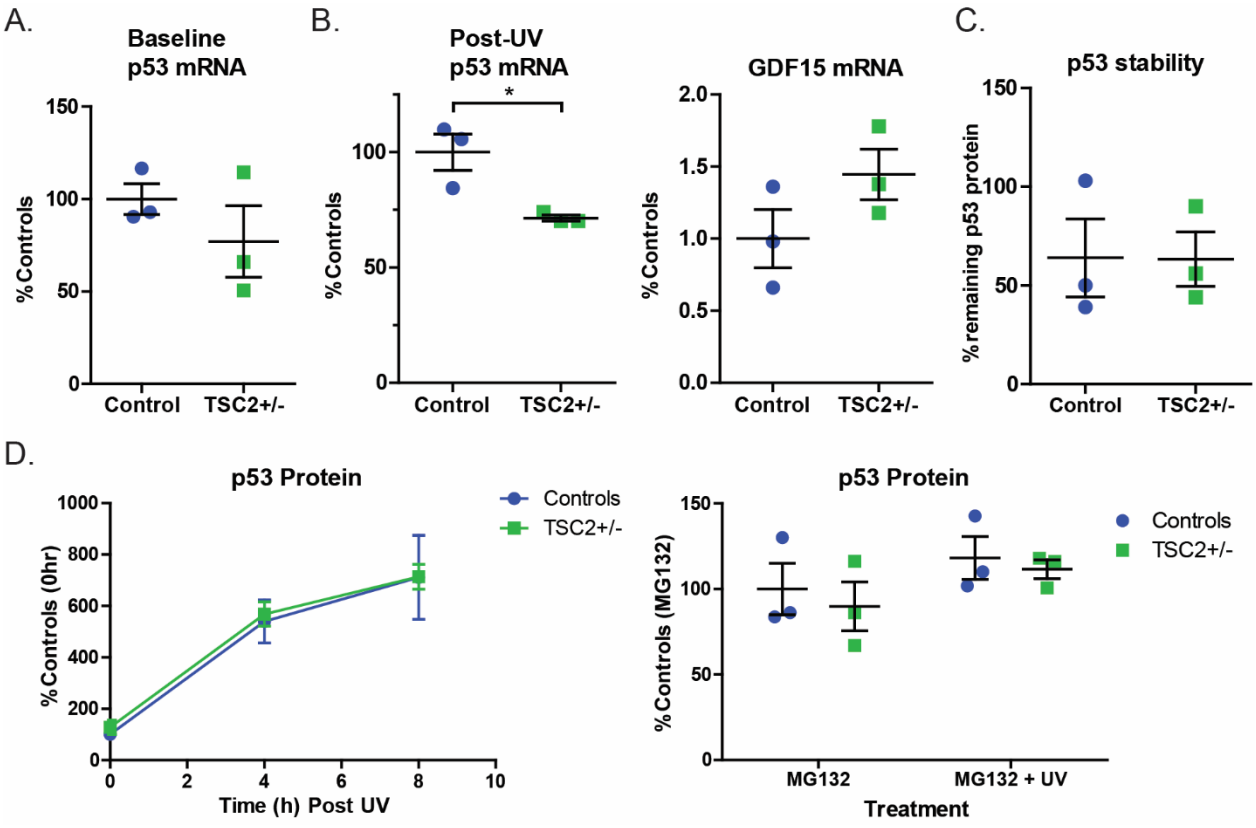

Figure 2.7. Stability, mRNA and translation of p53 in *TSC2*+/- fibroblasts.

(A) mRNA levels of *TP53* in fibroblasts were measured by qPCR at baseline using primers directed to the 3' end of the gene. Samples were normalized to *ACTIN* and *PGK1*. (*n*=3, 4 technical replicates; *p*=0.334, *t*-test) (**B**) Fibroblasts were challenged with UV light. Levels of *TP53* mRNA were measured twenty-four hours later by qPCR using primers directed to the 3' end (*n*=3, 4 technical replicates; *p*=0.023, *t*-test) Levels of *GDF15* mRNA (*n*=3, 4 technical replicates; *p*=0.171, *t*-test) (**C**) Fibroblasts were challenged with UV light and 15 hours later treated with the translation inhibitor cycloheximide (100 μM) for two hours. p53 protein levels were analyzed by immunoblot and normalized to p53 at time 0 for each individual (*n*=3). (**D**) Fibroblasts were treated with the proteasome inhibitor MG132 (1 μM) for 4 and 8 hours after UV challenge and p53 protein was measured by immunoblot (*n*=3). Fibroblasts were treated with MG132 (1 μM) for 6 hours with or without UV challenge. p53 protein levels were analyzed by immunoblot (*n*=3; interaction *p*=0.75, UV *p*=0.02, Genotype *p*=0.64, two-way ANOVA). See also Figure 5.2.

p53 is increased in *TSC2* heterozygous and homozygous mutant iPSCs

To confirm the interaction between tuberin and p53 was not limited to one cell type, we generated non-integrated *TSC2* heterozygous iPSC lines using Sendai viruses and measured p53 protein levels. Multiple iPSC clones from three controls and three TSC patients were treated with the DNA damaging agent neocarzinostatin. One of the control patients (CC) appeared to have lower p53 protein in both iPSC clones compared to the other controls leading to increased variability in the controls. p53 was significantly elevated in *TSC2* heterozygous mutant cells (Figure 2.8A, p=0.04). To further analyze the interaction between tuberin and p53, we also generated *TSC2* homozygous mutant human iPSCs using CRISPR-Cas9 technology (Mandegar et al 2016). At baseline, p53 is significantly elevated in *TSC2* homozygous mutant iPSCs compared to isogenic control lines (Figure 2.8B, p=0.03). *TSC2* homozygous mutant lines at baseline have unchanged phospho-S6, phospho-4E-BP1, and phospho-Akt^{Ser473} levels (Figure 2.8B). However, as iPSCs are maintained in mTeSR media that is nutrient-rich, these conditions likely do not reflect cell responses to changing stresses and metabolic demands. To address this point, we nutrient starved cells for 2.5 hours in DMEM without glucose or serum. Wildtype cells decreased mTORC1 signaling appropriately, reflecting a switch in cellular metabolism from anabolic to catabolic. In contrast, *TSC2* homozygous cells appeared unable to inhibit mTORC1 signaling with pS6 levels remaining high (Figure 2.8C, p=0.0002) However, when cells were starved in media without amino acids (HBSS), which signal to mTORC1 through Rag GTPases rather than tuberin/hamartin (Sancak et al 2008), both wildtype and *TSC2* homozygous mutant cells appropriately inhibited mTORC1 signaling (Figure 2.8C).

We were unable to find any change in p53 stability or translation/transcription in the heterozygous *TSC2* fibroblasts. However, because the fibroblasts required UV challenge to induce the p53 response it was difficult to appropriately time the cycloheximide or MG132 treatment with the UV treatment to detect a difference. However, *TSC2-/-* iPSCs eliminate this issue because they have increased p53 protein at baseline. We again measured p53 stability by cycloheximide treatment but found no difference between isogenic controls and *TSC2* homozygous iPSC lines (Figure 2.9A). Treatment with the protease inhibitor MG132 to isolate the contribution of transcription and translation to the p53 phenotype also did not reveal a difference between isogenic controls and *TSC2* homozygous iPSC lines (Figure 2.9B). Treatment of the iPSCs with the DNA damaging agent neocarzinostatin for 1-2 hours, increased p53 levels in both control and mutant lines. Homozygous mutant *TSC2* iPSCs displayed increased p53 levels relative to control lines (Figure 2.9C, p=0.04).

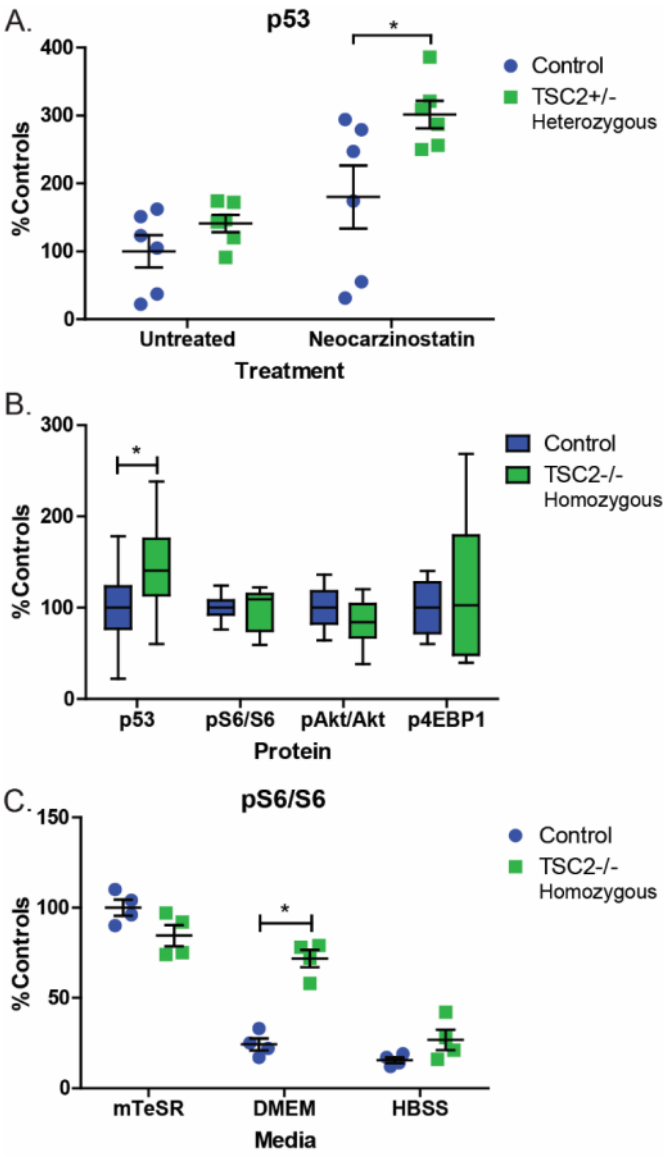

Figure 2.8. Increased p53 in heterozygous and homozygous *TSC2* mutant stem cells.

(A) Non-integrated iPSC lines generated from *TSC2* heterozygous patient fibroblast lines treated with the DNA damaging agent neocarzinostatin for 1 hour show increased p53 relative to controls. (n=6, 1-3 experimental repeats per sample; p=0.04 t-test) (**B**) Protein levels of p53 and mTORC1/mTORC2 related proteins were measured at baseline in homozygous knockout and control stem cells (n=14, 2 clones with 7 experimental repeats; p=0.03 t-test). (**C**) Homozygous *TSC2-/-* and isogenic control stem cells were nutrient starved for 2.5 hours in DMEM without glucose or HBSS media. Protein levels of pS6 were elevated in *TSC2-/-* iPSCs following nutrient starvation. (n=4, 2 clones with 2 experimental repeats; p=0.0002 t-test) See also Figure 5.3.

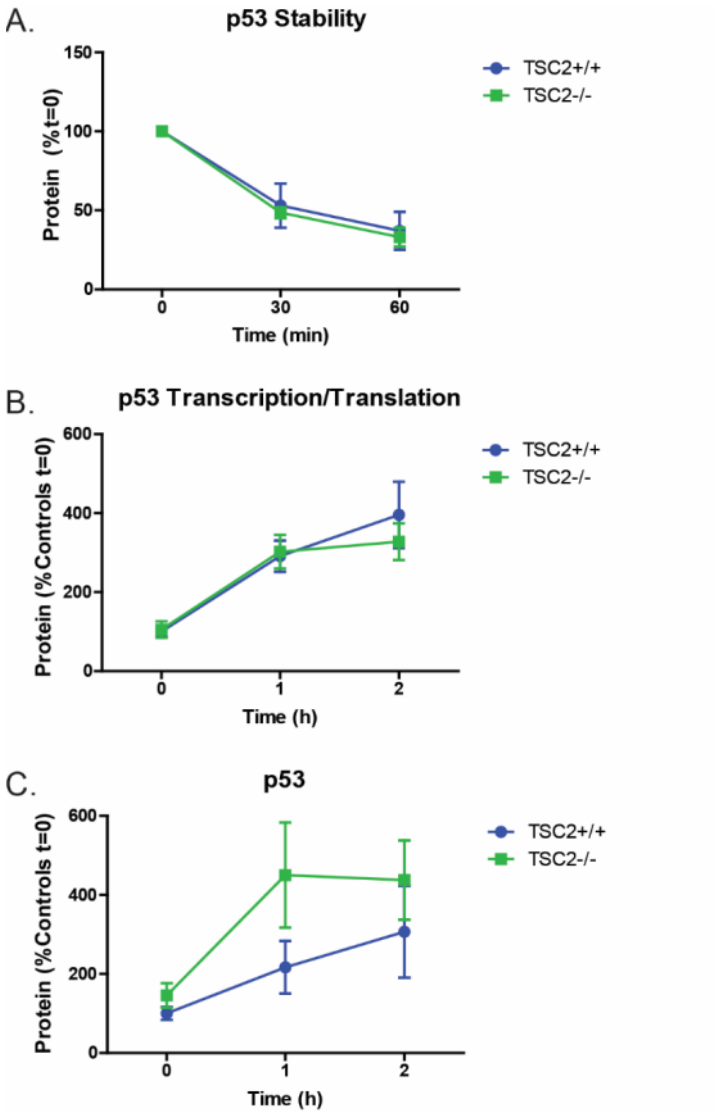

Figure 2.9. Stability, translation and DNA damage response in isogenic *TSC2*-/- stem cells.

(**A**) *TSC2*-/- and control iPSCs were treated with cycloheximide (100 μM) for 30-60 minutes and p53 was analyzed by immunoblot (*n*=4, 2 clones and 2 experimental replicates) (**B**) *TSC2*-/- and control iPSCs were treated with MG132 (1 μM) for 1-2 hours and p53 protein was analyzed by immunoblot (*n*=4, 2 clones and 2 experimental replicates). (**C**) iPSCs were challenged with DNA damaging agent neocarzinostatin for 1-2 hours. p53 protein levels were analyzed by immunoblot (*n*=4, 2 clones and 2 experimental replicates; interaction p=0.65, genotype p=0.039, treatment p=0.056 two-way ANOVA).

Discussion

Our initial intent was to generate heterozygous and homozygous *TSC2* mutant iPSCs from TSC patient fibroblasts to study the impact of gene dosage on somatic cell reprogramming and subsequent differentiation to various lineages impacted in TSC. This approach was designed to study the current favored "two hit" model of TSC where the initial genetic event is a germline mutation in either *TSC1* or *TSC2* followed by a second somatic mutation in the other allele of *TSC1* or *TSC2*. This model predicts that normal appearing tissues in patients with TSC to be heterozygous whereas any TSC associated focal abnormalities including skin lesions to be due to homozygous mutations. Despite deep sequencing of multiple primary lines, we were unable to find any homozygous mutant fibroblasts; all lines studied had only heterozygous mutations of *TSC2* and tuberin was clearly present albeit reduced. Consistent with genotyping results, no difference in mTORC1 signaling was observed in patient fibroblast cells. This suggests that homozygous fibroblasts do not survive during the transition to fibroblast culture or do not contribute significantly to hypopigmented macules or Shagreen patches. A recent publication reported that focal areas of hypopigmentation in patients with TSC result from loss of heterozygosity in melanocytes rather than fibroblasts (Cao et al 2017).

Unexpectedly, by reprogramming *TSC2* patient derived fibroblasts to make iPSCs, we also found strong evidence for an important role for p53. This supports a model of *TSC2* haploinsufficiency contributing to cell dysfunction and clinical manifestations. Previous reports support a connection between loss of *TSC1* or *TSC2* and increased p53, but the nature of this interaction remains unclear. Potential mechanisms include S6 kinase mediated phosphorylation and inhibition of MDM2, decreased Akt mediated phosphorylation and activation of MDM2, increased translation of MDM2-inhibitor ARF, or increased p53 translation or transcription (Goudarzi et al 2014, Lai et al 2010, Lee et al 2007, Miceli et al 2012, Ogawara et al 2002). The mTOR/p53 pathways may act together within a negative feedback loop where increased mTORC1 leads to increased p53 and sensitivity to DNA damage in proliferating cells. Completing this potential feedback loop, increased p53 activity in response to DNA damage or other cellular stress may inhibit mTORC1 to decrease the potential for excessive proliferation. Fibroblasts increase tuberin levels in response to DNA damaging agents; however, in the presence of a heterozygous mutation in *TSC2*, p53 levels increased above the usual response seen in control cells, suggesting that this critical feedback loop is disrupted. This may then contribute to one paradox seen in TSC, that despite having mutations in the mTORC1 pathway, cancer is very rarely seen.

Interestingly, the mTORC1 inhibitor, rapamycin, had diverging effects on apoptosis in control and TSP fibroblasts. Apoptosis was significantly increased in control fibroblasts while apoptosis was unchanged or decreased in TSP fibroblasts. Although loss of *TSC2* or *TSC1* sensitizes cells to cell death (Habib et al 2011, Lee et al 2007, Miceli et al 2012, Pai et al 2016, Zhang et al 2003), the effect of rapamycin on apoptosis and p53 is more complicated and appears to be cell type specific (reviewed in (Castedo et al 2002)). Our results suggest that rapamycin sensitizes cells to apoptosis in wildtype fibroblasts but in the setting of heterozygous loss of *TSC2*, which already have increased apoptosis, there is no change with rapamycin treatment.

The mTORC1 inhibitor, rapamycin, inhibited p53 accumulation following DNA damage, supporting an interaction between these two pathways. Although, no difference in mTORC1 signaling was observed in heterozygous fibroblasts at baseline, we did observe increased phospho-S6 in the nucleus following UV challenge. This suggests that differences in mTORC1 may be localized to subcellular compartments and require environmental/nutrient stresses. Following ribosomal stress and nucleolar breakdown, binding of ribosomal proteins to MDM2 leads to inhibition of MDM2 and stabilization of p53 protein (Boulon et al 2010). It is possible that heterozygous *TSC2* fibroblasts have localized changes in mTORC1 signaling in the nucleus that is sufficient to alter ribosomal dynamics and inhibit MDM2.

Tuberin and p53 may intersect in multiple ways; however, we did not find a significant increase in p53 stability, p53 transcription/translation, or *TP53* mRNA levels in *TSC2* heterozygous mutant cells. Some of these changes may simply be below the sensitivity of current methods of detection. As treatment with MG132 induces other stress pathways and *TSC2* homozygous mutant cells in general appear to be more sensitive to ER stress via proteasome inhibition (Kang et al 2011), it is possible that these other functions are obscuring any difference in p53 transcription or translation between controls and TSC patient cells. In the future, translation can be measured more directly using polysome profiling or radioactive labeling of proteins. Interestingly, we observed a decrease in *TP53* mRNA levels in *TSC2* heterozygous mutant fibroblasts compared to controls following UV exposure. There is conflicting evidence for p53 autoregulating its own transcription either positively or negatively (Benoit et al 2000, Deffie et al 1993, Ginsberg et al 1991, Hudson et al 1995). Our observation of inversely correlated patterns of *TP53* mRNA and protein levels with heterozygous loss of *TSC2* is most consistent with negative autoregulation.

Relative levels of p53 during reprogramming tightly correlate with reprogramming efficiency; knocking down or knocking out p53 enhances formation of pluripotent colonies while activating p53 with the pharmacological agent Nutlin inhibits reprogramming (Hong et al 2009, Kawamura et al 2009). However, permanent loss of p53 enhances reprogramming at the expense of later genomic instability (Marion et al 2009). The addition of shRNA to *TP53* to the episomal plasmids attempts to circumvent this issue by transiently knocking down p53 only during reprogramming. Then, with the expected loss of episomal plasmids during cell division, p53 levels are restored to normal levels following the reprogramming process. We found reprogramming efficiency correlated inversely with the theoretical levels of p53 in our fibroblasts, which was consistent with previous publications demonstrating increased reprogramming efficiency with knock-down or mutation of p53. However, the shRNA against p53 was not sufficient to completely rescue the TSC reprograming phenotype. We hypothesize that knock-down of p53 is required in *TSC2+/-* cells beyond the first few days of reprogramming. The percent of cells that have lost the plasmids increases from 32% by week 1 post-transfection to 72% by week 2 and finally 95% by week 3 (Okita et al 2011). If survival and reprogramming is impaired in cells that do not have continued knock-down of p53 and integration is a sufficiently rare event then this could account for the differences we see in heterozygous *TSC2* fibroblasts. However, we have not ruled out p53-independent mechanisms of decreased reprogramming efficiency in *TSC2+/-* fibroblasts. The transition of fibroblasts from partially reprogrammed cell to stable stem cell is regulated by a complicated network of changes and there are p53-independent interactions between the reprogramming factors and mTORC1 (Wang et al 2013, Wu et al 2015). Future studies will be necessary to dissect the contribution of *TSC2* to each stage of reprogramming and stem cell maintenance. One previous study of integration in episomally reprogrammed iPSCs observed that even wildtype fibroblasts had an increased tendency to integrate the *OCT4*/sh*TP53* plasmid over the other two plasmids, likely due to a growth advantage conferred by continued inhibition of p53 (Schlaeger et al 2015). We hypothesize that a similar mechanism is occurring in heterozygous cells but at a higher rate due to increased p53 in TSC patient-derived cells.

While a circuitous route was required to finally generate them, we now report the first generation of isogenic iPSCs with homozygous knock-out of the *TSC2* gene. Using CRISPR-Cas9 to generate isogenic lines, we were able to confirm that loss of tuberin leads to increased p53, both at baseline and in response to DNA damage. Further, we used a non-integrating Sendai viral method to reprogram heterozygous TSP fibroblasts to iPSCs. Using heterozygous TSP Sendai generated iPSCs, we were also able to confirm that the increased p53 seen in patient fibroblasts in response to DNA damage also applied to the pluripotent stem cell state.

Finally, our results suggest that loss of one copy of *TSC2* is sufficient to alter the cellular response to DNA damage and stress during reprogramming. The increased apoptosis in TSP derived lines then may further explain why cancer is quite rare in TSC and why any malignant transformation is

usually associated with p53 deletion (Habib et al 2011, Hayashi et al 2012). We further speculate that the increased rate of apoptosis may clarify why neural cells with second hits are either very rare or undetectable in the cortical lesions, (tubers) of patients with TSC. p53 also affects neural stem cell differentiation and self-renewal (Jacobs et al 2006, Li et al 2016, Meletis et al 2006, Mendrysa et al 2011, Tedeschi and Di Giovanni 2009) and we further hypothesize that even small disruptions in p53 pathways, like those seen in our heterozygous cells, could alter neural development. Future studies will address regulation of cell death and neural development by gene dosage and non-cell-autonomous effects using control, heterozygous and now homozygous mutant *TSC2* stem cell lines.

Materials and Methods

Statistics

All statistical analyses were conducted using GraphPad PRISM. Individual patient fibroblast lines or iPSC clones are treated as independent *n*. All other experimental or technical replicates are considered not independent and are averaged to obtain the final value for each patient clone/line. Four isogenic clones (two *TSC2+/+*, two *TSC2-/-*) were generated using CRISPR-Cas9. For experiments involving isogenic lines, both experimental and clone replicates are considered independent repeats and are shown in the data.

Cell Culture and Stem Cell Reprogramming

Fibroblasts were isolated from control volunteers (male, age 24 years, CA; female, age 18 years, CC; male, age 25 years, CX) or TSC patients (female, ages 2-12 years, Table 1.2) from normal-appearing skin and TSC associated skin lesions (Shagreen patches or hypopigmented macules). Fibroblasts were cultured in DMEM with 10% FBS, 1% non-essential amino acids, and 1% pen-strep.

Fibroblasts were reprogrammed by transfection of cells using the Neon system (Invitrogen) with plasmids expressing *KLF4*, *SOX2*, *OCT4*, *L-MYC* and *LIN28* with or without shRNA to *TP53* (Addgene #27076, 27077, 27078, 27080) according to previously published protocols (Okita et al 2011). Cells were switched to TeSR-E7 media (StemCell Technologies) 48 hours post-transfection. Three weeks post-transfection, some cultures were stained for alkaline phosphatase expression following fixation with 2% paraformaldehyde (Millipore SCR004). Pluripotent colonies positive for alkaline phosphatase were quantified in ImageJ (ver1.50e) by analyzing greyscale images, setting a threshold for positive staining, and counting the number of colonies with area ≥2 pixels (Schindelin et al 2012). Concurrently colonies from parallel plates were picked and transferred to Matrigel treated plates and grown in mTeSR1 media (Corning; StemCell Technologies). Sendai reprogramming was performed using the CytoTune iPS 2.0 Sendai Kit (ThermoFisher) in feeder-free conditions according to manufacturer's instructions. Nascent stem cells were passed to Matrigel and grown in mTeSR after one week.

Protein Stability and Translation

For p53 stability and translation analyses, cells were treated with 100 μM cycloheximide (Sigma 7698) or 1 μM MG132 (Millipore 474790). Appropriate doses were determined by in-cell Western assay to measure the dose at which puromycin incorporation into the nascent transcript was inhibited or p53 was stabilized.

Sequencing

Mutation screening of TSC fibroblast samples was performed using highly redundant exome sequencing in candidate genes. Genomic DNA was isolated and sheared; then exon-containing DNA was captured using SureSelect XT (Agilent). Next generation sequencing was done on an Illumina HiSeq2000 (Solexa) through the Vanderbilt Genome Sciences Resource. Variants were submitted to the *TSC2* Leiden Open Variant Database (http://www.LOVD.nl/TSC2). Confirmatory sequencing was performed on DNA or RNA isolated from fibroblast cultures using QuickExtract Buffer (epicentre) or Qiagen RNeasy or Invitrogen PureLink RNA kits. RNA was converted to cDNA using random hexamers and ThermoScientific Superscript First-Strand Synthesis Kit. PCR amplicons were isolated using QiaQuick PCR Purification Kit.

Quantitative PCR

RNA was isolated from fibroblast cultures as above and converted to cDNA. Quantitative PCR was performed using Life technologies SYBR Green Master Mix and run on a QuantStudio real-time qPCR machine through the Vanderbilt VANTAGE Core. Samples were run in duplicate or quadruplicate technical replicates and normalized to levels of *ACTIN* and *PGK1*.

Stem Cell Validation

Integration was assessed in cell lines after ≥10 passages post-reprogramming using primers for the WPRE and EBNA segments of the Yamanaka reprogramming plasmids.(Okita et al 2011) Primers immediately flanking the *shTP53* segment were used to distinguish between the three plasmids; presence or absence of the sh*TP53* plasmid was determined based on the size of the amplified fragment.

Pluripotency was assessed by the ability to differentiate to all three germline lineages using the hPSC Taqman Scorecard (ThermoFisher A15870). iPSCs were differentiated as embryoid bodies for one week in DMEM/F12 glutamax with 20% knockout serum replacement, non-essential amino acids and 55 μM β-mercaptoethanol. RNA was then isolated and converted to cDNA using the High-capacity Reverse Transcription Kit (ThermoFisher 4374966). Samples were analyzed by qPCR on the Applied Biosystems 7900HT through the Vanderbilt VANTAGE Core.

Karyotype analysis was performed using standard techniques (Genetics Associates, Inc. Nashville, TN).

Immunoblotting

Protein was isolated by lysing and scraping cells in RIPA buffer plus protease inhibitor cocktails 2 and 3 and phosphatase inhibitor cocktail (Sigma P5726, P0044, P8340). Samples were rotated for 30 minutes at 4°C, sonicated and then run on 4-12% NuPAGE BisTris gels in MOPS buffer. Gels were transferred to PVDF membrane at 95V for 90 minutes using the Bio-Rad Mini Trans-Blot Cell. Membranes were incubated overnight in primary antibody diluted in 5% BSA. Membranes were then incubated for 1 hour at room temperature in secondary antibody and imaged on an Odyssey Li-Cor machine. Samples were normalized to actin or to total protein measured using Li-Cor REVERT stain. To

control for intra-experimental differences in antibody concentration and Odyssey machine settings, normalized values are expressed as a percentage of the controls before averaging experimental replicates.

Nuclear-cytoplasmic extractions were performed using the NE-PER Kit according to manufacturer's instructions (ThermoFisher 78833).

Immunofluorescence

Cells were fixed in 4% paraformaldehyde for 20 min at room temperature, followed by 3x 5-minute PBS washes. For intracellular antibodies, cells were then permeabilized with 0.1% Triton in PBS for 20 minutes at room temperature and blocked in 0.1% Triton plus 5% normal goat serum for 1 hour at room temperature. For extracellular antibodies, cells were blocked in 5% normal goat serum for 1 hour at room temperature. Cells were then incubated in primary antibody rocking overnight at 4°C. Following 5x 10-minute PBS washes, cells were incubated with secondary antibody for 3 hours at room temperature.

Nuclear p53 was measured by immunofluorescence followed by analysis of images with ImageJ (Schindelin et al 2012). A nuclear mask was generated using Hoechst staining and mean fluorescent intensity of p53 was measured using the outlines.

DNA Damage

Primary fibroblasts were passed to 6 well plates at 100,000 cells per well or 96 well plates at 5,000 cells per well. Plates were then exposed to ~24 J/m^2 (30 seconds of UV light G51T8 bulb 4.9 Watts with wavelength 254 nm at a distance of approximately 0.706 meters). Analyses were conducted twenty-four hours later unless otherwise noted. iPSC lines were treated with 50 ng/ml of neocarzinostatin for 1-2 hours. Optimal neocarzinostatin doses were determined using a dose-response curve measured by in-cell Western assay for p53 response.

Flow Cytometry

Single cell suspensions of fibroblasts were obtained by trypsinizing adherent cells and collecting supernatant, followed by filtration through a 40 μm filter. Cells were then counted, stained with 5 μl Annexin V (AF488, ThermoScientific A1320) and 0.5 μl of 1 mg/ml propidium iodide (Sigma P4864) per 10^5 cells and immediately analyzed by flow cytometry. Cells were gated to exclude debris and doublets.

CRISPR

Doxycycline-inducible Cas9 iPSCs were generated and donated by the Conklin lab (Mandegar et al 2016). Cells were treated with 2 μM doxycycline for 24 hours prior to lipofection with Alt-R crRNA:trRNA complexes (IDTDNA). Guide sequences were designed using the online Zhang Lab CRISPR Design Tool (Hsu et al 2013). Guide RNA mixed with lipofectamine (1.5 μl 3 μM crRNA:trRNA, 0.3 μl lipofectamine 3000, 48.2 μl Opti-MEM) was added to a 96 well plate coated in Matrigel. Doxycycline-treated cells were isolated with Accutase and 40,000 cells were then added to each well. Two days later cells were expanded to a 6 well plate for subsequent colony picking or DNA isolation for T7 endonuclease analysis.

CHAPTER III

STEM CELL DYNAMICS AND SIGNALING IN PLASMID-INTEGRATED *TSC2+/-* IPSCS

Abstract

Functioning mTORC1 activity is critical for stem cell self-renewal and differentiation. However, it is unknown what effect heterozygous loss of *TSC2* would have on the stem cell state, and, further, how integration of the *OCT4/*sh*TP53* plasmid would affect this phenotype. *We hypothesized that the shRNA to p53 would be expressed and functioning leading to increased cell proliferation and survival but that heterozygous loss of TSC2 would not further alter stem cell dynamics.* Using non-integrated and integrated controls and TSP plasmid-reprogrammed human iPSCs we measured cell proliferation and mTORC1 signaling. However, while we confirmed increased cell proliferation in integrated lines, we were surprised to find decreased pluripotent stability and increased MEK1/2 signaling. Further, these changes were observed in integrated TSP lines but not integrated controls, suggesting an interaction between decreased p53 and decreased *TSC2* in the stem cell state.

Introduction

As described in previous chapters, TSC is a developmental disorder causing benign hamartomas in multiple organ systems. Several of the hamartomas, cortical tubers and cardiac rhabdomyomas, are detectable in TSC patients as early as 20 weeks of gestation suggesting an important role for hamartin and tuberin in early prenatal development (Muhler et al 2007, Northrup and Krueger 2013, Park et al 1997, Prabowo et al 2013, Tsai et al 2014). To better understand the impact of *TSC2* loss on development, we generated induced pluripotent stem cells (iPSCs) using human dermal fibroblasts obtained from TSC patients and control volunteers. We reprogrammed primary fibroblasts using established episomal methods employing three plasmids expressing *OCT4*, *KLF4*, *SOX2*, *L-MYC*, *LIN28*, and a shRNA knockdown targeted to *TP53* (Okita et al 2011). In Chapter II we showed that loss of one copy of *TSC2* is sufficient to increase p53 levels and inhibit reprogramming to iPSCs. These results indicate critical interactions between hamartin/tuberin, mTOR, and p53 to regulate stem cell reprogramming, cell maintenance, and cell death. mTOR regulation is critical to stem cell biology; loss of mTOR prevents mouse embryonic stem cells from growing *in vitro* and excess mTOR activity leads to inhibition of self-renewal and exhaustion of mouse hematopoietic stem cells (Chen et al 2008, Gangloff et al 2004, Murakami et al 2004). In human embryonic stem cells, treatment with the mTORC1 inhibitor rapamycin decreased expression of pluripotent proteins Nanog, Sox2 and Oct4 (Zhou et al 2009). Further, rapamycin treatment during embryoid body differentiation enhanced mesoderm/endoderm protein expression and decreased ectoderm protein expression (Zhou et al 2009). Large increases and decreases in mTORC1 activity alters stem cell biology, but it is unclear what effect heterozygous mutations in *TSC2* will have on human stem cells or how the mutations will interact with integration of the *OCT4*/sh*TP53* plasmid. We hypothesized that integration of the shRNA to p53 will decrease p53 protein leading to increased cell proliferation and survival, but this will affect both controls and TSP integrated lines. We confirmed increased cell proliferation and survival in integrated lines but, surprisingly, found evidence for an interaction between *TSC2* mutations and knockdown of p53 in the maintenance of pluripotency.

Results

To model neurodevelopment in TSC we generated induced pluripotent stem cells from patient and control volunteer fibroblasts using reprogramming plasmids. The reprogramming plasmids are expected to remain episomal and not integrate into the transfected cell genome. The plasmids are unable to be replicated and they should be lost following reprogramming as the cells continue to divide. However, as there is a chance that the plasmids will become integrated into the genome, all iPSC lines were checked for continued presence of the plasmids by PCR. Control lines had the expected low rate of integration, consistent with previous publications. However, iPSC lines from TSC patients integrated the plasmids at a significantly higher rate (Chapter II, Figure 2.3). Interestingly, the only plasmid the TSC lines integrated was the *OCT4*/*shTP53* plasmid. In the previous chapter we showed that TSP fibroblasts have increased p53 potentially driving selection of colonies integrating the shRNA to p53.

First, we wanted to confirm that the integrated *TSC2*+/- iPS lines had decreased tuberin expression and that the integration event was not altering tuberin mRNA or protein. We did observe a significant decrease in *TSC2* mRNA, however, the reduction in tuberin protein in integrated *TSC2*+/- iPSCs did not quite reach significance (Figure 3.1A p=0.004, 3.1B, p=0.06). One line, T21-3, was generated from fibroblasts with a frameshift mutation in *TSC2* which should result in a stop codon eight amino acids later. However, this iPS line had no change in tuberin protein (106.7% controls) or mRNA (101.6% controls). The frameshift mutation likely causes formation of abnormal tuberin protein rather than nonsense mediated decay; as such, this line has been excluded from Figure 3.1.

Although we did not find any differences in mTORC1 expression in fibroblasts with heterozygous loss of *TSC2,* we wondered whether the stem cell state would prove more sensitive to heterozygous loss of tuberin than the terminally differentiated fibroblasts. To measure mTORC1 activity we quantified phospho-S6 levels by immunoblot. Surprisingly, integrated *TSC2*+/- iPSC lines had decreased mTORC1 activity rather than increased (Figure 3.1C). Control integrated iPS lines also had decreased mTORC1 activity. These results suggest that although integration of the OCT4/shp53 does not alter tuberin protein or mRNA, it is inhibiting mTORC1 activity.

If the TSC iPSCs are integrating the shp53 plasmid in order to overcome increased levels of p53 protein, then we would expect that the plasmid would need to be integrated in such a way that the shRNA continues to be expressed. To determine whether the integrated shp53 was functioning, we measured p53 protein levels in control and integrated TSP iPS lines. All but one (T8-22) of the integrated iPSC lines had decreased p53 protein levels compared to non-integrated controls, suggesting that the shRNA is still expressed in the integrated iPSC lines. Overall, p53 protein levels in integrated TSP lines averaged 65% of non-integrated controls; however, the difference did not reach significance because of the outlier T8-22 (Figure 3.2A, p=0.11). A recent report showed that human stem cells acquire mutations in p53 in culture (Merkle et al 2017). We wondered whether the TSP outlier, T8-22, had acquired a mutation in p53 such that it continued to express p53 protein but in a mutated form, effectively circumventing the need for *shTP53*. To test this, we sequenced p53 in T8-22 at sixteen of the most common “hot spots” acquired in iPSC culture; however, we did not find evidence of any p53 mutations.

In order to obtain non-integrated TSP iPSCs, we reprogrammed three fibroblast lines with heterozygous *TSC2*+/- mutations, T20, T23 and T31, using the Sendai viral method. In contrast to integrated plasmid-reprogrammed TSP iPSCs, p53 protein levels at baseline were unaltered in Sendai-reprogrammed TSP iPSCs (Figure 3.2B and Chapter II Figure 2.8A). Sendai-reprogrammed iPSCs also had decreased tuberin protein but did not have any change in mTORC1 activity (Figure 3.3A-B). This supports the hypothesis that it is integration of the OCT4/shp53 plasmid causing decreased p53 protein in iPSCs.

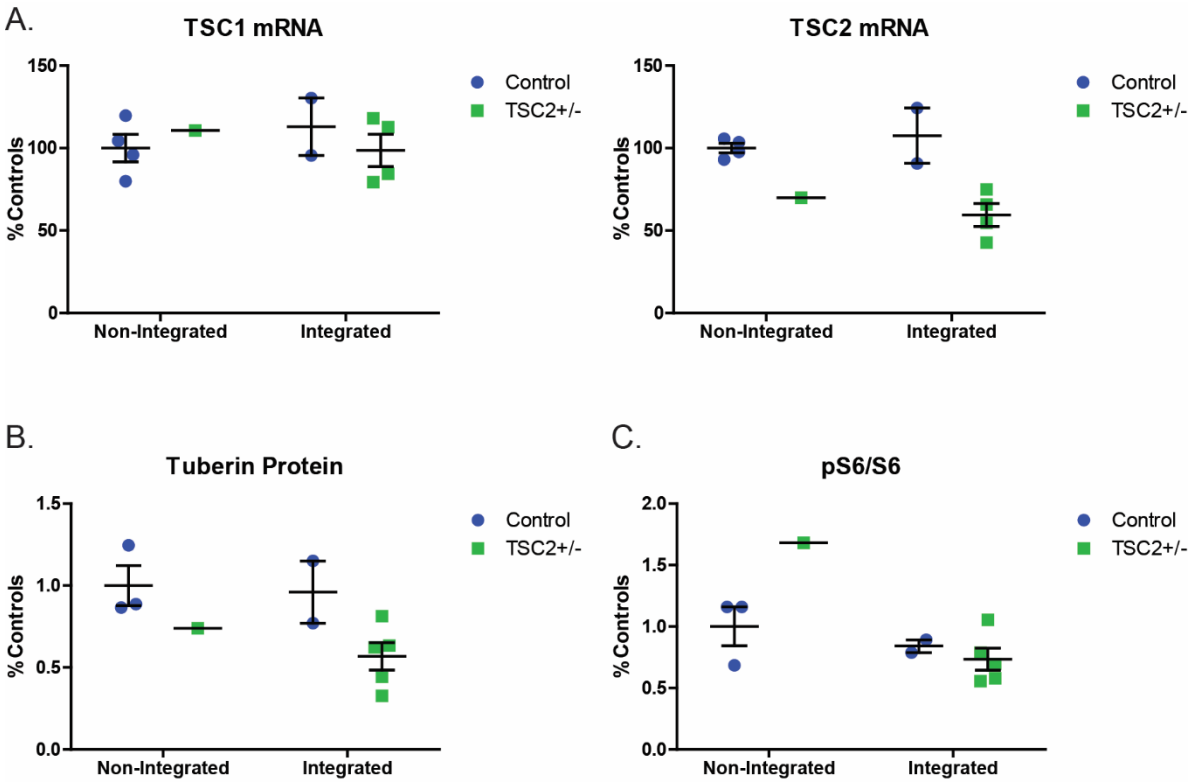

Figure 3.1. Heterozygous nonsense mutations in *TSC2* result in reduced *TSC2* mRNA and tuberin protein levels in plasmid-reprogrammed iPSCs.

(A) *TSC1* and *TSC2* mRNA quantified by qPCR in control and TSP iPSCs (*n*=2-4 average of four technical replicates; *TSC2* mRNA interaction *p*=0.37, genotype *p*=0.004, integration *p*=0.88 two-way ANOVA) (**B**) Protein was isolated from plasmid-reprogrammed control and TSP iPSCs and analyzed by immunoblot for tuberin protein (*n*=1-5, average of 2-3 experimental replicates; interaction *p*=0.67, genotype *p*=0.06, integration *p*=0.50 two-way ANOVA) (**C**) mTORC1 signaling measured by phospho-$S6^{Ser240/244}$ normalized to total S6 (*n*=1-6, average of 3-5 experimental replicates; interaction *p*=0.04, genotype *p*=0.10, integration *p*=0.008 two-way ANOVA)

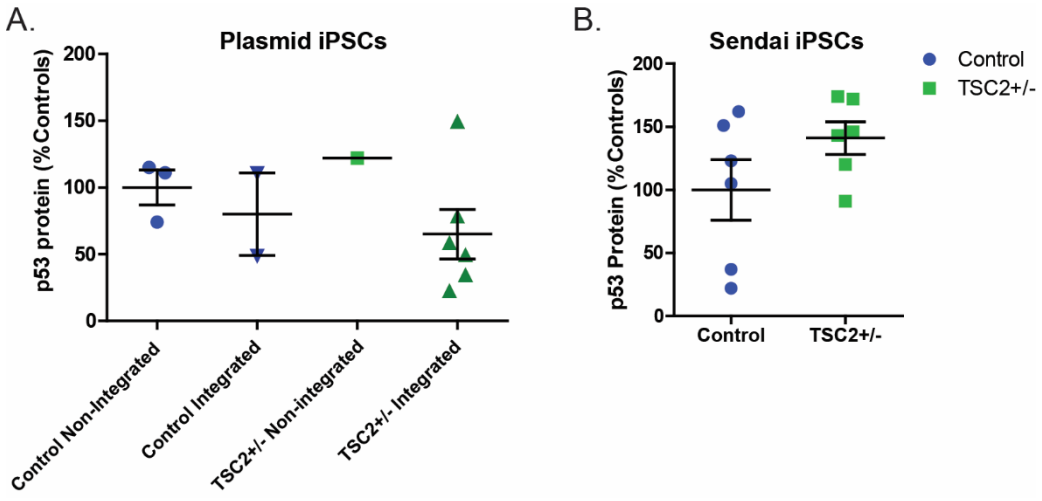

Figure 3.2. p53 protein expression in integrated TSP iPSCs.

(**A**) Protein was isolated from plasmid-reprogrammed control and TSP iPSCs and analyzed by immunoblot for p53 protein (n=1-6, average of 3-4 experimental replicates per clone; interaction p=0.43, genotype p=0.91, integration p=0.11) (**B**) Non-integrated iPSC lines generated from *TSC2* heterozygous patient and controls were analyzed by immunoblot for p53 protein (n=6, average of 1-3 experimental replicates per clone)

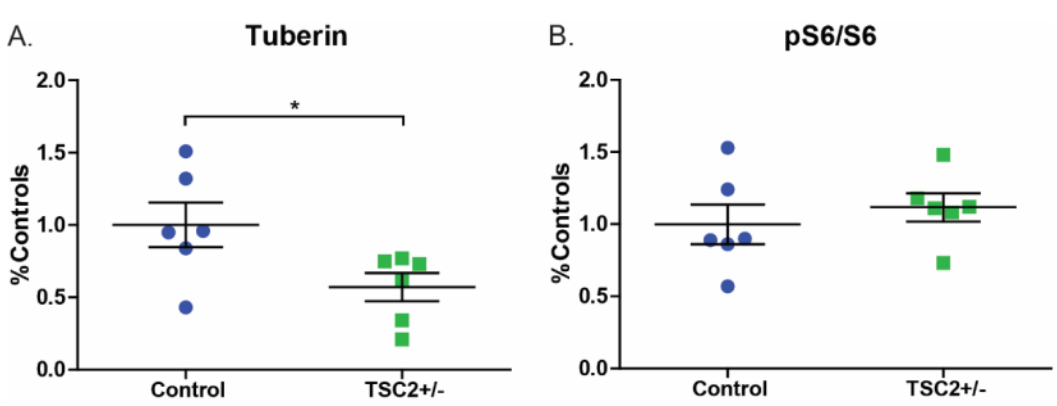

Figure 3.3. Heterozygous nonsense mutations in *TSC2* result in reduced tuberin protein in Sendai-reprogrammed iPSCs.

(**A**) Protein was isolated from Sendai-reprogrammed control and TSP iPSCs and analyzed by immunoblot for tuberin protein (n=6, average of 1-3 experimental replicates; p=0.02 t-test) (**B**) mTORC1 signaling measured by phospho-S6$^{Ser240/244}$ normalized to total S6 (n=6, average of 1-3 experimental replicates)

We validated all iPSCs for the ability to form pluripotent colonies and differentiate to all three germ layers (Chapter II, Figure 2.2). Although we were able to find TSP iPSC colonies which stained positively for pluripotent markers, we observed that during routine culture TSP iPSCs were more difficult to maintain and tended to spontaneously differentiate at a higher rate than controls. To measure the rate of spontaneous differentiation, colonies from three non-integrated controls, one integrated control and five integrated TSP iPSCs were purified using mechanical dissociation. Following growth in culture all cells were dissociated and analyzed by flow cytometry for the pluripotent marker TRA-1-60. As expected, the majority of control cells were pluripotent stem cells (Figure 3.4). In contrast, the integrated heterozygous TSP iPSCs had significantly lower percentages of pluripotent stem cells compared to non-integrated controls (Figure 3.4 p=0.02). Interestingly, the one integrated control line CC2 did not show the dramatic decrease in TRA-1-60 staining seen in integrated TSP iPSCs. Although we have not directly measured pluripotent stability in the non-integrated Sendai lines, we have not noted any problems with spontaneous differentiation during routine maintenance and passage. This suggests that the increase in spontaneous differentiation seen in integrated TSP iPSCs is a result of the combination of decreased p53 and decreased tuberin.

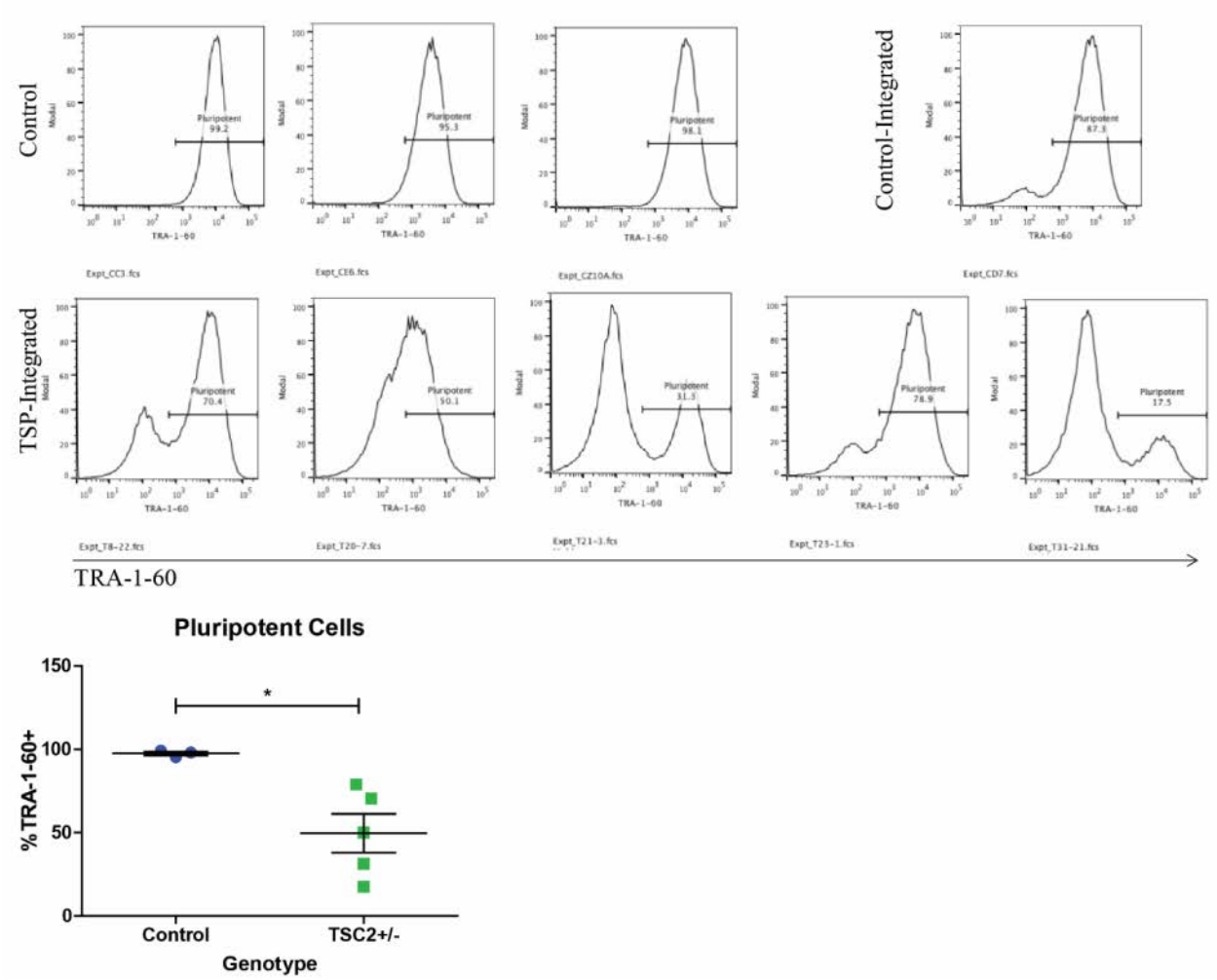

Figure 3.4. Decreased pluripotent stability in integrated TSP iPSC lines.

Colonies from control and integrated TSP iPSC lines were isolated and passaged mechanically. Following expansion in culture cells were stained for the pluripotent marker TRA-1-60 and analyzed by flow cytometry. TSP iPSCs had fewer pluripotent cells than controls (n=3-5; p=0.02 t-test)

When we analyzed control and TSP iPSC colonies for expression of pluripotent markers we observed a number of Oct4 bright cells in TSP cultures (Figure 3.5). These cells were always located at the edge of or outside the colony, suggesting exit from the colony structure. When control iPSCs spontaneously differentiate, the differentiating cells migrating away from the colony do not express pluripotent markers. This suggests that the integrated TSP iPSCs not only have increased rates of spontaneous differentiation but also the differentiating cells are differentiating abnormally. The TSP iPSCs all integrated the reprogramming plasmid with the *OCT4*/shp53 genes, so the *OCT4* gene on the reprogramming plasmid could be contributing to the Oct4-bright cells. However, we do not see any differences in Oct4 staining within the colony itself (Figure 3.5). Despite the increase in spontaneous differentiation, when cells were differentiated as embryoid bodies we did not observe any preference towards one lineage (Chapter II Figure 2.2). There was a slight tendency to maintain expression of pluripotent transcripts which is consistent with our observation of continued expression of Oct4 protein outside of the colony.

During routine passaging of stem cells, we noticed that heterozygous TSC patient iPS cells were much more tolerant of single cell passaging than controls. To quantify this, we counted the cells and plated them at equal numbers. The following day the plates were fixed and quantified by nuclear Hoechst fluorescence by plate reader. Integrated TSC patient lines had 379% more cells survive single cell passaging on average compared to controls (Figure 3.6A, p=0.035). We hypothesized that the increase in cell number was due to either decreased cell death during single cell suspension or increased cell proliferation. To address these possibilities, we first measured cell doubling time to determine whether increased proliferation. Control and integrated *TSC2+/-* iPSCs were plated into replicate 96 well plates and cell counts were obtained over four days. Integrated *TSC2+/-* iPSCs had increased cell numbers over four days and decreased cell doubling time compared to controls (Figure 3.6B, p=0.008). Next, we measured cell death in cells grown overnight in adherent conditions or single cell suspension culture. The following day, cells were stained with Annexin V and Propidium Iodide to detect apoptotic and dead cells, respectively (Figure 3.6C). Although not significant, integrated heterozygous *TSC2+/-* cells had a small increase in Propidium Iodide negative (live and early apoptotic) cells compared to controls (Figure 3.6C p=0.318), so we can't rule out the possibility that increased cell survival in single-cell suspension contributes to the phenotype.

ERK1/2 phosphorylation of tuberin inhibits the TSC complex and activates Rheb/mTORC1. ERK-mediated inhibition of tuberin has been proposed as potential pseudo-second hit in TSC tubers which have heterozygous mutations in *TSC2* (Ma et al 2005). Integrated TSP iPSCs had increased MEK1/2 signaling, measured by phospho-ERK1/2, compared to control iPSCs (Figure 3.7A p=0.045). As TSP iPSCs consist of a mix of pluripotent colonies and spontaneously differentiating cells, we wondered whether the difference in signaling was a reflection of the differences in cell types in culture. To isolate signaling in the pluripotent cells we measured phosphoERK1/2 in TRA-1-60 positive cells by flow cytometry. An increase in the mean fluorescent signal of phospho-ERK1/2 was confirmed in two out the three TSP lines (Figure 3.7B).

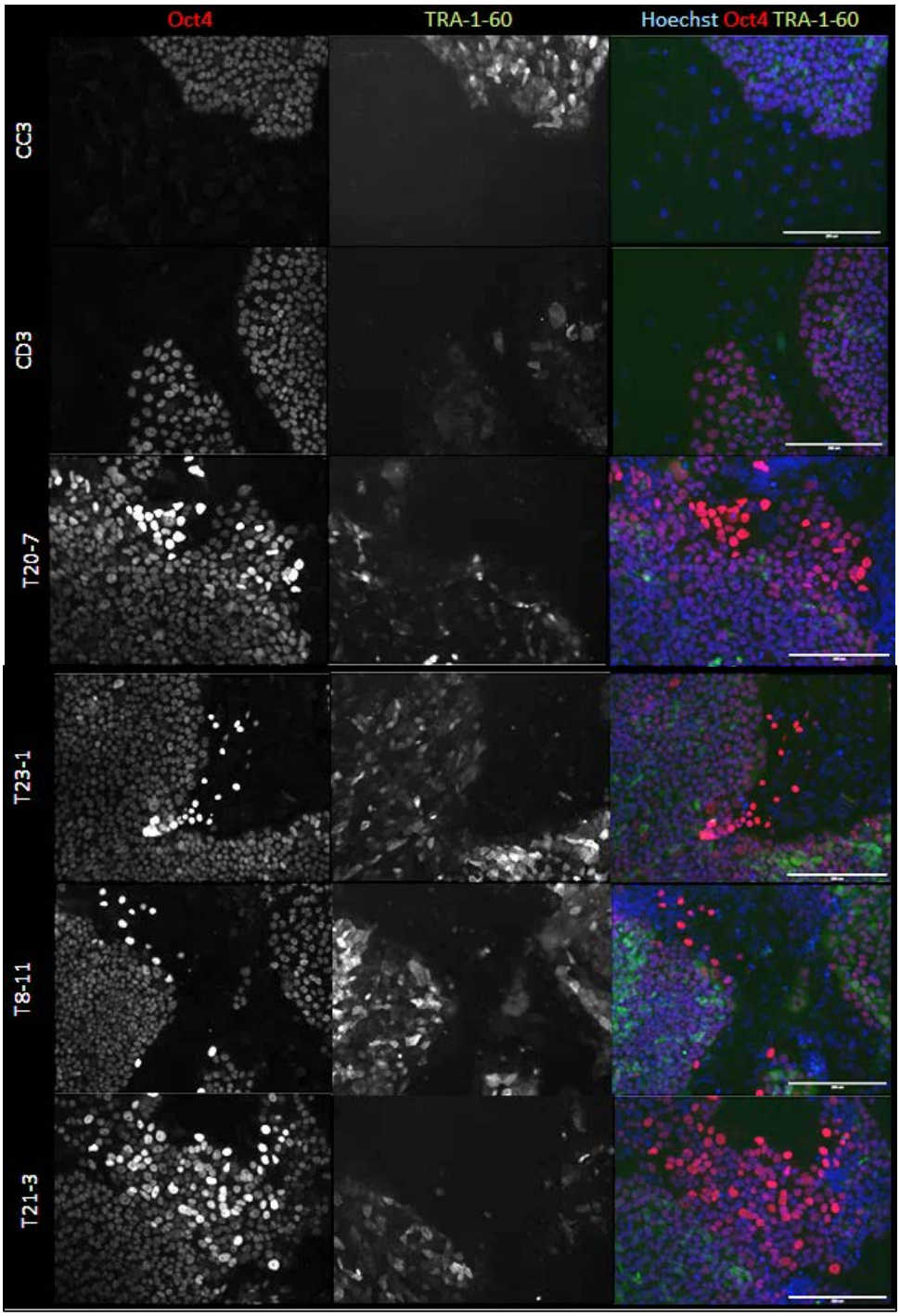

Figure 3.5. Abnormal spontaneous differentiation in TSP iPSCs

Colonies from control and integrated TSP iPSC lines were stained for the pluripotent markers TRA-1-60 and OCT4 and analyzed by immunofluorescence.

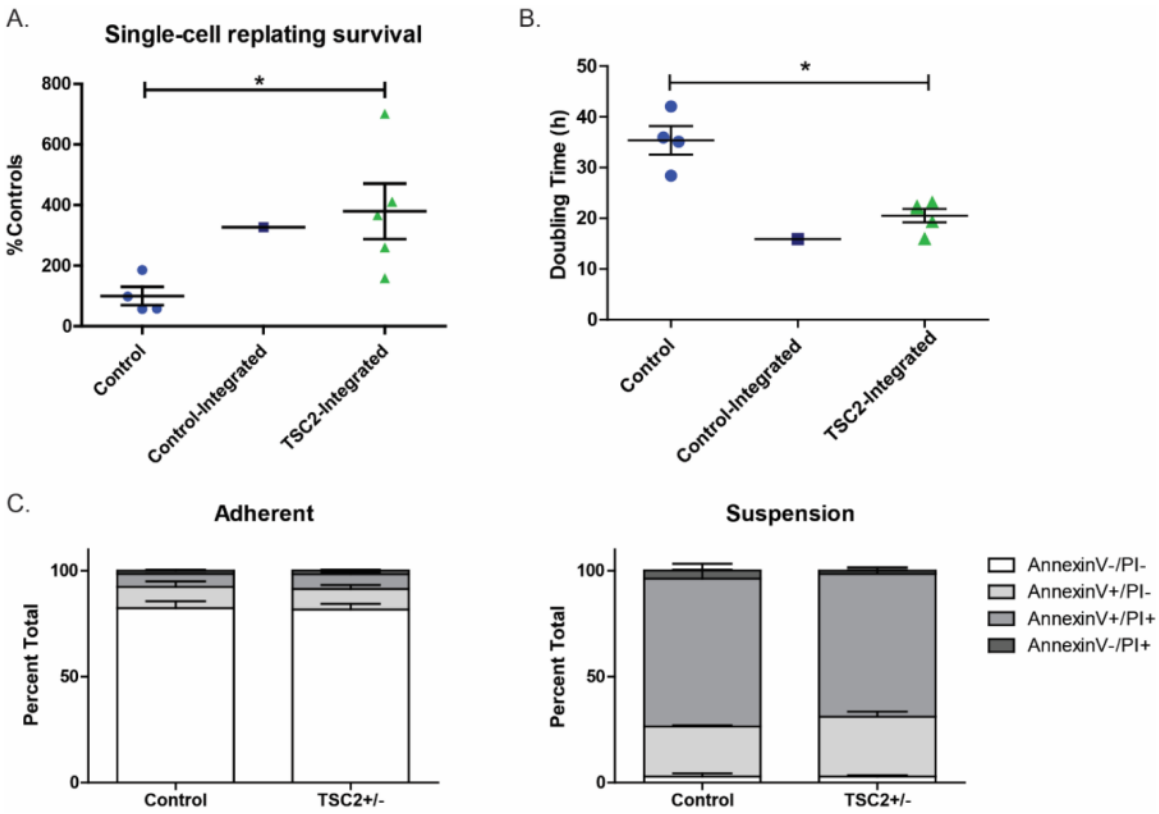

Figure 3.6 Integrated *TSC2+/-* iPSCs have increased cell survival and proliferation

(**A**) Control and *TSC2+/-* iPS cells were passaged as single cells to 96 well plates. Cell number was quantified by nuclear stain Hoechst fluorescence by plate reader (n=4-5 individual lines, average of 2-4 experimental replicates per line; p=0.035 *t*-test). (**B**) Control and integrated *TSC2+/-* cells were counted and plated into 96 well plates. One plate was fixed every twenty-four hours and cell counts were measured by fluorescence of the nuclear stain Hoechst by plate reader. (*n*=4-5 individual lines, average of 2-4 experimental replicates; *p*=0.008) (**C**) Control and integrated *TSC2+/-* iPSCs were grown in adherent or suspension culture for 21 hours without rock inhibitor. Cell death was measured by Annexin V and Propidium Iodide staining by flow cytometry. (*n*=2 controls and 3 TSP, *p*=0.318 *t*-test PI negative)

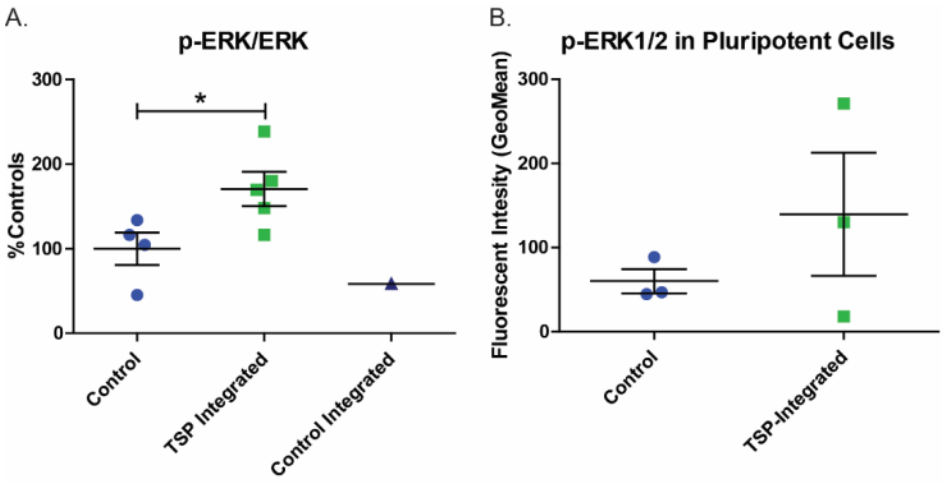

Figure 3.7 Increased MEK1/2 signaling in integrated *TSC2+/-* iPSCs

(**A**) Protein was isolated from control and TSP iPSCs and analyzed by immunoblot for expression of phospho-ERK1/2. Phosphorylated protein was normalized to total ERK1/2 (*n*=4-5 individual lines; average of 2-4 experimental replicates; *p*=0.045 *t*-test) (**B**) Control and integrated stem cells were analyzed by flow cytometry. Following gating for TRA-1-60 positive pluripotent cells, the fluorescent intensity of phospho-ERK1/2 was analyzed.

Discussion

We have generated integrated plasmid-reprogrammed as well as non-integrated Sendai-reprogrammed iPSCs to explore the contribution of tuberin and p53 to stem cell maintenance. We initially sought to model early neural development in TSC using iPSCs generated from heterozygous *TSC2+/-* patient fibroblasts. However, in the process of generating TSC and control stem cells we discovered an important contribution of *TSC2* to the reprogramming process, such that most of the TSP patient lines had integrated the OCT4/shp53 plasmid. This was further explored in Chapter II, where we showed that *TSC2+/-* fibroblasts have elevated levels of p53 protein following cell stress. We hypothesized that the *TSC2+/-* clones with continued expression of the shRNA to p53 would overcome the elevated p53 levels to proliferate and survive the reprogramming process. To test whether the shp53 is functioning and expressed in the integrated iPSCs we measured p53 protein levels by immunoblot. The integrated plasmid-reprogrammed iPSCs have reduced p53 protein; this is in contrast to the non-integrated Sendai reprogrammed lines which have normal (or elevated following DNA damage) p53 protein levels.

In chapter II, we saw that tuberin protein levels rose in response to UV challenge. Previous studies have shown that p53 binds to and upregulates *TSC2* mRNA and protein (Feng et al 2005, Feng et al 2007). We wondered whether continued expression of the shRNA to p53 would alter *TSC2* mRNA or tuberin protein levels. However, we showed that integration of the OCT4/shp53 plasmid does not alter tuberin protein or mRNA expression; heterozygous *TSC2+/-* stem cells have similarly decreased *TSC2* protein in both the integrated plasmid-reprogrammed lines and the Sendai-reprogrammed lines.

Surprisingly, we observed decreased mTORC1 signaling measured by phospho-S6$^{Ser240/244}$ in both the control and TSP integrated lines. This suggests that it is the integration causing decreased mTORC1 signaling. There is evidence for p53 participating in a negative feedback loop to inhibit mTORC1 (Agarwal et al 2016), so we hypothesized that continued expression of the shRNA to p53 would release this feedback loop and lead to increased mTORC1 in integrated lines. However, we observed the opposite result in the integrated iPSCs, suggesting there are other interactions that we have not explored.

The integrated TSP iPSCs, but not the control integrated iPSCs, have elevated phospho-ERK1/2. This finding is especially interesting as ERK1/2 phosphorylates and inhibits tuberin; elevated phospho-ERK1/2 observed in tubers has been proposed as potential molecular "second-hit" to inhibit the remaining tuberin protein. Our findings are consistent with these previous studies. However, more studies are needed to determine whether the increase in phospho-ERK1/2 is due to heterozygous loss of *TSC2* alone or whether it requires p53 knock-down as well. Future studies examining ERK1/2 signaling in the non-integrated Sendai lines will further clarify this potentially interesting interaction.

During routine maintenance of the integrated TSP stem cells, we observed increased spontaneous differentiation and increased cell number following single cell passage. Our results suggest that increased cell proliferation and increased cell survival in suspension underlie our observation of increased cell number following routine passaging. The time point chosen for the cell suspension experiment was likely too long as most cells in either control or TSC patient groups had died. However, these results are consistent with previous results in our lab (E. Armour Dissertation, Vanderbilt University) describing increased recovery of pluripotency markers in integrated TSC iPSCs following single-cell passage. We also observed increased cell survival and proliferation in our integrated control lines suggesting that integration of the OCT4/shp53 plasmid is causative in these phenotypes. Indeed, p53 is an important cell cycle and apoptotic regulator, such that loss of p53 would be expected to decrease cell doubling time and decrease cell death following single cell suspension. However, mTORC1 has also been shown to regulate cyclins and we have not formally ruled out a potential contribution of heterozygous loss of *TSC2* to the increased proliferation in these lines.

In contrast to the cell proliferation and survival phenotypes, the integrated control line CC2 did not display decreased pluripotent stability, suggesting that heterozygous loss of *TSC2* is contributing to increased differentiation. Further, decreased p53 protein, in addition to increasing survival and proliferation, has been proposed to enhance reprogramming by increasing expression pluripotent genes, so it is unlikely to be responsible for the pluripotent instability in integrated TSP iPSCs. This is an interesting finding which will require further exploration in the non-integrated Sendai iPSC lines.

We have shown that integration of the OCT/shp53 plasmid and heterozygous loss of *TSC2* interact in several ways which contribute to our understanding of how the p53 and mTOR pathway function in stem cells. Future studies will use non-integrated heterozygous iPSCs to more fully dissect these intriguing pathways.

Materials and Methods

Statistics

All statistical analyses were conducted using GraphPad PRISM. Individual patient-derived iPSC clones are treated as independent *n*. All other experimental or technical replicates are considered not independent and are averaged to obtain the final value for each patient clone/line.

Cell Proliferation

Control and *TSC2+/-* iPSC cells were detached using Accutase, resuspended in mTeSR media with ROCK inhibitor and then plated in mTeSR at a concentration of 5X 10^3 cells per 96 well. A standard curve from 1.6E5 to 2.5E3 was prepared at the same time. Plates were fixed every twenty-four hours for four days in 4% paraformaldehyde and stained with nuclear marker Hoechst. Black well plates were then read on a BIO-TEK Synergy HT Microtiter Platereader. Cell survival was estimated based on Day 0 cell numbers. Doubling time was calculated using exponential growth equation (least squares fit, weighted by $1/Y^2$) in GraphPad Prism. Doubling times >72 hours were interpreted as not proliferating and were excluded from analysis.

Flow cytometry

iPSCs were isolated as single cells by enzymatic Accutase treatment and resuspended in 2.5% normal goat serum in PBS on ice. For surface TRA-1-60 staining, no cell permeabilization was used. Cells were filtered through a 40 μm filter and counted. Cells were then stained with 10μl/test TRA-1-60 antibody (BD Biosciences #560193) or equivalent concentration of PE IgM isotype control.

For measurements of detachment-triggered apoptosis, cells were grown in adherent cultures on Matrigel in mTeSR or in low adherence plates without rock inhibitor. Cells were stained with 5 μl Annexin V (AF488, ThermoScientific A1320) and 0.5 μl of 1 mg/ml propidium iodide (Sigma P4864) per 10^5 cells and immediately analyzed by flow cytometry. Cells were gated to exclude debris and doublets.

Immunofluorescence

Cells were fixed in 4% paraformaldehyde for 20 min at room temperature, followed by 3x 5-minute PBS washes. For intracellular antibodies, cells were then permeabilized with 0.1% Triton in PBS for 20 minutes at room temperature and blocked in 0.1% Triton plus 5% normal goat serum for 1 hour at room temperature. For extracellular antibodies, cells were blocked in 5% normal goat serum for 1 hour at room temperature. Cells were then incubated in primary antibody rocking overnight at 4°C. Following 5x 10-minute PBS washes, cells were incubated with secondary antibody for 3 hours at room temperature.

Immunoblotting

Protein was isolated by lysing and scraping cells in RIPA buffer plus protease inhibitor cocktails 2 and 3 and phosphatase inhibitor cocktail (Sigma P5726, P0044, P8340). Samples were rotated for 30 minutes at 4°C, sonicated and then run on 4-12% NuPAGE BisTris gels in MOPS buffer. Gels were transferred to PVDF membrane at 95V for 90 minutes using the Bio-Rad Mini Trans-Blot Cell. Membranes were incubated overnight in primary antibody diluted in 5% BSA. Membranes were then incubated for 1 hour at room temperature in secondary antibody and imaged on an Odyssey Li-Cor machine. Samples were normalized to actin or total protein levels using Li-Cor REVERT stain. To control for intra-experimental differences in antibody concentration and Odyssey machine settings, normalized values are expressed as a percentage of the controls before averaging experimental replicates.

CHAPTER IV

HOMOZYGOUS LOSS OF *TSC2* CAUSES IMPAIRED MTOR REGULATION DURING NEURODEVELOPMENT

Abstract

Tuberous Sclerosis Complex causes refractory epilepsy and intellectual disability but the pathogenesis of the neurological symptoms is not understood. Identifying when and in what cell types mutations in *TSC1* or *TSC2* lead to neurological dysfunction is the first step to better and more targeted treatments. Induced pluripotent stem cells provide the opportunity to study these processes in human model of neurodevelopment. *We hypothesized that heterozygous and homozygous loss of TSC2 would lead to dysregulation of mTOR signaling in neural progenitors and impair neural differentiation.* Here we show that homozygous loss of *TSC2* leads to increased mTORC1 in neural progenitors and decreased neural progenitor formation. Future studies will be necessary to explore how heterozygous loss of *TSC2* alters neural differentiation in non-integrated iPSCs.

Introduction

The most debilitating symptoms of TSC are a consequence of brain involvement. Patients frequently have intellectual disability and refractory epilepsy. mTORC1 inhibitors have been used to effectively treat some of the hamartomatous growths in TSC; however, the effect is limited to the treatment period (Bissler et al 2008, Cardamone et al 2014, Franz et al 2006, McCormack et al 2011, Sasongko et al 2016). While mTORC1 inhibitors have a clear cytostatic effect both *in vitro* and *in vivo*, it is not known how effective they will be in treating symptoms not directly related to expanding hamartomas. Studies are underway to determine whether mTORC1 inhibitors are effective in treating epilepsy and cognitive symptoms, however a better understanding of the developmental impact of *TSC1* and *TSC2* mutations could lead to more impactful treatment targeted to a specific time point and cell type. As mTORC1 activity is important in maintaining proliferating pluripotent cells, we hypothesized that mTORC1 activity would decrease during directed differentiation in wild-type cells and that TSC lines would be unable to inhibit mTORC1 activity during this period. Increased mTORC1 activity in other stem cell populations (hematopoietic, germline) causes increased differentiation and stem cell exhaustion (Chen et al 2008, Magri and Galli 2013, Sun et al 2010, Zhou et al 2009) and we hypothesized that the same would be true of neural stem cells with homozygous mutations in *TSC2*.

To better understand the impact of heterozygous and homozygous *TSC2* loss on neurodevelopment, we used heterozygous induced pluripotent stem cells (iPSCs) generated from patient fibroblasts using plasmid-reprogramming methods and isogenic homozygous *TSC2-/-* iPSCs generated using CRISPR-Cas9 techniques to edit the genome. Here we show that homozygous *TSC2* stem cells are unable to regulate mTORC1 and mTORC2 activity during neural differentiation and, further, homozygous mutations in *TSC2* impair formation of neural progenitors.

Results

To determine how heterozygous loss of *TSC2* alters early neural differentiation we differentiated non-integrated control and integrated TSC line TSP16-11 to neural progenitors. No mutation was identified in TSC patient TSP16 by exome sequencing of *TSC1* or *TSC2* (E. Armour Dissertation, Vanderbilt University). However, the patient meets the clinical criteria of TSC. Further, clone TSP16-8 had decreased *TSC2* mRNA levels and protein levels, although the variability in the control protein levels makes it difficult to draw any conclusions (Figure 4.1A-B). This suggests that the cells had a large deletion in *TSC2* that would be missed by exome sequencing. Stem cells were differentiated to neural progenitors using a dual-SMAD inhibition protocol in adherent cultures (neural differentiation protocol #1) for 7 days. Cells isolated from day 0, day 3, day 5, and day 7 of neural differentiation were analyzed by flow cytometry. Forward-scatter and side-scatter are broad measurements of cell size and cell complexity, respectively. Based on the forward-scatter and side-scatter measurements, there are dramatic changes over the course of differentiation. On day 3, there is an initial increase in side-scatter or cell complexity (Figure 4.2). This may reflect the cellular response to the growth factors and small molecule inhibitors added to the media to induce differentiation. The sudden switch from pluripotency to neural differentiation involves a switch in transcription programs likely leading to increased cellular proteins. After this initial burst of cellular complexity, the side-scatter values decrease slightly, although they never return to the levels of day 0 cells (Figure 4.2). The forward-scatter showed that the cell size shrinks below their starting point by day 5 and day 7 (Figure 4.2). These patterns are similar in both control and TSP lines.

To study the timing of cellular transition from pluripotent stem cell to neural progenitor we stained cells for the pluripotent marker Oct4 and the neural progenitor marker Pax6 and analyzed cells by flow cytometry (Figure 4.2). As expected, the pluripotent marker Oct4 is rapidly lost and by day 5 no Oct4 positive pluripotent stem cells were detected in the control line. At the same time, the control cells begin turning on Pax6 expression; by day 5 37% of the cells are positive and 78% are positive by day 7. In contrast, the integrated TSP line T16-11 appropriately downregulated Oct4 but did not upregulate Pax6 signal.

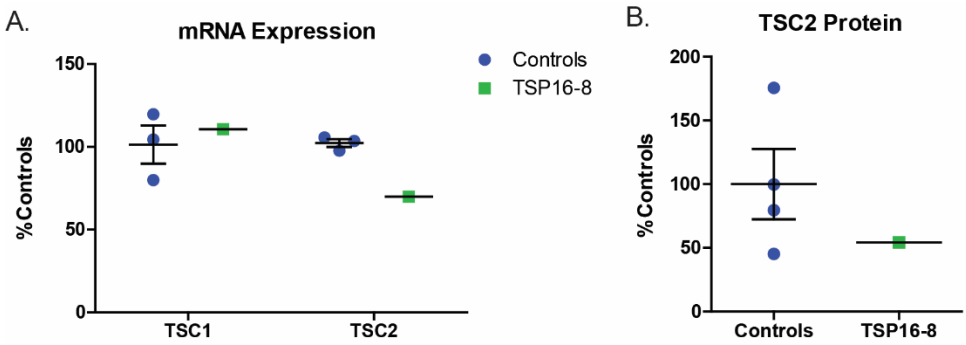

Figure 4.1 TSC2 mRNA and protein expression in TSP16-8

(A) *TSC1* and *TSC2* mRNA quantified by qPCR in control and TSP16-8 iPSCs. (**B**) TSC2 protein quantified by immunoblot in control and TSP16-8 iPSCs.

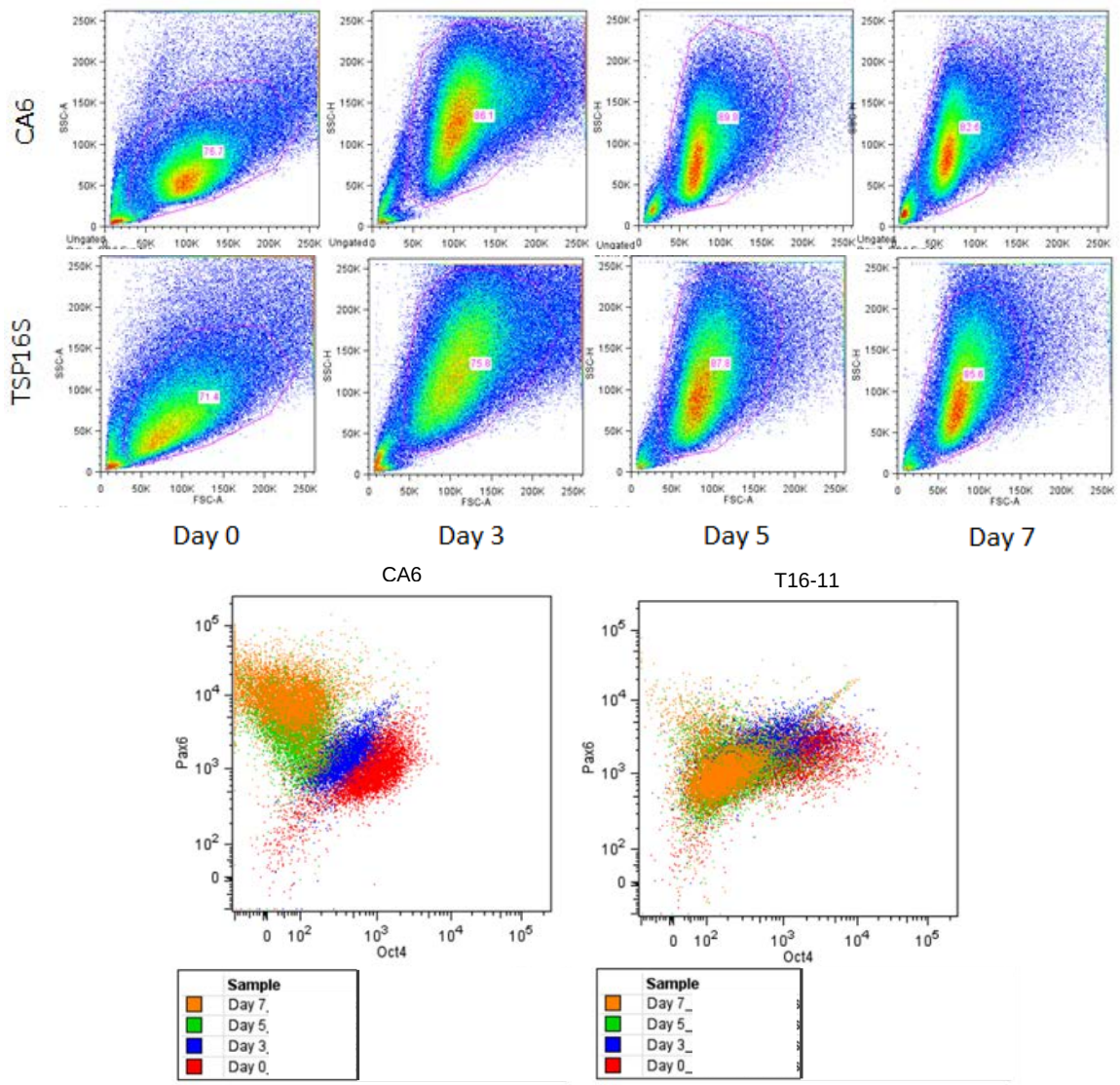

Figure 4.2. Impaired formation of neural progenitors in integrated TSC iPSC line TSP16-11

Control line CA6 and TSC line TSP16-11 were differentiated to neural progenitors using dual-SMAD inhibition in adherent cultures. Cells were isolated on Day 0, 3, 5, and 7 of neural differentiation and analyzed by flow cytometry. (**A**) Forward- and side-scatter show that both the control line and TSP line undergo similar changes in cell size and complexity during the first week of directed differentiation. (**B**) Both control and TSP lines downregulate pluripotency marker Oct4 during directed differentiation. TSP line TSP16-11 fails to upregulate neural progenitor marker Pax6.

To test the contribution of mTORC1 to neural differentiation, we treated cells with the mTORC1 inhibitor rapamycin and analyzed cells by immunoblot. As was observed by flow cytometry, Pax6 levels were lower in TSP16-11 patient cells (Figure 4.3C genotype p=0.0003, post-test p<0.01). Although rapamycin inhibited mTORC1 markers phospho-S6 and phospho-4E-BP1 levels to 44-69% of normal (Figure 4.3A-B, p<0.0001 and p=0.006), treatment failed to increase Pax6 protein levels in the TSP16-11 patient cells (Figure 4.3C).

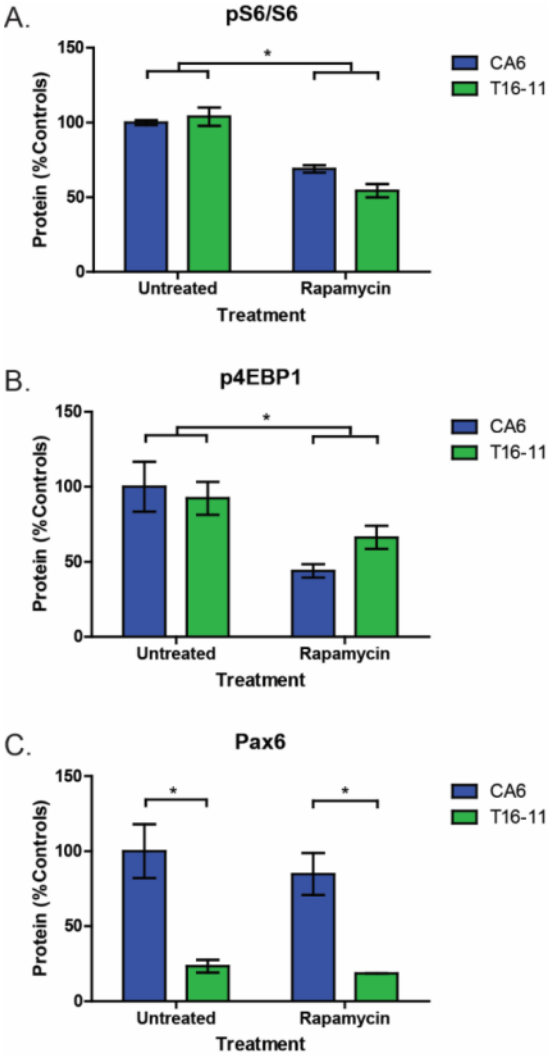

Figure 4.3 Impaired formation of neural progenitors in integrated TSC iPSC line TSP16-11 is mTORC1-independent

Control iPSC line CA6 and TSP line TSP16-11 were differentiated to neural progenitors with or without 20 nM rapamycin treatment. Protein was isolated on day 7 and analyzed for phospho-S6, phospho-4E-BP1 and Pax6 levels. (**A**) Phospho-S6 protein normalized to total S6 (n=3 replicate wells; interaction p=0.05, genotype p=0.226, rapamycin p<0.0001) (**B**) Phospho-4E-BP1 protein normalized to actin (n=3 replicate wells; interaction p=0.207, genotype p=0.5233, rapamycin p=0.006). (**C**) Pax6 protein normalized to actin (n=3 replicate wells; interaction p=0.665, genotype p=0.0003, rapamycin p=0.415, Bonferroni post-test p<0.01)

To further explore the relationship between mTORC1 and mTORC2 signaling and neural differentiation, we monitored phospho-S6 and phospho-Akt protein levels by immunoblot during the first week of neural differentiation using iPS lines CA6, CC3, T20-7 and T16-11. Controls decreased phospho-S6 levels from day 2 to day 7 suggesting inhibition of mTORC1 activity. However, integrated TSP iPSCs also appropriately inhibited mTORC1 (Figure 4.4).

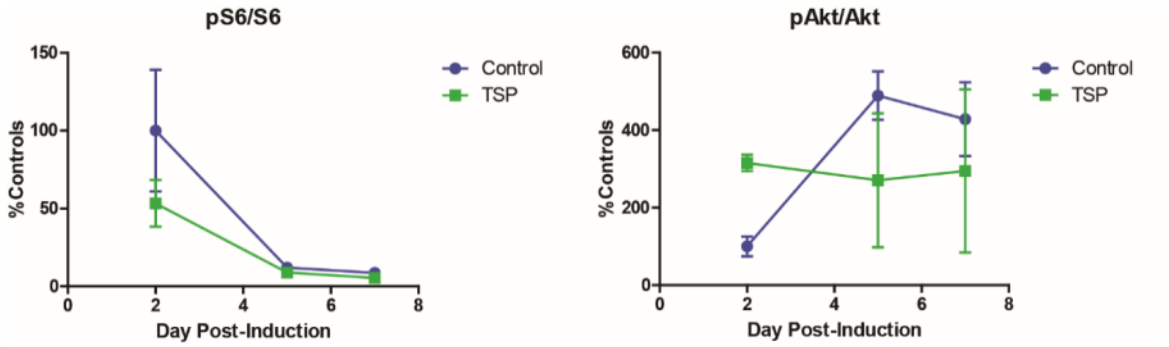

Figure 4.4 mTORC1 activity decreases and mTORC2 activity increases during neural differentiation of plasmid-reprogrammed iPSCs

Control iPSC lines (CA6, CC3) and TSP iPSC lines (TSP20-7, TSP16-11) were differentiated to neural progenitors. Protein was isolated on Day 2, 5 and 7 of directed differentiation and analyzed by immunoblot for phospho-S6 and phospho-Akt (n=2, average of 3 replicate wells for each line).

To better isolate the contribution of *TSC2* to neural development, we generated isogenic homozygous *TSC2* knock-out stem cells. Using wildtype and homozygous *TSC2* mutant lines we differentiated the stem cells towards neural progenitors using dual-SMAD inhibition in adherent cultures (neural differentiation protocol #2). We isolated protein and imaged cells weekly during the first four weeks of neural development. *TSC2* mutant lines display impaired neural differentiation, consistent with what we previously observed with heterozygous line T16-11. Protein levels of Pax6, a transcription factor upregulated in neural progenitors, increase during the first few weeks of neural differentiation, peaking at week 2 in controls. In contrast, the homozygous *TSC2-/-* cells have lower levels of Pax6 protein, peaking at approximately 60% of controls (Figure 4.5A, Figure 4.6). Nestin is an intermediate filament expressed in neural progenitors, but it shows a slightly different time course compared to Pax6. The anti-nestin antibody detects two bands by immunoblot. Previous reports have suggested that nestin can be phosphorylated by cdk5 or cdc2 (Sahlgren et al 2001, Sahlgren et al 2003). The lower nestin band was expressed slightly earlier than the upper band (week 1 vs week 2). Although there was no difference between wildtype and *TSC2* mutant cells in their expression of the lower band, there may be decreased expression of the upper nestin band in *TSC2* mutant cells (Figure 4.5B p=0.113); however, this did not reach significance and further studies will be necessary to determine the identity of the two nestin bands. Interestingly, neuronal marker beta-tubulin III, does not show differences between wildtype and *TSC2* mutant cells (Figure 4.5C).

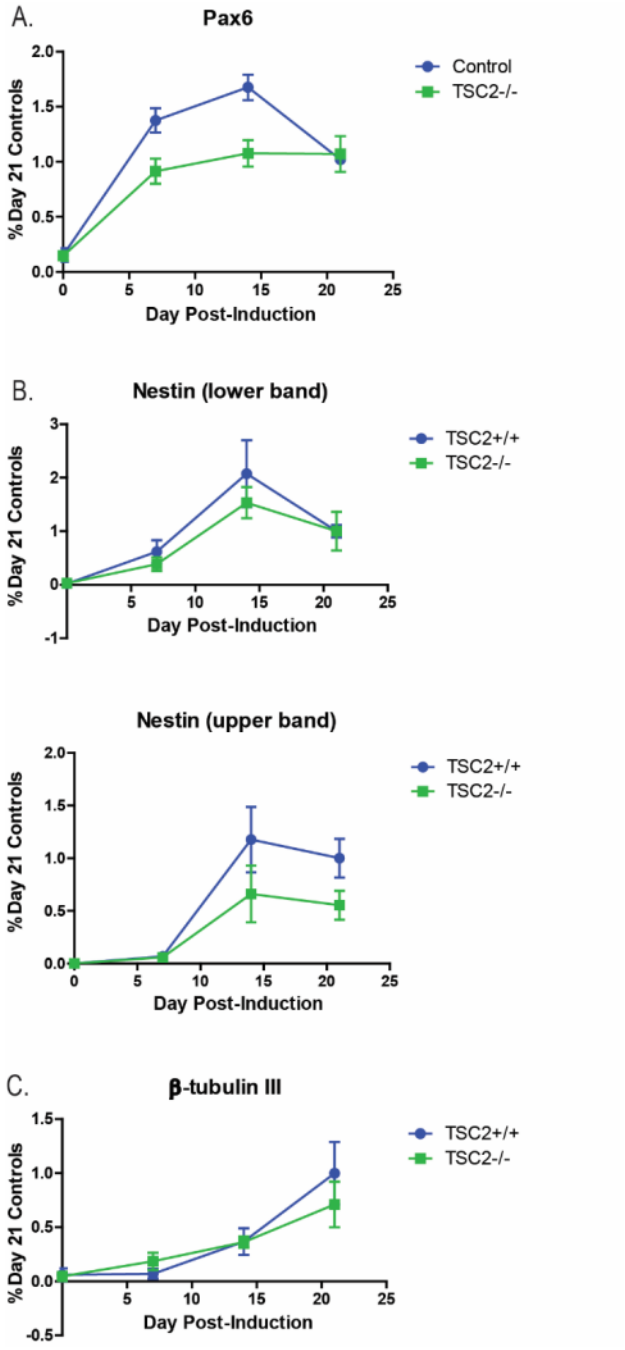

Figure 4.5 Impaired formation of neural progenitors from *TSC2-/-* iPSCs

Protein was isolated from iPSC-derived neural progenitors over the course of three weeks of directed differentiation and analyzed by immunoblot for neuronal markers (**A**) Pax6 (n=6; interaction p=0.004, time p<0.0001, genotype p=0.012 two-way ANOVA; Bonferroni post-test Day 7 p<0.05 Day 14 p<0.001) (**B**) Nestin lower band (n=6; interaction p=0.678, time p=0.001, genotype p=0.441) Nestin upper band (n=6; interaction p=0.304, time p=0.0002, genotype p=0.113 two-way ANOVA) (**C**) β-Tubulin III (n=4)

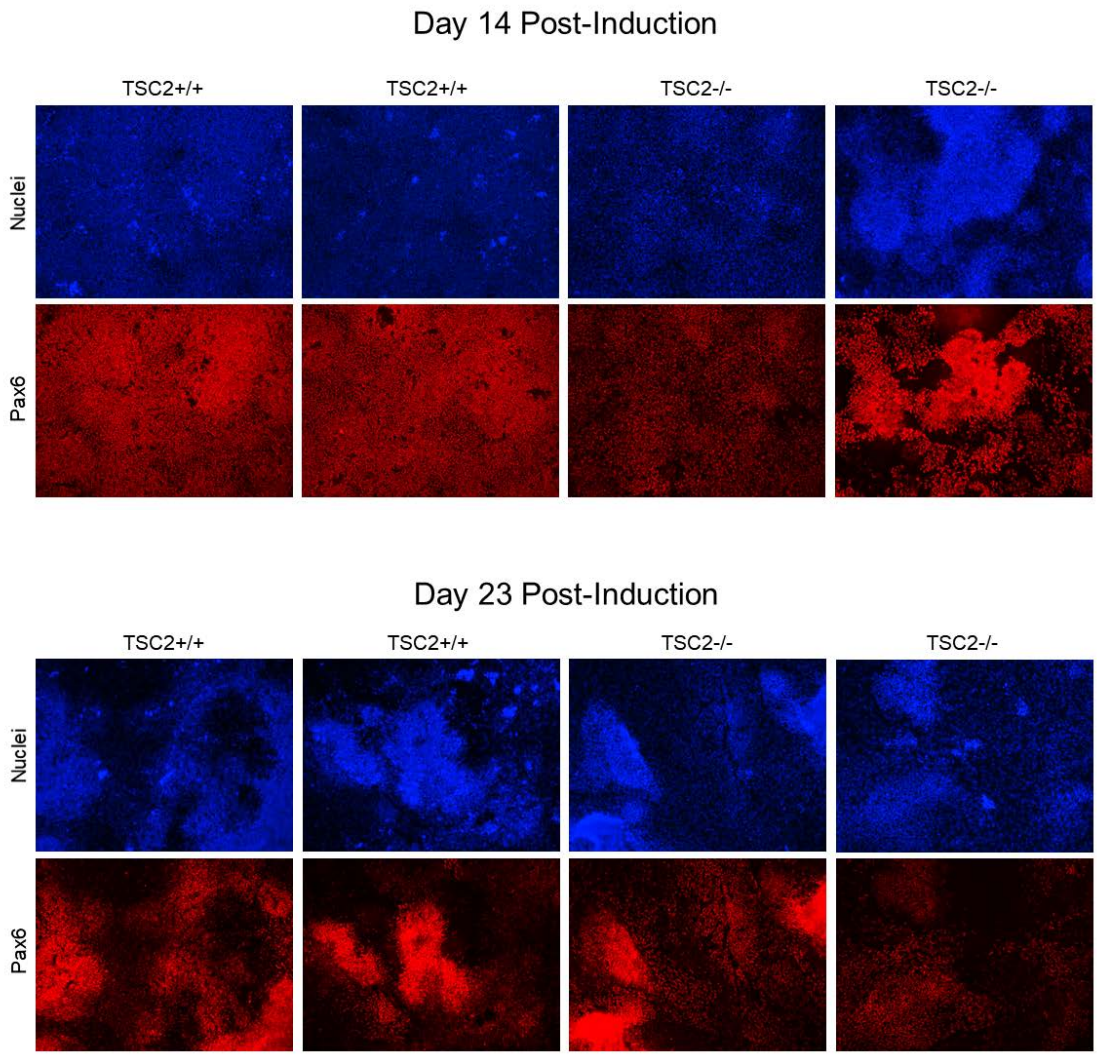

Figure 4.6 Expression of neural progenitor marker Pax6 during directed differentiation

Expression of neural progenitor marker Pax6 was analyzed by immunofluorescence imaged at 10x magnification on day 14 and day 23 of neural differentiation

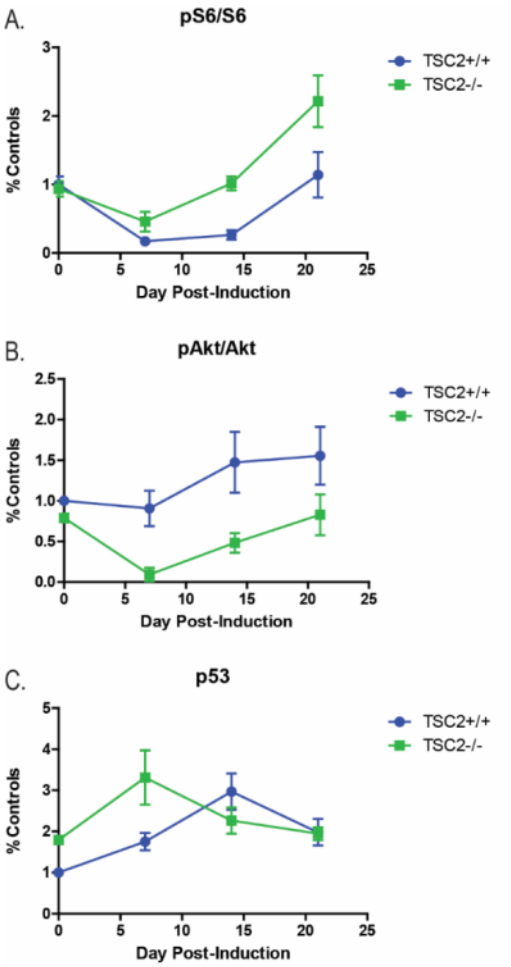

Figure 4.7 Changes in mTORC1 and mTORC2 signaling during neural differentiation of iPSCs

Protein was isolated from iPSC-derived neural progenitors over the course of three weeks of directed differentiation and analyzed by immunoblot. (**A**) pS6/S6 (n=6; interaction p=0.019, time p<0.0001, genotype p=0.015 two-way ANOVA; Bonferroni post-test Day 14 p<0.05, Day 21 p<0.01) (**B**) pAkt/Akt (n=6; interaction p=0.251, time p=0.012, genotype p=0.007 two-way ANOVA; Bonferroni post-test Day 14 p<0.05) (**C**) p53 (n=6; interaction p=0.002, time p=0.0003, genotype p=0.26 two-way ANOVA; Bonferroni post-test Day 7 p<0.01)

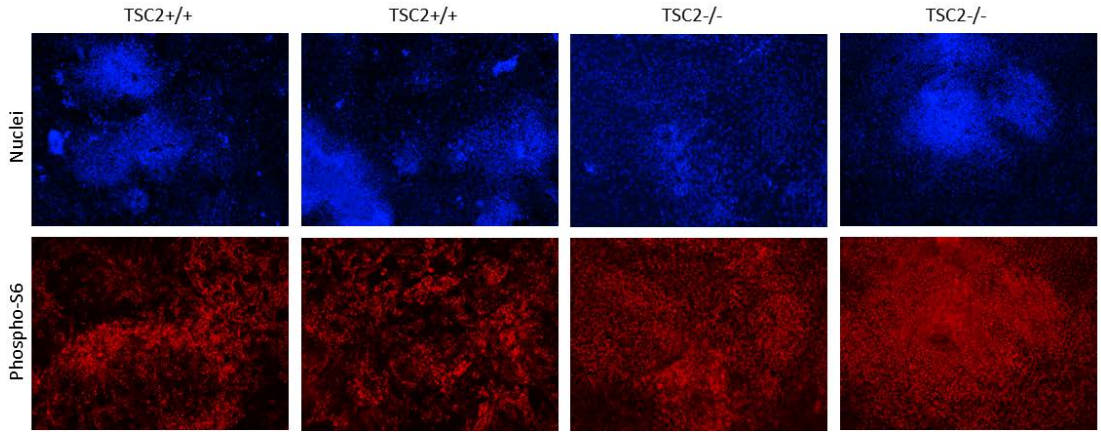

Figure 4.8 mTORC1 signaling during neural differentiation of iPSCs

Expression of phospho-S6 was analyzed by immunofluorescence at 10x magnification on day 23 of neural differentiation.

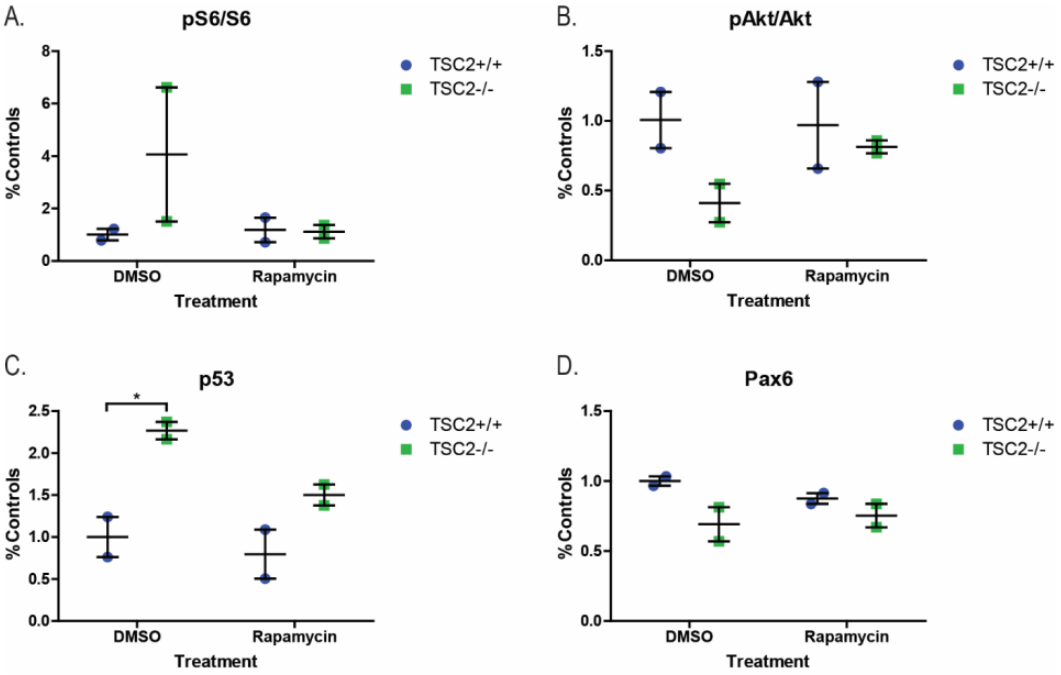

Figure 4.9 Impaired early neural differentiation of *TSC2-/-* iPSCs is mTORC1-independent

TSC2+/+ and *TSC2-/-* iPSCs were differentiated to neural progenitors for one week and treated with 0.2nM rapamycin or vehicle throughout directed differentiation (**A**) phospho-S6$^{Ser240/244}$ normalized to S6 (n=2; interaction p=0.309, rapamycin p=0.354, genotype 0.410, two-way ANOVA) (**B**) phospho-Akt^{Ser473} normalized to total Akt (n=2; interaction p=0.176, rapamycin p=0.229, genotype 0.286, two-way ANOVA) (**C**) p53 (n=2; interaction p=0.139, rapamycin p=0.054, genotype p=0.066 two-way ANOVA; Bonferroni post-test p<0.05) (**D**) Pax6 (n=2; interaction p=0.041, rapamycin p=0.251, genotype p=0.186 two-way ANOVA)

Next, we explored how mTORC1 and mTORC2 signaling changes during neural development. In control cells, mTORC1 signaling, measured by pS6 protein levels, initially drops to 17% of starting day 0 values before rising to 114% by day 21. In contrast, without tuberin, *TSC2-/-* cells are unable to decrease pS6 as dramatically, and pS6 eventually reaches 220% of day 0 controls by day 21 of neural differentiation (Figure 4.7A, Figure 4.8). mTORC2 signaling, measured by phospho-Akt^{Ser473}, increases slightly during neural differentiation in control cells but homozygous *TSC2* mutants have decreased mTORC2 signaling (Figure 4.7B). Although p53 levels were increased at baseline in homozygous *TSC2* cells, consistent with what was observed previously, both wildtype and *TSC2* mutant cells increased p53 during neural differentiation to similar levels.

To test whether the increased mTORC1 and decreased mTORC2 signaling were causative in the impaired differentiation of homozygous *TSC2-/-* stem cells, we treated stem cells with the mTORC1 inhibitor rapamycin during directed differentiation. Rapamycin corrected the abnormalities in mTORC1 and mTORC2 signaling in homozygous *TSC2-/-* cells at day 7 of differentiation (Figure 4.9A-B). Further, rapamycin partially corrected the elevated p53 protein at day 7 of differentiation (Figure 4.9C). However, rapamycin did not correct Pax6 protein levels in *TSC2-/-* cells. In fact, Pax6 protein was slightly decreased in controls, likely due to slowed growth. However, these results are from one round of differentiation and will require replication.

Discussion

To explore the effects of heterozygous and homozygous *TSC2* mutations on early neurodevelopment, we generated heterozygous and homozygous *TSC2* iPSCs and then directed them towards a neural progenitor fate. Integrated TSC line T16-11 displayed impaired formation of Pax6 positive neural progenitors despite appropriately exiting the stem cell state. Unlike increased p53 protein, loss of p53 in mice does not cause alterations in neural development, so it is more likely that this phenotype is due to mutations in the TSC genes or an interaction between the two genes. Alternatively, given the results in Chapter II, it is likely that spontaneous differentiation of T16-11 before neural induction even began impaired the efficiency of neural differentiation. However, formation of neural progenitors was also inhibited in isogenic homozygous *TSC2* lines, supporting altered neural differentiation regardless of gene dosage. Surprisingly, inhibition of mTORC1 activity with rapamycin failed to rescue formation of neural progenitors at day 7 in either heterozygous or homozygous TSC lines. However, in both experiments rapamycin appeared to slightly inhibit formation of neural progenitors in controls as well. This could be due to slowed growth delaying emergence of Pax6 positive cells. Future studies using a longer time course will be required to determine whether the decrease in neural progenitors with rapamycin treatment is actually just a delay in the neural differentiation time course. The ability of homozygous TSC mutant lines to form early β-tubulin III+ neurons despite decreased neural progenitor formation suggests that *TSC2* cells may be moving rapidly through the neural progenitor stage to produce early neurons rather than expand the neural progenitor pool. Future studies will be necessary to track Pax6 positive cells as they divide and differentiate and to explore what cell types the Pax6 negative cells are forming.

Costa et al. showed decreased formation of post-mitotic neurons from neural progenitors in both heterozygous and homozygous *TSC2* human stem cells, suggesting that *TSC* mutant cells form fewer cells at every stage of neural differentiation (Costa et al 2016).This is consistent with our hypothesis that *TSC2* mutant cells undergo increased differentiation at the expense of self-renewal. Interestingly, they were also unable to rescue the neuronal differentiation phenotype with rapamycin treatment. Given these results, the dominant effect of rapamycin during neural differentiation is likely slowed proliferation, pointing to the need for different or more precisely timed treatments.

The double band observed when analyzing the neural progenitor marker nestin by immunoblot was an interesting finding because each band had a slightly different time course and differences in the homozygous *TSC2-/-* lines were only seen in the upper band. We hypothesize that this larger band may represent a phosphorylated form of nestin. Nestin can be phosphorylated by cdc2 or cdk5 (Sahlgren et al 2001, Sahlgren et al 2003). While the developmental significance of nestin phosphorylation is unclear, cdk5 has been shown to be essential for normal cortical development and its activity is highest in post-mitotic neurons (reviewed in (Lopes and Agostinho 2011). Interestingly, cdk5 is upregulated in cortical tubers and SEGAs in TSC while cdc2 is decreased in patient fibroblasts (Ess et al 2004, Ess et al 2005, Wataya-Kaneda et al 2001). Elevated cdk5 would be expected to result in increased phospho-nestin but in our experiments, we observed decreased expression of the larger nestin band. Additional studies are needed to confirm that the larger band we are observing is the phosphorylated form and how TSC is affecting nestin regulation.

Homozygous *TSC2-/-* iPSCs are unable to regulate mTORC1 and mTORC2 activity during neural development. No differences in mTORC1 or mTORC2 signaling are observed in *TSC2-/-* iPSCs in mTeSR due to the high concentration of stimulatory signals; however, neural differentiation media is similarly replete with growth factors and glucose. Despite this fact, we did find differences in mTORC1 and mTORC2 signaling in *TSC2-/-* lines, suggesting that neural stem cells are especially sensitive to loss of tuberin.

Although different neural differentiation methods and different TSC stem cell lines were used, the results between both experiments were consistent. Both experiments showed a decrease in phospho-S6 levels during early neural differentiation. Both heterozygous and homozygous *TSC2* mutant lines had impaired differentiation to Pax6 positive progenitor cells, but with no apparent defect in β-tubulin III neuron formation in the homozygous *TSC2* lines. However, if the stem cells are undergoing differentiation at the expense of self-renewal then we expect that *TSC2* neural progenitors will form fewer β-tubulin III+ neurons over a longer time course. Future studies using TSC iPSCs to dissect neural progenitor proliferation versus differentiation will advance our understanding of how *TSC2* is regulating neural progenitor dynamics. Furthermore, using heterozygous and homozygous *TSC2* iPSCs we can begin to model loss-of-heterozygosity and non-cell autonomous mechanisms of neural dysfunction.

Materials and Methods

Neural Differentiation Protocol #1

Protocol modified from (Neely et al 2012). Cells were isolated using Accutase, counted and re-plated at 7E4 cells/24 well in mTeSR with rock inhibitor. Once cells reach 80-90% confluency the media is switched from mTeSR to neural differentiation media. Neural differentiation media: 41 ml KO DMEM/F12, 7.5 ml KO serum replacement, 0.5 ml L-glutamine, 0.5 ml pen-strep, 0.5 ml non-essential amino acids, 0.193 µl BMe plus 0.5 µM DMH1 and 10 µM SB431542.

Neural Differentiation Protocol #2

Protocol modified from (Shi et al 2012a, Shi et al 2012b). Cells were isolated using Accutase, counted and re-plated at 1E6 cells/12 well in mTeSR with rock inhibitor. Once cells reach 80-90% confluency the media is switched from mTeSR to neural induction media. Change media daily. Pass each well of 12-well to one 6-well on day 8 using Dispase. On day 11 cells were switched from neural induction media to neural maintenance media. Supplement media with 20 ng/ml FGF2 on days 16-18. Pass cells 1:3 to three wells of 6-well plate on day 20 using Dispase.

Neural differentiation media:

DMEM/F12 GlutaMAX	242.5 ml
Neurobasal	241.25 ml
N-2 (100x)	2.5 ml
B-27 (50x)	5 ml
2.5 µg/mL insulin (4 mg/mL stock)	312.5 ml
1.5 mM l-glutamine (200 mM stock) or glutamax	3.75 ml
100 uM NEAA	2.5 ml
10 uM BME (1.43M)	1.75µl
50 U/mL penicillin + 50 mg/mL streptomycin	5ml

For neural induction, supplement neural maintenance media with SMAD inhibitors 2 µM DMH1 10 µM SB431542.

Immunoblotting

Protein was isolated by lysing and scraping cells in RIPA buffer plus protease inhibitor cocktails 2 and 3 and phosphatase inhibitor cocktail (Sigma P5726, P0044, P8340). Samples were rotated for 30 minutes at 4°C, sonicated and then run on 4-12% NuPAGE BisTris gels in MOPS buffer. Gels were transferred to PVDF membrane at 95V for 90 minutes using the Bio-Rad Mini Trans-Blot Cell. Membranes were incubated overnight in primary antibody diluted in 5% BSA. Membranes were then incubated for 1 hour at room temperature in secondary antibody and imaged on an Odyssey Li-Cor machine. Samples were normalized to actin or to total protein measured using Li-Cor REVERT stain. To control for intra-experimental differences in antibody concentration and Odyssey machine settings, normalized values are expressed as a percentage of the controls before averaging experimental replicates.

Statistics

All statistical analyses were conducted using GraphPad PRISM. Unless otherwise noted, individual patient-derived iPSC clones are treated as independent *n*. All other experimental or technical replicates are considered not independent and are averaged to obtain the final value for each patient clone/line. Four isogenic clones (two *TSC2+/+*, two *TSC2-/-*) were generated using CRISPR-Cas9. For experiments involving isogenic lines, both experimental and clone replicates are considered independent repeats and are shown in the data.

CHAPTER V

PATHOGENESIS AND TREATMENT OF TSC

TSC is a pediatric disorder which frequently causes debilitating intellectual disability and refractory epilepsy. Despite the fact that clinicians can diagnose TSC prenatally, there are still limited treatment options to offer. Considerable progress has been made since the identification of the *TSC1* and *TSC2* genes in 1993 and 1997. The identification of the TSC complex as a regulator of the mTOR pathway led to much hope for the effectiveness of mTORC1 inhibitors in the treatment of disease. However, many questions remain including when to treat, what cell types need to be targets, and how mutations in *TSC1* or *TSC2* alter early development. In this chapter, I will summarize findings to date using human stem cells with TSC mutations and speculate how the results fit into our understanding of the pathogenesis of neurological dysfunction in TSC.

Mechanisms of Cortical Dysfunction in TSC

Hamartomas in TSC are generally thought to arise from a "second-hit" somatic mutation in the other allele of *TSC1* or *TSC2,* resulting in excess mTORC1 activity in the affected cell but leaving the surrounding heterozygous tissue functionally normal. Accumulating evidence suggests few cells in the cortex of TSC patients acquire a second-hit. As most cells in the patients' brains apparently only harbor heterozygous mutations, it is very important to consider alternative hypotheses. First, heterozygous loss of *TSC1* or *TSC2* may be sufficient to alter cell dynamics and mTORC1 signaling. This could be in response to specific triggers (removal of growth factors or DNA damage), could occur in specific cell types or time points (neural progenitors) or might occur only in precise subcellular compartments (lysosome, nucleus neuronal axon). Second, non-cell autonomous mechanisms could be causing formation of tubers and disrupting neurodevelopment. Small numbers of cells with loss of heterozygosity (e.g. some giant cells within the tubers) could be secreting factors which disrupt neighboring neurodevelopment. Further, given our findings of increased p53 and apoptosis, the cells with loss of heterozygosity may die at a higher rate, making detection even more difficult. Notably, these possibilities are not mutually exclusive.

Long-term goals of the TSC community include defining the cellular response to stress and potential environmental exposures contributing to the variability in disease presentation (Sahin et al 2016). Cellular reprograming is a stress-filled process; it requires transcriptional and epigenetic modifications as well as increased proliferation and a metabolic shift from oxidative phosphorylation to glycolysis and further subjects the cells to DNA damage and replicative stress (Firas and Polo 2017, Hsu et al 2016, Ruiz et al 2015). In the process of generating TSP iPSCs we discovered that heterozygous *TSC2* mutant cells are more sensitive to reprogramming stress than control fibroblasts, such that they have a higher rate of integration and decreased reprogramming efficiency. We further showed that TSP fibroblast and stem cells had an exaggerated response to DNA damaging agents, UV light and neocarzinostatin, increasing p53 levels above the wildtype response. Environmental stress or growth signals (DNA damage, growth factors, and nutrients) feed into the mTORC1 pathway. During development, heterozygous cells may be exposed to an environmental "second-hit" which alters cellular differentiation. Our results strengthen the hypothesis that heterozygous cells are not normal and, as such, could be contributing to disease manifestations in TSC.

Given the number of upstream stimuli that feed into mTORC1, it is logical that appreciable signaling differences following *TSC1* or *TSC2* mutations are context dependent. Even our homozygous

TSC2-/- stem cells did not display differences in mTORC1 signaling until they were nutrient starved or differentiated towards neurons. We showed that following UV damage there may be increased phospho-S6 in the nucleus of *TSC2+/-* fibroblasts. Subcellular localization of the TSC complex and mTORC1 is critical to its function (Menon et al 2014). Thus, while heterozygous mutations in *TSC1* or *TSC2* may not appear to cause dramatic differences in mTORC1 signaling, the subcellular distribution of the TSC complex or downstream effectors could affect cellular function. The localization of the TSC complex may be especially important in neurons which contain multiple discrete compartments. Previous studies have shown that mTORC1 signaling is elevated in axons and tuberin/mTORC1 components are preferentially localized to the axons but not dendrites of neurons (Choi et al 2008, Nie et al 2010).

Hamartomas in TSC follow a different developmental timeline depending on the affected organ. The onset of hamartomas varies from prenatal to post-puberty and while some regress others continue to grow. These differences point to differences in the tissue specific pathogenesis of TSC lesions. Cortical populations, in particular, appear to be especially sensitive to TSC mutations. While formation of AML and SEGA hamartomas requires a second-hit, the cortical tubers and white matter abnormalities apparently do not. Understanding these tissue-specific differences is critical to treating TSC effectively. The goal of treatment of AML or SEGA may be to paradoxically increase enhance cellular dysfunction in homozygous cells to increase cell death and eliminate the growing hamartoma. Meanwhile, treatment of the neurological symptoms may require inhibiting mTORC1, but only in subsets of cells during a specific developmental time periods.

Mouse models have confirmed that mutations of *Tsc1* or *Tsc2* can alter learning, social interaction and neuronal morphology. However, there are dramatic differences between mouse cortical development and human cortical development. The mouse cortex develops in the classical inside-out layering with progenitors in the ventricular zone and intermediate progenitors in the subventricular zone. In contrast, human cortex develops two separate bands of proliferating progenitors- the ventricular zone/inner subventricular zone and the outer subventricular zone. It is thought that this additional layer of intermediate progenitors contributes to the increased size of human cortex. Secondly, the human cortex develops much more slowly than mouse cortex. It takes the mouse 9 days (E9-E18) to develop progenitors and all six cortical layers; in contrast, it takes humans 25 weeks. Fortunately, these differences in timing and layering are at least partially conserved in cell cultures of mouse and human stem cells differentiating to neurons (van den Ameele et al 2014). Human iPSCs then represent an opportunity to overcome species-specific differences to enable more valid modeling of early neurodevelopment in TSC.

iPSCs also allow an opportunity to define specific time points during neurodevelopment that are sensitive to *TSC1/2* mutations. Using wildtype cells, we showed that mTORC1 signaling decreases during the first few weeks of directed differentiation. As the TSC complex is the major mTORC1 inhibitor, the transition to neural progenitors may be especially sensitive to loss of functioning tuberin and hamartin proteins. Indeed, when we differentiated *TSC2-/-* cells to neural progenitors they had increased mTORC1, increased p53 and decreased mTORC2 signaling. Further, homozygous cells had impaired formation of neural progenitors. We found similar results in our plasmid-reprogrammed integrated lines. Interestingly, rapamycin failed to rescue neural progenitor differentiation at one week despite correcting mTORC1, mTORC2, and p53 signaling. Future studies will be required to confirm the phenotype in non-integrated heterozygous lines and measure subcellular localization of the TSC complex during neural development. Further, immunofluorescent studies are necessary to determine whether TSC mutations are changing neural progenitor number or organization.

Although homozygous mutations in *Tsc1* or *Tsc2* are embryonic lethal in mice (Kobayashi et al 1999, Onda et al 1999), second-hits in a small subset of cells or occurring later in development could survive long enough to disrupt neighboring cell development. Mice lacking *Tsc1* only in neurons have a reduction in myelin production and fewer mature oligodendrocytes. The authors then confirmed that

neuronal cultures from mice with knockdown or knockout of *TSC1/2* and patient iPSC-derived neurons secrete more CTGF (connective tissue growth factor) which blocks oligodendrocyte maturation (Ercan et al 2017). This is consistent with decreased myelin and oligodendrocytes observed in cortical tubers (Muhlebner et al 2016, Scholl et al 2016). Further, it provides evidence for a secreted factor regulated by *TSC1/TSC2* function which could disrupt cortical development in a non-cell autonomous manner.

A potential non-cell autonomous mechanism could be further explored using the heterozygous and homozygous *TSC1/TSC2* iPSCs we generated. Do homozygous neurons secrete signaling molecules at baseline or in response to injury/stress? Do heterozygous cells respond to secreted factors in the same way as wildtype cells? These studies would begin to answer questions about potential non-cell autonomous mechanisms contributing to TSC pathology.

Costa et al. generated homozygous and heterozygous *TSC2* neural stem cells from hESCs (Costa et al 2016). When the neural stem cells were differentiated to post-mitotic neurons, heterozygous and homozygous cells formed fewer post-mitotic neurons in a dose dependent manner. They also observed an increase in cell death in differentiating homozygous *TSC2*-/- neural stem cells. This along with our findings of increased p53 and impaired formation of neural progenitors suggests that homozygous *TSC2* mutant cells have increased apoptosis at multiple stages of neural development. This may help explain why second-hits are so rare in cortical cells but it leads to more questions. Are neurons more sensitive to loss of *TSC2*? What are the tissue specific differences that allow for formation of hamartomas without loss-of-heterozygosity in the cortex but not in the kidney? Future studies using iPSC-derived cells representing the major organs affected in TSC will begin to answer questions about the tissue specific pathogenesis of TSC.

Treatment of TSC

TSC is a heterogeneous disorder affecting multiple organs and causing diverse symptoms. When the *TSC1*/2 genes were discovered and shown to inhibit mTORC1, it was hoped that mTORC1 inhibitors would be able cure TSC. Although mTORC1 inhibitors are effective at treating some aspects of the disease, such a varied disease may require multiple treatment options.

mTORC1 inhibitors have robust inhibiting effects on cell proliferation and growth *in vitro* and *in vivo.* This has been employed to successfully treat kidney AMLs or the SEGA brain tumors. However, this appears to be a static therapy as benefits are limited to the treatment period; once mTORC1 inhibitors are discontinued hamartomas begin to regrow. These limitations suggest that perhaps our goal in treatment of AML and SEGA should not be to transiently reverse the phenotype but instead to kill the proliferating cells. AMLs and SEGAs have acquired a second-hit resulting in excess mTORC1 activity, growth and proliferation. By treating these cells with mTORC1 inhibitors, clinicians may be shifting the cells back towards a more normal phenotype while exposed to the drugs. Cells then stop expanding and multiplying but the TSC complex is still absent and unable to appropriately regulate mTORC1 activity. Once the “brakes” are removed from mTORC1, cells will return to expanding and proliferating. An alternative strategy then may be to drive these hyper-proliferative cells towards cell death either through coupling mTORC1 inhibition with additional medications, a strategy frequently employed in cancer treatment, or through entirely new targets.

Given our results suggesting increased sensitivity to cell death and apoptosis in cells with mutations in *TSC1/2*, a potential new therapeutic approach would be to enhance the apoptotic phenotype in AMLs and SEGAs. Using heterozygous and homozygous *TSC1/2* iPSCs, we could screen for treatments which increase cell death in homozygous but not heterozygous cells. An ideal treatment would

kill homozygous *TSC1/2* cells in AMLs and SEGAs without damaging the heterozygous cells which make up the majority of the patient's body.

TSC patients have a high rate of epilepsy (75-85%) and frequently develop refractory epilepsy (Chu-Shore et al 2010, Jones et al 1999). Furthermore, most patients present with seizures within the first year and cognitive outcomes are correlated with age of onset (Chu-Shore et al 2010). Treatment of epilepsy and neurocognitive disorders would significantly improve outcomes in TSC patients. Unfortunately, the use of mTORC1 inhibitors in the treatment of TSC-related epilepsy is less well supported by clinical trials. The first trial published in 2013 reported a reduction in seizure frequency in 17 out of 20 patients who had a history of refractory epilepsy (Krueger et al 2013). A subsequent study, the EXIST-1 trial, found no difference between the treatment and placebo arm; however, as seizure frequency was not the primary endpoint of that study the patients were not balanced appropriately between the two arms, complicating interpretation (Franz et al 2013). These results suggest that the mechanisms of epilepsy as well as neurocognitive symptoms of TSC may be different than the excessive growth of AMLs and SEGAs. These differences could be related to gene dosage effects or developmental differences.

If ongoing research uncovers evidence to support a non-cell autonomous mechanism of cortical dysfunction then it may be possible to target the homozygous dysfunctional cells using a similar strategy as AMLs and SEGAs. However, even if eliminating the disruptive homozygous *TSC1/2* mutant cells would cure the neurocognitive symptoms, we would need a better understanding of when during development to target these cells. The fact that tubers are formed prenatally suggests that the pathological events are occurring early in development. Our results support the idea that there may be developmental time points especially sensitive to changes in *TSC1* or *TSC2*.

However, since the majority of the cortical cells in TSC patients are heterozygous *TSC1/2* cells the goal would be to correct the phenotype rather than eliminate offending cells. Our and other's results suggest that mTORC1 inhibitors may not be able to correct the abnormal neural differentiation in TSC. The overwhelming cytostatic effect of rapamycin may be obscuring any beneficial effect on developmental pathways. Inhibitors or activators targeting a subset of downstream effectors of mTORC1 (i.e. S6K, 4EBP1, autophagy) may be required to correct neurodevelopmental phenotypes. However, other studies have shown rescue of abnormal excitability in iPSC-derived neurons, suggesting there may be some hope for treatment even without correcting early developmental abnormalities (Costa et al 2016).

Summary

Human iPSCs will allow us to answer questions about the basic function of *TSC1* and *TSC2* in multiple developing tissue types but most especially in neural progenitors. Understanding when during development and in what cell types cellular dysfunction first occurs will allow for much more targeted and effective therapies in patients. The clinical presentation of TSC is highly variable even among patients with identical gene mutations. Using iPSCs to model TSC offers great potential as a method to address genotype-phenotype correlations and potential modifiers. Much of the promise of patient-derived iPSC technology is hampered by the inherent variability of lines from different individuals. Use of CRISPR-Cas9 to generate isogenic lines either by replicating the mutation in a wildtype line or correcting the mutation in a patient line will overcome many of these limitations. Defining a robust phenotype in isogenic lines is the first step to then analyzing differences in individual patient lines. The goal is to not only understand more about the basic biology of TSC, but to be able to use patient iPSC lines to predict disease severity and response to various treatments.

APPENDIX

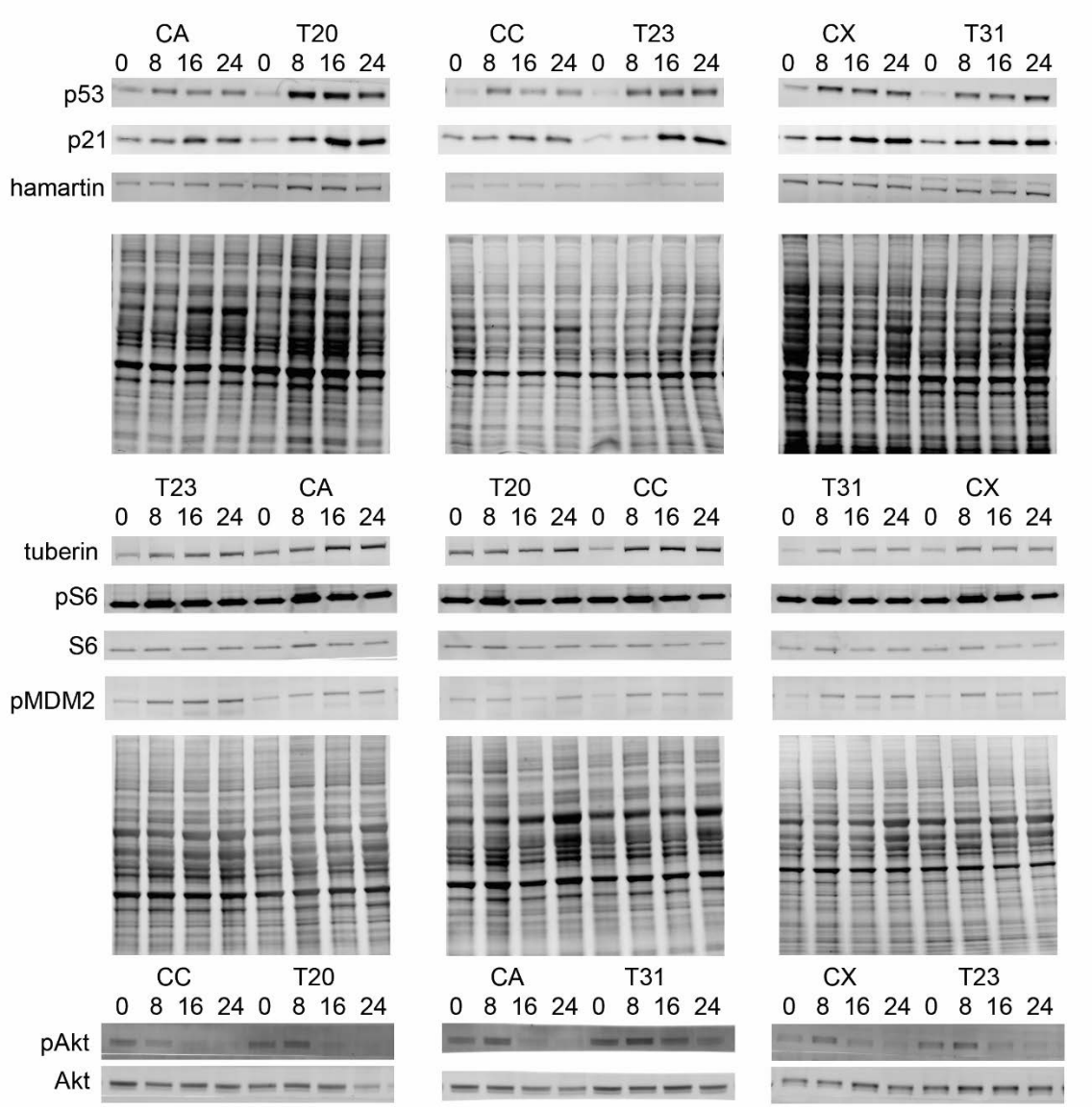

Figure 5.1. Immunoblot of fibroblast time course response to UV challenge

Fibroblast lines were exposed to UV light and protein isolated at 0, 8 16, and 24 hours post-exposure was analyzed by immunoblot. Protein levels were normalized to total protein.

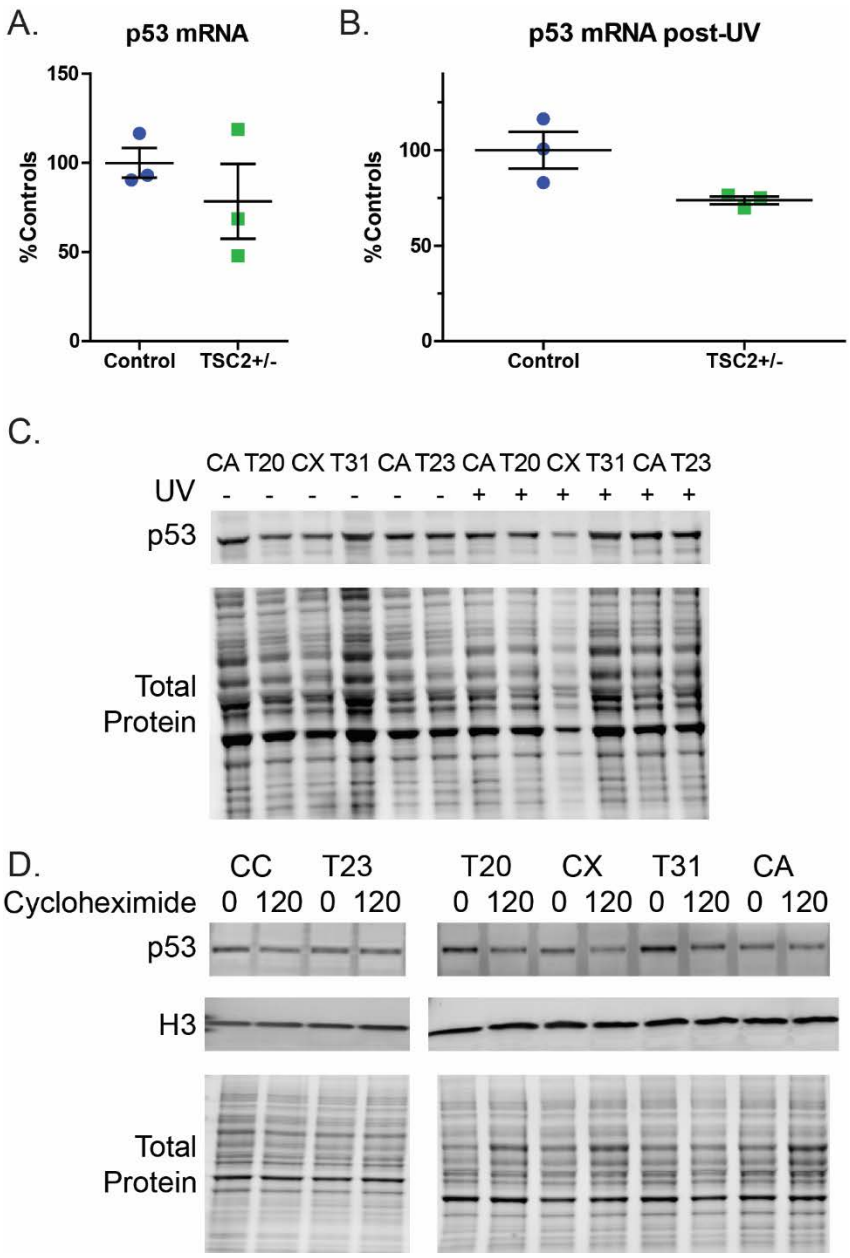

Figure 5.2 mRNA, translation and stability of p53 in fibroblasts

(**A**) mRNA levels of *TP53* in fibroblasts were measured by qPCR at baseline using primers directed to the 5' end. Samples were normalized to *ACTIN* and *PGK1*. (n=3, p=0.395, t-test) (**B**) Fibroblasts were challenged with UV light and RNA was isolated 24 hours later. Levels of *TP53* mRNA were measured by qPCR using primers directed to the 5' end (n=3, genotype p=0.056, t-test) (**C**) Fibroblasts were treated with the proteasome inhibitor MG132 (1 μM) for 6 hours with or without UV challenge. p53 protein levels were analyzed by immunoblot. (**D**) Fibroblasts were challenged with UV light and 15 hours later treated with the translation inhibitor cycloheximide (100 μM) for two hours. p53 protein levels were analyzed by immunoblot.

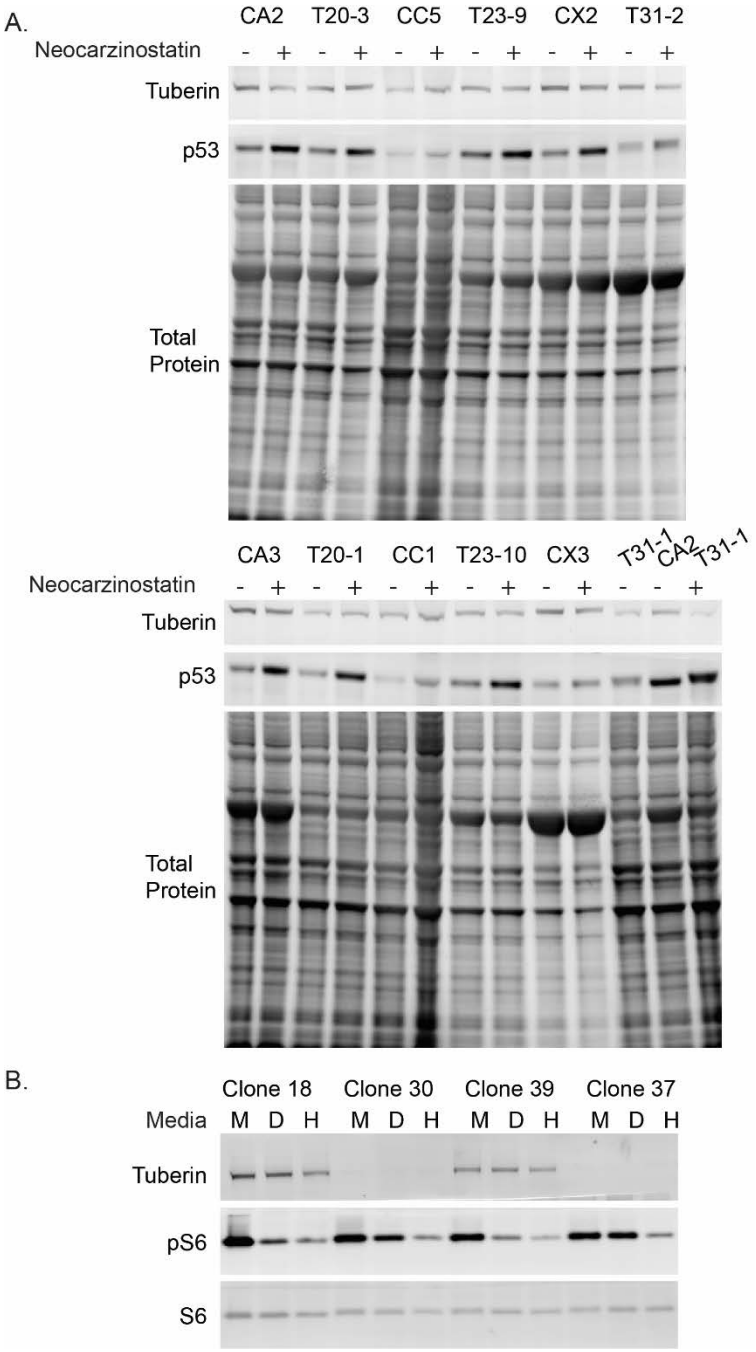

Figure 5.3 Immunoblot of *TSC2* heterozygous and homozygous stem cells

(A) Non-integrated iPS lines generated from *TSC2* heterozygous patient fibroblast lines treated with the DNA damaging agent neocarzinostatin for 1 hour show increased p53 relative to controls. (*n*=6, 1-3 experimental repeats per sample; *p*=0.04 *t*-test) **(B)** Homozygous *TSC2-/-* and isogenic control stem cells were nutrient starved for 2.5 hours in DMEM without glucose or HBSS media. Protein levels of pS6 were elevated in *TSC2-/-* iPS cells following nutrient starvation. (*n*=4, 2 clones with 2 experimental repeats; *p*=0.0002 *t*-test)

REFERENCES

Agarwal S, Bell CM, Taylor SM, Moran RG (2016). p53 Deletion or Hotspot Mutations Enhance mTORC1 Activity by Altering Lysosomal Dynamics of TSC2 and Rheb. *Mol Cancer Res* **14:** 66-77.

Alfaiz AA, Micale L, Mandriani B, Augello B, Pellico MT, Chrast J *et al* (2014). TBC1D7 mutations are associated with intellectual disability, macrocrania, patellar dislocation, and celiac disease. *Hum Mutat* **35:** 447-451.

Altman NR, Purser RK, Post MJ (1988). Tuberous sclerosis: characteristics at CT and MR imaging. *Radiology* **167:** 527-532.

Amin S, Lux A, Calder N, Laugharne M, Osborne J, O'Callaghan F (2016). Causes of mortality in individuals with tuberous sclerosis complex. *Dev Med Child Neurol*.

Arulrajah S, Ertan G, Jordan L, Tekes A, Khaykin E, Izbudak I *et al* (2009). Magnetic resonance imaging and diffusion-weighted imaging of normal-appearing white matter in children and young adults with tuberous sclerosis complex. *Neuroradiology* **51:** 781-786.

Bateman JM, McNeill H (2004). Temporal control of differentiation by the insulin receptor/tor pathway in Drosophila. *Cell* **119:** 87-96.

Benoit V, Hellin AC, Huygen S, Gielen J, Bours V, Merville MP (2000). Additive effect between NF-kappaB subunits and p53 protein for transcriptional activation of human p53 promoter. *Oncogene* **19:** 4787-4794.

Bilanges B, Argonza-Barrett R, Kolesnichenko M, Skinner C, Nair M, Chen M *et al* (2007). Tuberous sclerosis complex proteins 1 and 2 control serum-dependent translation in a TOP-dependent and -independent manner. *Mol Cell Biol* **27:** 5746-5764.

Bissler JJ, McCormack FX, Young LR, Elwing JM, Chuck G, Leonard JM *et al* (2008). Sirolimus for angiomyolipoma in tuberous sclerosis complex or lymphangioleiomyomatosis. *N Engl J Med* **358:** 140-151.

Boisvert FM, Lamond AI (2010). p53-Dependent subcellular proteome localization following DNA damage. *Proteomics* **10:** 4087-4097.

Bolton PF, Park RJ, Higgins JN, Griffiths PD, Pickles A (2002). Neuro-epileptic determinants of autism spectrum disorders in tuberous sclerosis complex. *Brain* **125:** 1247-1255.

Boulon S, Westman BJ, Hutten S, Boisvert FM, Lamond AI (2010). The nucleolus under stress. *Mol Cell* **40:** 216-227.

Bourneville D (1880). Sclerose tubereuse des circonvolutions cerebrales: idiotie et epilepsie hemiplegique. *Arch Neurol (Paris)* **1:** 81-91.

Brown EJ, Albers MW, Shin TB, Ichikawa K, Keith CT, Lane WS *et al* (1994). A mammalian protein targeted by G1-arresting rapamycin-receptor complex. *Nature* **369:** 756-758.

Brugarolas J, Lei K, Hurley RL, Manning BD, Reiling JH, Hafen E *et al* (2004). Regulation of mTOR function in response to hypoxia by REDD1 and the TSC1/TSC2 tumor suppressor complex. *Genes & development* **18:** 2893-2904.

Buccoliero AM, Franchi A, Castiglione F, Gheri CF, Mussa F, Giordano F *et al* (2009). Subependymal giant cell astrocytoma (SEGA): Is it an astrocytoma? Morphological, immunohistochemical and ultrastructural study. *Neuropathology* **29:** 25-30.

Budanov AV, Karin M (2008). p53 target genes sestrin1 and sestrin2 connect genotoxic stress and mTOR signaling. *Cell* **134:** 451-460.

Cam M, Bid HK, Xiao L, Zambetti GP, Houghton PJ, Cam H (2014). p53/TAp63 and AKT regulate mammalian target of rapamycin complex 1 (mTORC1) signaling through two independent parallel pathways in the presence of DNA damage. *J Biol Chem* **289:** 4083-4094.

Cao J, Tyburczy ME, Moss J, Darling TN, Widlund HR, Kwiatkowski DJ (2017). Tuberous sclerosis complex inactivation disrupts melanogenesis via mTORC1 activation. *J Clin Invest* **127:** 349-364.

Capo-Chichi JM, Tcherkezian J, Hamdan FF, Decarie JC, Dobrzeniecka S, Patry L *et al* (2013). Disruption of TBC1D7, a subunit of the TSC1-TSC2 protein complex, in intellectual disability and megalencephaly. *J Med Genet* **50:** 740-744.

Cardamone M, Flanagan D, Mowat D, Kennedy SE, Chopra M, Lawson JA (2014). Mammalian target of rapamycin inhibitors for intractable epilepsy and subependymal giant cell astrocytomas in tuberous sclerosis complex. *J Pediatr* **164:** 1195-1200.

Castedo M, Ferri KF, Kroemer G (2002). Mammalian target of rapamycin (mTOR): pro- and anti-apoptotic. *Cell Death Differ* **9:** 99-100.

Chandra PS, Salamon N, Nguyen ST, Chang JW, Huynh MN, Cepeda C *et al* (2007). Infantile spasm-associated microencephaly in tuberous sclerosis complex and cortical dysplasia. *Neurology* **68:** 438-445.

Chauvin C, Koka V, Nouschi A, Mieulet V, Hoareau-Aveilla C, Dreazen A *et al* (2014). Ribosomal protein S6 kinase activity controls the ribosome biogenesis transcriptional program. *Oncogene* **33:** 474-483.

Chen C, Liu Y, Liu R, Ikenoue T, Guan KL, Zheng P (2008). TSC-mTOR maintains quiescence and function of hematopoietic stem cells by repressing mitochondrial biogenesis and reactive oxygen species. *J Exp Med* **205:** 2397-2408.

Choi YJ, Di Nardo A, Kramvis I, Meikle L, Kwiatkowski DJ, Sahin M *et al* (2008). Tuberous sclerosis complex proteins control axon formation. *Genes Dev* **22:** 2485-2495.

Chu-Shore CJ, Major P, Camposano S, Muzykewicz D, Thiele EA (2010). The natural history of epilepsy in tuberous sclerosis complex. *Epilepsia* **51:** 1236-1241.

Costa V, Aigner S, Vukcevic M, Sauter E, Behr K, Ebeling M *et al* (2016). mTORC1 Inhibition Corrects Neurodevelopmental and Synaptic Alterations in a Human Stem Cell Model of Tuberous Sclerosis. *Cell Rep* **15:** 86-95.

Dabora SL, Jozwiak S, Franz DN, Roberts PS, Nieto A, Chung J *et al* (2001). Mutational analysis in a cohort of 224 tuberous sclerosis patients indicates increased severity of TSC2, compared with TSC1, disease in multiple organs. *Am J Hum Genet* **68:** 64-80.

Deffie A, Wu H, Reinke V, Lozano G (1993). The tumor suppressor p53 regulates its own transcription. *Mol Cell Biol* **13:** 3415-3423.

Devlin LA, Shepherd CH, Crawford H, Morrison PJ (2006). Tuberous sclerosis complex: clinical features, diagnosis, and prevalence within Northern Ireland. *Dev Med Child Neurol* **48:** 495-499.

DeYoung MP, Horak P, Sofer A, Sgroi D, Ellisen LW (2008). Hypoxia regulates TSC1/2-mTOR signaling and tumor suppression through REDD1-mediated 14-3-3 shuttling. *Genes Dev* **22:** 239-251.

Dibble CC, Elis W, Menon S, Qin W, Klekota J, Asara JM *et al* (2012). TBC1D7 is a third subunit of the TSC1-TSC2 complex upstream of mTORC1. *Mol Cell* **47:** 535-546.

Ehninger D, Han S, Shilyansky C, Zhou Y, Li W, Kwiatkowski DJ *et al* (2008). Reversal of learning deficits in a Tsc2+/- mouse model of tuberous sclerosis. *Nat Med* **14:** 843-848.

Eker R (1954). Familial renal adenomas in Wistar rats; a preliminary report. *Acta Pathol Microbiol Scand* **34:** 554-562.

Ekong R, Nellist M, Hoogeveen-Westerveld M, Wentink M, Panzer J, Sparagana S *et al* (2016). Variants Within TSC2 Exons 25 and 31 Are Very Unlikely to Cause Clinically Diagnosable Tuberous Sclerosis. *Hum Mutat* **37:** 364-370.

Eluvathingal TJ, Behen ME, Chugani HT, Janisse J, Bernardi B, Chakraborty P *et al* (2006). Cerebellar lesions in tuberous sclerosis complex: neurobehavioral and neuroimaging correlates. *J Child Neurol* **21:** 846-851.

Ercan E, Han JM, Di Nardo A, Winden K, Han MJ, Hoyo L *et al* (2017). Neuronal CTGF/CCN2 negatively regulates myelination in a mouse model of tuberous sclerosis complex. *J Exp Med* **214:** 681-697.

Ess KC, Uhlmann EJ, Li W, Li H, Declue JE, Crino PB *et al* (2004). Expression profiling in tuberous sclerosis complex (TSC) knockout mouse astrocytes to characterize human TSC brain pathology. *Glia* **46:** 28-40.

Ess KC, Kamp CA, Tu BP, Gutmann DH (2005). Developmental origin of subependymal giant cell astrocytoma in tuberous sclerosis complex. *Neurology* **64:** 1446-1449.

European (1993). Identification and characterization of the tuberous sclerosis gene on chromosome 16. *Cell* **75:** 1305-1315.

Feliciano DM, Lin TV, Hartman NW, Bartley CM, Kubera C, Hsieh L *et al* (2013). A circuitry and biochemical basis for tuberous sclerosis symptoms: from epilepsy to neurocognitive deficits. *Int J Dev Neurosci* **31:** 667-678.

Feng Z, Zhang H, Levine AJ, Jin S (2005). The coordinate regulation of the p53 and mTOR pathways in cells. *Proc Natl Acad Sci U S A* **102:** 8204-8209.

Feng Z, Hu W, de Stanchina E, Teresky AK, Jin S, Lowe S *et al* (2007). The regulation of AMPK beta1, TSC2, and PTEN expression by p53: stress, cell and tissue specificity, and the role of these gene products in modulating the IGF-1-AKT-mTOR pathways. *Cancer Res* **67:** 3043-3053.

Ferreira-Cerca S, Poll G, Gleizes PE, Tschochner H, Milkereit P (2005). Roles of eukaryotic ribosomal proteins in maturation and transport of pre-18S rRNA and ribosome function. *Mol Cell* **20:** 263-275.

Firas J, Polo JM (2017). Towards understanding transcriptional networks in cellular reprogramming. *Curr Opin Genet Dev* **46:** 1-8.

Fischer M (2017). Census and evaluation of p53 target genes. *Oncogene* **36:** 3943-3956.

Francoz S, Froment P, Bogaerts S, De Clercq S, Maetens M, Doumont G *et al* (2006). Mdm4 and Mdm2 cooperate to inhibit p53 activity in proliferating and quiescent cells in vivo. *Proc Natl Acad Sci U S A* **103:** 3232-3237.

Franz DN, Leonard J, Tudor C, Chuck G, Care M, Sethuraman G *et al* (2006). Rapamycin causes regression of astrocytomas in tuberous sclerosis complex. *Ann Neurol* **59:** 490-498.

Franz DN (2013). Everolimus in the treatment of subependymal giant cell astrocytomas, angiomyolipomas, and pulmonary and skin lesions associated with tuberous sclerosis complex. *Biologics : targets & therapy* **7:** 211-221.

Franz DN, Belousova E, Sparagana S, Bebin EM, Frost M, Kuperman R *et al* (2013). Efficacy and safety of everolimus for subependymal giant cell astrocytomas associated with tuberous sclerosis complex (EXIST-1): a multicentre, randomised, placebo-controlled phase 3 trial. *Lancet* **381:** 125-132.

Fuhs H (1925). Über Naevus multiplex Pringle. *Archiv für Dermatologie und Syphilis* **148:** 509-515.

Gangloff YG, Mueller M, Dann SG, Svoboda P, Sticker M, Spetz JF *et al* (2004). Disruption of the mouse mTOR gene leads to early postimplantation lethality and prohibits embryonic stem cell development. *Mol Cell Biol* **24:** 9508-9516.

Ganley IG, Lam du H, Wang J, Ding X, Chen S, Jiang X (2009). ULK1.ATG13.FIP200 complex mediates mTOR signaling and is essential for autophagy. *J Biol Chem* **284:** 12297-12305.

Garaci FG, Floris R, Bozzao A, Manenti G, Simonetti A, Lupattelli T *et al* (2004). Increased brain apparent diffusion coefficient in tuberous sclerosis. *Radiology* **232:** 461-465.

Garelick MG, Mackay VL, Yanagida A, Academia EC, Schreiber KH, Ladiges WC *et al* (2013). Chronic rapamycin treatment or lack of S6K1 does not reduce ribosome activity in vivo. *Cell Cycle* **12:** 2493-2504.

Gingras AC, Raught B, Gygi SP, Niedzwiecka A, Miron M, Burley SK *et al* (2001). Hierarchical phosphorylation of the translation inhibitor 4E-BP1. *Genes Dev* **15:** 2852-2864.

Ginsberg D, Mechta F, Yaniv M, Oren M (1991). Wild-type p53 can down-modulate the activity of various promoters. *Proc Natl Acad Sci U S A* **88:** 9979-9983.

Goodman M, Lamm SH, Engel A, Shepherd CW, Houser OW, Gomez MR (1997). Cortical tuber count: a biomarker indicating neurologic severity of tuberous sclerosis complex. *J Child Neurol* **12:** 85-90.

Goorden SM, van Woerden GM, van der Weerd L, Cheadle JP, Elgersma Y (2007). Cognitive deficits in Tsc1+/- mice in the absence of cerebral lesions and seizures. *Ann Neurol* **62:** 648-655.

Goudarzi KM, Nister M, Lindstrom MS (2014). mTOR inhibitors blunt the p53 response to nucleolar stress by regulating RPL11 and MDM2 levels. *Cancer Biol Ther* **15:** 1499-1514.

Gressner AM, Wool IG (1974). The phosphorylation of liver ribosomal proteins in vivo. Evidence that only a single small subunit protein (S6) is phosphorylated. *J Biol Chem* **249:** 6917-6925.

Gunther M, Penrose L (1935). The genetics of epiloia. *Journal of Genetics* **31:** 413-430.

Habib SL, Yadav A, Mahimainathan L, Valente AJ (2011). Regulation of PI 3-K, PTEN, p53, and mTOR in Malignant and Benign Tumors Deficient in Tuberin. *Genes Cancer* **2:** 1051-1060.

Harrington LS, Findlay GM, Gray A, Tolkacheva T, Wigfield S, Rebholz H *et al* (2004). The TSC1-2 tumor suppressor controls insulin-PI3K signaling via regulation of IRS proteins. *J Cell Biol* **166:** 213-223.

Hartdegen A (1881). Ein Fall von multipler Verhärtung des Grosshirns nebst histologisch eigenartigen harten Geschwülsten der Seitenventrikel („Glioma gangliocellulare “) bei einem Neugeborenen. *Eur Arch Psychiatry Clin Neurosci* **11:** 117-131.

Haupt Y, Maya R, Kazaz A, Oren M (1997). Mdm2 promotes the rapid degradation of p53. *Nature* **387:** 296-299.

Hayashi T, Koike K, Kumasaka T, Saito T, Mitani K, Terao Y *et al* (2012). Uterine angiosarcoma associated with lymphangioleiomyomatosis in a patient with tuberous sclerosis complex: an autopsy case report with immunohistochemical and genetic analysis. *Hum Pathol* **43:** 1777-1784.

He G, Zhang YW, Lee JH, Zeng SX, Wang YV, Luo Z *et al* (2014). AMP-activated protein kinase induces p53 by phosphorylating MDMX and inhibiting its activity. *Mol Cell Biol* **34:** 148-157.

He J, Kang L, Wu T, Zhang J, Wang H, Gao H *et al* (2012). An elaborate regulation of Mammalian target of rapamycin activity is required for somatic cell reprogramming induced by defined transcription factors. *Stem Cells Dev* **21:** 2630-2641.

Henske EP, Scheithauer BW, Short MP, Wollmann R, Nahmias J, Hornigold N *et al* (1996). Allelic loss is frequent in tuberous sclerosis kidney lesions but rare in brain lesions. *Am J Hum Genet* **59:** 400-406.

Hinton RB, Prakash A, Romp RL, Krueger DA, Knilans TK (2014). Cardiovascular manifestations of tuberous sclerosis complex and summary of the revised diagnostic criteria and surveillance and management recommendations from the International Tuberous Sclerosis Consensus Group. *J Am Heart Assoc* **3:** e001493.

Hirose T, Scheithauer BW, Lopes MB, Gerber HA, Altermatt HJ, Hukee MJ *et al* (1995). Tuber and subependymal giant cell astrocytoma associated with tuberous sclerosis: an immunohistochemical, ultrastructural, and immunoelectron and microscopic study. *Acta Neuropathol* **90:** 387-399.

Hong H, Takahashi K, Ichisaka T, Aoi T, Kanagawa O, Nakagawa M *et al* (2009). Suppression of induced pluripotent stem cell generation by the p53-p21 pathway. *Nature* **460:** 1132-1135.

Horton LE, Bushell M, Barth-Baus D, Tilleray VJ, Clemens MJ, Hensold JO (2002). p53 activation results in rapid dephosphorylation of the eIF4E-binding protein 4E-BP1, inhibition of ribosomal protein S6 kinase and inhibition of translation initiation. *Oncogene* **21:** 5325-5334.

Hosokawa N, Hara T, Kaizuka T, Kishi C, Takamura A, Miura Y *et al* (2009). Nutrient-dependent mTORC1 association with the ULK1-Atg13-FIP200 complex required for autophagy. *Mol Biol Cell* **20:** 1981-1991.

Hsu PD, Scott DA, Weinstein JA, Ran FA, Konermann S, Agarwala V *et al* (2013). DNA targeting specificity of RNA-guided Cas9 nucleases. *Nat Biotechnol* **31:** 827-832.

Hsu YC, Chen CT, Wei YH (2016). Mitochondrial resetting and metabolic reprogramming in induced pluripotent stem cells and mitochondrial disease modeling. *Biochim Biophys Acta* **1860:** 686-693.

Hudson JM, Frade R, Bar-Eli M (1995). Wild-type p53 regulates its own transcription in a cell-type specific manner. *DNA Cell Biol* **14:** 759-766.

Humphrey A, Higgins JN, Yates JR, Bolton PF (2004). Monozygotic twins with tuberous sclerosis discordant for the severity of developmental deficits. *Neurology* **62:** 795-798.

Inoki K, Li Y, Zhu T, Wu J, Guan KL (2002). TSC2 is phosphorylated and inhibited by Akt and suppresses mTOR signalling. *Nat Cell Biol* **4:** 648-657.

Inoki K, Li Y, Xu T, Guan KL (2003a). Rheb GTPase is a direct target of TSC2 GAP activity and regulates mTOR signaling. *Genes Dev* **17:** 1829-1834.

Inoki K, Zhu T, Guan KL (2003b). TSC2 mediates cellular energy response to control cell growth and survival. *Cell* **115:** 577-590.

Inoki K, Ouyang H, Zhu T, Lindvall C, Wang Y, Zhang X *et al* (2006). TSC2 integrates Wnt and energy signals via a coordinated phosphorylation by AMPK and GSK3 to regulate cell growth. *Cell* **126:** 955-968.

Jacobs WB, Kaplan DR, Miller FD (2006). The p53 family in nervous system development and disease. *J Neurochem* **97:** 1571-1584.

Jambaque I, Cusmai R, Curatolo P, Cortesi F, Perrot C, Dulac O (1991). Neuropsychological aspects of tuberous sclerosis in relation to epilepsy and MRI findings. *Dev Med Child Neurol* **33:** 698-705.

Jansen FE, Braams O, Vincken KL, Algra A, Anbeek P, Jennekens-Schinkel A *et al* (2008a). Overlapping neurologic and cognitive phenotypes in patients with TSC1 or TSC2 mutations. *Neurology* **70:** 908-915.

Jansen FE, Vincken KL, Algra A, Anbeek P, Braams O, Nellist M *et al* (2008b). Cognitive impairment in tuberous sclerosis complex is a multifactorial condition. *Neurology* **70:** 916-923.

Jones AC, Shyamsundar MM, Thomas MW, Maynard J, Idziaszczyk S, Tomkins S *et al* (1999). Comprehensive mutation analysis of TSC1 and TSC2-and phenotypic correlations in 150 families with tuberous sclerosis. *Am J Hum Genet* **64:** 1305-1315.

Julien LA, Carriere A, Moreau J, Roux PP (2010). mTORC1-activated S6K1 phosphorylates Rictor on threonine 1135 and regulates mTORC2 signaling. *Mol Cell Biol* **30:** 908-921.

Jung CH, Jun CB, Ro SH, Kim YM, Otto NM, Cao J *et al* (2009). ULK-Atg13-FIP200 complexes mediate mTOR signaling to the autophagy machinery. *Mol Biol Cell* **20:** 1992-2003.

Kabat D (1970). Phosphorylation of ribosomal proteins in rabbit reticulocytes. Characterization and regulatory aspects. *Biochemistry (Mosc)* **9:** 4160-4175.

Kang YJ, Lu MK, Guan KL (2011). The TSC1 and TSC2 tumor suppressors are required for proper ER stress response and protect cells from ER stress-induced apoptosis. *Cell Death Differ* **18:** 133-144.

Kawamura T, Suzuki J, Wang YV, Menendez S, Morera LB, Raya A *et al* (2009). Linking the p53 tumour suppressor pathway to somatic cell reprogramming. *Nature* **460:** 1140-1144.

Khalaileh A, Dreazen A, Khatib A, Apel R, Swisa A, Kidess-Bassir N *et al* (2013). Phosphorylation of ribosomal protein S6 attenuates DNA damage and tumor suppression during development of pancreatic cancer. *Cancer Res* **73:** 1811-1820.

Kim TH, Leslie P, Zhang Y (2014). Ribosomal proteins as unrevealed caretakers for cellular stress and genomic instability. *Oncotarget* **5:** 860-871.

Kobayashi T, Nishizawa M, Hirayama Y, Kobayashi E, Hino O (1995). cDNA structure, alternative splicing and exon-intron organization of the predisposing tuberous sclerosis (Tsc2) gene of the Eker rat model. *Nucleic Acids Res* **23:** 2608-2613.

Kobayashi T, Minowa O, Kuno J, Mitani H, Hino O, Noda T (1999). Renal carcinogenesis, hepatic hemangiomatosis, and embryonic lethality caused by a germ-line Tsc2 mutation in mice. *Cancer Res* **59:** 1206-1211.

Koh S, Jayakar P, Dunoyer C, Whiting SE, Resnick TJ, Alvarez LA *et al* (2000). Epilepsy surgery in children with tuberous sclerosis complex: presurgical evaluation and outcome. *Epilepsia* **41:** 1206-1213.

Kothare SV, Singh K, Chalifoux JR, Staley BA, Weiner HL, Menzer K *et al* (2014). Severity of manifestations in tuberous sclerosis complex in relation to genotype. *Epilepsia* **55:** 1025-1029.

Kovacina KS, Park GY, Bae SS, Guzzetta AW, Schaefer E, Birnbaum MJ *et al* (2003). Identification of a proline-rich Akt substrate as a 14-3-3 binding partner. *J Biol Chem* **278:** 10189-10194.

Krishnan ML, Commowick O, Jeste SS, Weisenfeld N, Hans A, Gregas MC *et al* (2010). Diffusion features of white matter in tuberous sclerosis with tractography. *Pediatr Neurol* **42:** 101-106.

Krueger DA, Wilfong AA, Holland-Bouley K, Anderson AE, Agricola K, Tudor C *et al* (2013). Everolimus treatment of refractory epilepsy in tuberous sclerosis complex. *Ann Neurol*.

Kruger T, Zentgraf H, Scheer U (2007). Intranucleolar sites of ribosome biogenesis defined by the localization of early binding ribosomal proteins. *J Cell Biol* **177:** 573-578.

Kubbutat MH, Jones SN, Vousden KH (1997). Regulation of p53 stability by Mdm2. *Nature* **387:** 299-303.

Kwiatkowski DJ, Whittemore VH, Thiele EA (2011). *Tuberous Sclerosis Complex: Genes, Clinical Features and Therapeutics*. Wiley.

Lai KP, Leong WF, Chau JF, Jia D, Zeng L, Liu H *et al* (2010). S6K1 is a multifaceted regulator of Mdm2 that connects nutrient status and DNA damage response. *EMBO J* **29:** 2994-3006.

Laplante M, Sabatini DM (2012). mTOR signaling in growth control and disease. *Cell* **149:** 274-293.

Lee CH, Inoki K, Karbowniczek M, Petroulakis E, Sonenberg N, Henske EP *et al* (2007). Constitutive mTOR activation in TSC mutants sensitizes cells to energy starvation and genomic damage via p53. *EMBO J* **26:** 4812-4823.

Lee CW, Wong LL, Tse EY, Liu HF, Leong VY, Lee JM *et al* (2012). AMPK promotes p53 acetylation via phosphorylation and inactivation of SIRT1 in liver cancer cells. *Cancer Res* **72:** 4394-4404.

Lewis WW, Sahin M, Scherrer B, Peters JM, Suarez RO, Vogel-Farley VK *et al* (2013). Impaired language pathways in tuberous sclerosis complex patients with autism spectrum disorders. *Cereb Cortex* **23:** 1526-1532.

Li H, Collado M, Villasante A, Strati K, Ortega S, Canamero M *et al* (2009). The Ink4/Arf locus is a barrier for iPS cell reprogramming. *Nature* **460:** 1136-1139.

Li S, Thangapazham RL, Wang JA, Rajesh S, Kao TC, Sperling L *et al* (2011). Human TSC2-null fibroblast-like cells induce hair follicle neogenesis and hamartoma morphogenesis. *Nat Commun* **2:** 235.

Li Y, Stockton ME, Bhuiyan I, Eisinger BE, Gao Y, Miller JL *et al* (2016). MDM2 inhibition rescues neurogenic and cognitive deficits in a mouse model of fragile X syndrome. *Sci Trans Med* **8:** 336ra361.

Lopes JP, Agostinho P (2011). Cdk5: multitasking between physiological and pathological conditions. *Prog Neurobiol* **94:** 49-63.

Lopes MB, Altermatt HJ, Scheithauer BW, Shepherd CW, VandenBerg SR (1996). Immunohistochemical characterization of subependymal giant cell astrocytomas. *Acta Neuropathol* **91:** 368-375.

Loughery J, Cox M, Smith LM, Meek DW (2014). Critical role for p53-serine 15 phosphorylation in stimulating transactivation at p53-responsive promoters. *Nucleic Acids Res* **42:** 7666-7680.

Ma L, Chen Z, Erdjument-Bromage H, Tempst P, Pandolfi PP (2005). Phosphorylation and functional inactivation of TSC2 by Erk implications for tuberous sclerosis and cancer pathogenesis. *Cell* **121:** 179-193.

Magri L, Cambiaghi M, Cominelli M, Alfaro-Cervello C, Cursi M, Pala M *et al* (2011). Sustained activation of mTOR pathway in embryonic neural stem cells leads to development of tuberous sclerosis complex-associated lesions. *Cell Stem Cell* **9:** 447-462.

Magri L, Galli R (2013). mTOR signaling in neural stem cells: from basic biology to disease. *Cell Mol Life Sci* **70:** 2887-2898.

Maheshwar MM, Sandford R, Nellist M, Cheadle JP, Sgotto B, Vaudin M *et al* (1996). Comparative analysis and genomic structure of the tuberous sclerosis 2 (TSC2) gene in human and pufferfish. *Hum Mol Genet* **5:** 562.

Makki MI, Chugani DC, Janisse J, Chugani HT (2007). Characteristics of abnormal diffusivity in normal-appearing white matter investigated with diffusion tensor MR imaging in tuberous sclerosis complex. *AJNR Am J Neuroradiol* **28:** 1662-1667.

Mandegar MA, Huebsch N, Frolov EB, Shin E, Truong A, Olvera MP *et al* (2016). CRISPR Interference Efficiently Induces Specific and Reversible Gene Silencing in Human iPSCs. *Cell Stem Cell* **18:** 541-553.

Manning BD, Tee AR, Logsdon MN, Blenis J, Cantley LC (2002). Identification of the tuberous sclerosis complex-2 tumor suppressor gene product tuberin as a target of the phosphoinositide 3-kinase/akt pathway. *Mol Cell* **10:** 151-162.

Marcel V, Dichtel-Danjoy ML, Sagne C, Hafsi H, Ma D, Ortiz-Cuaran S *et al* (2011). Biological functions of p53 isoforms through evolution: lessons from animal and cellular models. *Cell Death Differ* **18:** 1815-1824.

Marcotte L, Aronica E, Baybis M, Crino PB (2012). Cytoarchitectural alterations are widespread in cerebral cortex in tuberous sclerosis complex. *Acta Neuropathol* **123:** 685-693.

Marine JC, Francoz S, Maetens M, Wahl G, Toledo F, Lozano G (2006). Keeping p53 in check: essential and synergistic functions of Mdm2 and Mdm4. *Cell Death Differ* **13:** 927-934.

Marion RM, Strati K, Li H, Murga M, Blanco R, Ortega S *et al* (2009). A p53-mediated DNA damage response limits reprogramming to ensure iPS cell genomic integrity. *Nature* **460:** 1149-1153.

Martin-Perez J, Thomas G (1983). Ordered phosphorylation of 40S ribosomal protein S6 after serum stimulation of quiescent 3T3 cells. *Proc Natl Acad Sci U S A* **80:** 926-930.

Martin KR, Zhou W, Bowman MJ, Shih J, Au KS, Dittenhafer-Reed KE *et al* (2017). The genomic landscape of tuberous sclerosis complex. *Nat Commun* **8:** 15816.

Martina JA, Chen Y, Gucek M, Puertollano R (2012). MTORC1 functions as a transcriptional regulator of autophagy by preventing nuclear transport of TFEB. *Autophagy* **8:** 903-914.

McCormack FX, Inoue Y, Moss J, Singer LG, Strange C, Nakata K *et al* (2011). Efficacy and safety of sirolimus in lymphangioleiomyomatosis. *N Engl J Med* **364:** 1595-1606.

Meletis K, Wirta V, Hede SM, Nister M, Lundeberg J, Frisen J (2006). p53 suppresses the self-renewal of adult neural stem cells. *Development* **133:** 363-369.

Mendrysa SM, Ghassemifar S, Malek R (2011). p53 in the CNS: Perspectives on Development, Stem Cells, and Cancer. *Genes Cancer* **2:** 431-442.

Menon S, Dibble CC, Talbott G, Hoxhaj G, Valvezan AJ, Takahashi H *et al* (2014). Spatial control of the TSC complex integrates insulin and nutrient regulation of mTORC1 at the lysosome. *Cell* **156:** 771-785.

Merkle FT, Ghosh S, Kamitaki N, Mitchell J, Avior Y, Mello C *et al* (2017). Human pluripotent stem cells recurrently acquire and expand dominant negative P53 mutations. *Nature* **545:** 229-233.

Meyuhas O (2015). Ribosomal Protein S6 Phosphorylation: Four Decades of Research. *Int Rev Cell Mol Biol* **320:** 41-73.

Miceli AP, Saporita AJ, Weber JD (2012). Hypergrowth mTORC1 signals translationally activate the ARF tumor suppressor checkpoint. *Mol Cell Biol* **32:** 348-364.

Mieulet V, Roceri M, Espeillac C, Sotiropoulos A, Ohanna M, Oorschot V *et al* (2007). S6 kinase inactivation impairs growth and translational target phosphorylation in muscle cells maintaining proper regulation of protein turnover. *Am J Physiol Cell Physiol* **293:** C712-722.

Montagne J, Stewart MJ, Stocker H, Hafen E, Kozma SC, Thomas G (1999). Drosophila S6 kinase: a regulator of cell size. *Science* **285:** 2126-2129.

Muhlebner A, van Scheppingen J, Hulshof HM, Scholl T, Iyer AM, Anink JJ *et al* (2016). Novel Histopathological Patterns in Cortical Tubers of Epilepsy Surgery Patients with Tuberous Sclerosis Complex. *PLoS One* **11:** e0157396.

Muhler MR, Rake A, Schwabe M, Schmidt S, Kivelitz D, Chaoui R *et al* (2007). Value of fetal cerebral MRI in sonographically proven cardiac rhabdomyoma. *Pediatric radiology* **37:** 467-474.

Murakami M, Ichisaka T, Maeda M, Oshiro N, Hara K, Edenhofer F *et al* (2004). mTOR is essential for growth and proliferation in early mouse embryos and embryonic stem cells. *Mol Cell Biol* **24:** 6710-6718.

Nakashima A, Yoshino K, Miyamoto T, Eguchi S, Oshiro N, Kikkawa U *et al* (2007). Identification of TBC7 having TBC domain as a novel binding protein to TSC1-TSC2 complex. *Biochem Biophys Res Commun* **361:** 218-223.

Neely MD, Litt MJ, Tidball AM, Li GG, Aboud AA, Hopkins CR *et al* (2012). DMH1, a highly selective small molecule BMP inhibitor promotes neurogenesis of hiPSCs: comparison of PAX6 and SOX1 expression during neural induction. *ACS Chem Neurosci* **3:** 482-491.

Nie D, Di Nardo A, Han JM, Baharanyi H, Kramvis I, Huynh T *et al* (2010). Tsc2-Rheb signaling regulates EphA-mediated axon guidance. *Nat Neurosci* **13:** 163-172.

Niida Y, Stemmer-Rachamimov AO, Logrip M, Tapon D, Perez R, Kwiatkowski DJ *et al* (2001). Survey of somatic mutations in tuberous sclerosis complex (TSC) hamartomas suggests different genetic mechanisms for pathogenesis of TSC lesions. *Am J Hum Genet* **69:** 493-503.

Northrup H, Krueger DA (2013). Tuberous sclerosis complex diagnostic criteria update: recommendations of the 2012 Iinternational Tuberous Sclerosis Complex Consensus Conference. *Pediatr Neurol* **49:** 243-254.

O'Callaghan FJ, Shiell AW, Osborne JP, Martyn CN (1998). Prevalence of tuberous sclerosis estimated by capture-recapture analysis. *Lancet* **351:** 1490.

Ogawara Y, Kishishita S, Obata T, Isazawa Y, Suzuki T, Tanaka K *et al* (2002). Akt enhances Mdm2-mediated ubiquitination and degradation of p53. *J Biol Chem* **277:** 21843-21850.

Okita K, Matsumura Y, Sato Y, Okada A, Morizane A, Okamoto S *et al* (2011). A more efficient method to generate integration-free human iPS cells. *Nat Methods* **8:** 409-412.

Onda H, Lueck A, Marks PW, Warren HB, Kwiatkowski DJ (1999). Tsc2(+/-) mice develop tumors in multiple sites that express gelsolin and are influenced by genetic background. *J Clin Invest* **104:** 687-695.

Pai GM, Zielinski A, Koalick D, Ludwig K, Wang ZQ, Borgmann K *et al* (2016). TSC loss distorts DNA replication programme and sensitises cells to genotoxic stress. *Oncotarget* **7:** 85365-85380.

Park SH, Pepkowitz SH, Kerfoot C, De Rosa MJ, Poukens V, Wienecke R *et al* (1997). Tuberous sclerosis in a 20-week gestation fetus: immunohistochemical study. *Acta neuropathologica* **94:** 180-186.

Pende M, Um SH, Mieulet V, Sticker M, Goss VL, Mestan J *et al* (2004). S6K1(-/-)/S6K2(-/-) mice exhibit perinatal lethality and rapamycin-sensitive 5'-terminal oligopyrimidine mRNA translation and reveal a mitogen-activated protein kinase-dependent S6 kinase pathway. *Mol Cell Biol* **24:** 3112-3124.

Peters JM, Sahin M, Vogel-Farley VK, Jeste SS, Nelson CA, 3rd, Gregas MC *et al* (2012). Loss of white matter microstructural integrity is associated with adverse neurological outcome in tuberous sclerosis complex. *Acad Radiol* **19:** 17-25.

Potter CJ, Pedraza LG, Xu T (2002). Akt regulates growth by directly phosphorylating Tsc2. *Nat Cell Biol* **4:** 658-665.

Povey S, Burley MW, Attwood J, Benham F, Hunt D, Jeremiah SJ *et al* (1994). Two loci for tuberous sclerosis: one on 9q34 and one on 16p13. *Ann Hum Genet* **58:** 107-127.

Prabowo AS, Anink JJ, Lammens M, Nellist M, van den Ouweland AM, Adle-Biassette H *et al* (2013). Fetal brain lesions in tuberous sclerosis complex: TORC1 activation and inflammation. *Brain Pathol* **23:** 45-59.

Qin W, Chan JA, Vinters HV, Mathern GW, Franz DN, Taillon BE *et al* (2010). Analysis of TSC cortical tubers by deep sequencing of TSC1, TSC2 and KRAS demonstrates that small second-hit mutations in these genes are rare events. *Brain Pathol* **20:** 1096-1105.

Rayer PFO (1835). *Traité théorique et pratique des maladies de la peau, avec un atlas ... Seconde édition ... refondue*. Baillière.

Rennebeck G, Kleymenova EV, Anderson R, Yeung RS, Artzt K, Walker CL (1998). Loss of function of the tuberous sclerosis 2 tumor suppressor gene results in embryonic lethality characterized by disrupted neuroepithelial growth and development. *Proc Natl Acad Sci U S A* **95:** 15629-15634.

Ridler K, Bullmore ET, De Vries PJ, Suckling J, Barker GJ, Meara SJ *et al* (2001). Widespread anatomical abnormalities of grey and white matter structure in tuberous sclerosis. *Psychol Med* **31:** 1437-1446.

Rosset C, Netto CBO, Ashton-Prolla P (2017). TSC1 and TSC2 gene mutations and their implications for treatment in Tuberous Sclerosis Complex: a review. *Genet Mol Biol* **40:** 69-79.

Roux PP, Ballif BA, Anjum R, Gygi SP, Blenis J (2004). Tumor-promoting phorbol esters and activated Ras inactivate the tuberous sclerosis tumor suppressor complex via p90 ribosomal S6 kinase. *Proc Natl Acad Sci U S A* **101:** 13489-13494.

Ruiz S, Lopez-Contreras AJ, Gabut M, Marion RM, Gutierrez-Martinez P, Bua S *et al* (2015). Limiting replication stress during somatic cell reprogramming reduces genomic instability in induced pluripotent stem cells. *Nat Commun* **6:** 8036.

Ruvinsky I, Sharon N, Lerer T, Cohen H, Stolovich-Rain M, Nir T *et al* (2005). Ribosomal protein S6 phosphorylation is a determinant of cell size and glucose homeostasis. *Genes Dev* **19:** 2199-2211.

Sabatini DM, Erdjument-Bromage H, Lui M, Tempst P, Snyder SH (1994). RAFT1: a mammalian protein that binds to FKBP12 in a rapamycin-dependent fashion and is homologous to yeast TORs. *Cell* **78:** 35-43.

Sahin M, Henske EP, Manning BD, Ess KC, Bissler JJ, Klann E *et al* (2016). Advances and Future Directions for Tuberous Sclerosis Complex Research: Recommendations From the 2015 Strategic Planning Conference. *Pediatr Neurol* **60:** 1-12.

Sahlgren CM, Mikhailov A, Hellman J, Chou YH, Lendahl U, Goldman RD *et al* (2001). Mitotic reorganization of the intermediate filament protein nestin involves phosphorylation by cdc2 kinase. *J Biol Chem* **276:** 16456-16463.

Sahlgren CM, Mikhailov A, Vaittinen S, Pallari HM, Kalimo H, Pant HC *et al* (2003). Cdk5 regulates the organization of Nestin and its association with p35. *Mol Cell Biol* **23:** 5090-5106.

Sampson JR, Scahill SJ, Stephenson JB, Mann L, Connor JM (1989). Genetic aspects of tuberous sclerosis in the west of Scotland. *J Med Genet* **26:** 28-31.

Sancak O, Nellist M, Goedbloed M, Elfferich P, Wouters C, Maat-Kievit A *et al* (2005). Mutational analysis of the TSC1 and TSC2 genes in a diagnostic setting: genotype--phenotype correlations and comparison of diagnostic DNA techniques in Tuberous Sclerosis Complex. *Eur J Hum Genet* **13:** 731-741.

Sancak Y, Thoreen CC, Peterson TR, Lindquist RA, Kang SA, Spooner E *et al* (2007). PRAS40 is an insulin-regulated inhibitor of the mTORC1 protein kinase. *Mol Cell* **25:** 903-915.

Sancak Y, Peterson TR, Shaul YD, Lindquist RA, Thoreen CC, Bar-Peled L *et al* (2008). The Rag GTPases bind raptor and mediate amino acid signaling to mTORC1. *Science* **320:** 1496-1501.

Sarbassov DD, Guertin DA, Ali SM, Sabatini DM (2005). Phosphorylation and regulation of Akt/PKB by the rictor-mTOR complex. *Science* **307:** 1098-1101.

Sardiello M, Palmieri M, di Ronza A, Medina DL, Valenza M, Gennarino VA *et al* (2009). A gene network regulating lysosomal biogenesis and function. *Science* **325:** 473-477.

Sasongko TH, Ismail NF, Zabidi-Hussin Z (2016). Rapamycin and rapalogs for tuberous sclerosis complex. *Cochrane Database Syst Rev* **7:** CD011272.

Schindelin J, Arganda-Carreras I, Frise E, Kaynig V, Longair M, Pietzsch T *et al* (2012). Fiji: an open-source platform for biological-image analysis. *Nat Methods* **9:** 676-682.

Schlaeger TM, Daheron L, Brickler TR, Entwisle S, Chan K, Cianci A *et al* (2015). A comparison of non-integrating reprogramming methods. *Nat Biotechnol* **33:** 58-63.

Scholl T, Muhlebner A, Ricken G, Gruber V, Fabing A, Samueli S *et al* (2016). Impaired oligodendroglial turnover is associated with myelin pathology in focal cortical dysplasia and tuberous sclerosis complex. *Brain Pathol*.

Settembre C, Zoncu R, Medina DL, Vetrini F, Erdin S, Huynh T *et al* (2012). A lysosome-to-nucleus signalling mechanism senses and regulates the lysosome via mTOR and TFEB. *EMBO J* **31:** 1095-1108.

Shi Y, Kirwan P, Livesey FJ (2012a). Directed differentiation of human pluripotent stem cells to cerebral cortex neurons and neural networks. *Nat Protoc* **7:** 1836-1846.

Shi Y, Kirwan P, Smith J, Robinson HP, Livesey FJ (2012b). Human cerebral cortex development from pluripotent stem cells to functional excitatory synapses. *Nat Neurosci* **15:** 477-486, S471.

Shima H, Pende M, Chen Y, Fumagalli S, Thomas G, Kozma SC (1998). Disruption of the p70(s6k)/p85(s6k) gene reveals a small mouse phenotype and a new functional S6 kinase. *EMBO J* **17:** 6649-6659.

Simao G, Raybaud C, Chuang S, Go C, Snead OC, Widjaja E (2010). Diffusion tensor imaging of commissural and projection white matter in tuberous sclerosis complex and correlation with tuber load. *AJNR Am J Neuroradiol* **31:** 1273-1277.

Stambolic V, MacPherson D, Sas D, Lin Y, Snow B, Jang Y *et al* (2001). Regulation of PTEN transcription by p53. *Mol Cell* **8:** 317-325.

Sun P, Quan Z, Zhang B, Wu T, Xi R (2010). TSC1/2 tumour suppressor complex maintains Drosophila germline stem cells by preventing differentiation. *Development* **137:** 2461-2469.

Takahashi K, Yamanaka S (2006). Induction of pluripotent stem cells from mouse embryonic and adult fibroblast cultures by defined factors. *Cell* **126:** 663-676.

Tapon N, Ito N, Dickson BJ, Treisman JE, Hariharan IK (2001). The Drosophila tuberous sclerosis complex gene homologs restrict cell growth and cell proliferation. *Cell* **105:** 345-355.

Tavazoie SF, Alvarez VA, Ridenour DA, Kwiatkowski DJ, Sabatini BL (2005). Regulation of neuronal morphology and function by the tumor suppressors Tsc1 and Tsc2. *Nat Neurosci* **8:** 1727-1734.

Tedeschi A, Di Giovanni S (2009). The non-apoptotic role of p53 in neuronal biology: enlightening the dark side of the moon. *EMBO Rep* **10:** 576-583.

Tee AR, Manning BD, Roux PP, Cantley LC, Blenis J (2003). Tuberous sclerosis complex gene products, Tuberin and Hamartin, control mTOR signaling by acting as a GTPase-activating protein complex toward Rheb. *Curr Biol* **13:** 1259-1268.

Thoreen CC, Kang SA, Chang JW, Liu Q, Zhang J, Gao Y *et al* (2009). An ATP-competitive mammalian target of rapamycin inhibitor reveals rapamycin-resistant functions of mTORC1. *J Biol Chem* **284:** 8023-8032.

Tsai V, Parker WE, Orlova KA, Baybis M, Chi AW, Berg BD *et al* (2014). Fetal brain mTOR signaling activation in tuberous sclerosis complex. *Cereb Cortex* **24:** 315-327.

Tyburczy ME, Wang JA, Li S, Thangapazham R, Chekaluk Y, Moss J *et al* (2014). Sun exposure causes somatic second-hit mutations and angiofibroma development in tuberous sclerosis complex. *Hum Mol Genet* **23:** 2023-2029.

Tyburczy ME, Dies KA, Glass J, Camposano S, Chekaluk Y, Thorner AR *et al* (2015). Mosaic and Intronic Mutations in TSC1/TSC2 Explain the Majority of TSC Patients with No Mutation Identified by Conventional Testing. *PLoS Genet* **11:** e1005637.

Utikal J, Polo JM, Stadtfeld M, Maherali N, Kulalert W, Walsh RM *et al* (2009). Immortalization eliminates a roadblock during cellular reprogramming into iPS cells. *Nature* **460:** 1145-1148.

van den Ameele J, Tiberi L, Vanderhaeghen P, Espuny-Camacho I (2014). Thinking out of the dish: what to learn about cortical development using pluripotent stem cells. *Trends Neurosci* **37:** 334-342.

van Slegtenhorst M, de Hoogt R, Hermans C, Nellist M, Janssen B, Verhoef S *et al* (1997). Identification of the tuberous sclerosis gene TSC1 on chromosome 9q34. *Science* **277:** 805-808.

van Slegtenhorst M, Nellist M, Nagelkerken B, Cheadle J, Snell R, van den Ouweland A *et al* (1998). Interaction Between Hamartin and Tuberin, the TSC1 and TSC2 Gene Products. *Hum Mol Genet* **7:** 1053-1057.

Vander Haar E, Lee SI, Bandhakavi S, Griffin TJ, Kim DH (2007). Insulin signalling to mTOR mediated by the Akt/PKB substrate PRAS40. *Nat Cell Biol* **9:** 316-323.

Vogt P (1908). Zur Pathologie und pathologischen Anatomie der verschiedenen Idiotieformen. pp. 106–117. *Eur Neurol* **24:** 106-117.

Von Recklinghausen F (1862). Ein Herz von einem Neugeborenen welches mehrere Theils nach aussen, Theils nach den Hohlen prominirende Tumoren (Myomen) trug. *Monatschr Geburtsheilkd* **20:** 1-2.

Waltereit R, Welzl H, Dichgans J, Lipp HP, Schmidt WJ, Weller M (2006). Enhanced episodic-like memory and kindling epilepsy in a rat model of tuberous sclerosis. *J Neurochem* **96:** 407-413.

Waltereit R, Japs B, Schneider M, de Vries PJ, Bartsch D (2011). Epilepsy and Tsc2 haploinsufficiency lead to autistic-like social deficit behaviors in rats. *Behav Genet* **41:** 364-372.

Wang S, Xia P, Ye B, Huang G, Liu J, Fan Z (2013). Transient activation of autophagy via Sox2-mediated suppression of mTOR is an important early step in reprogramming to pluripotency. *Cell Stem Cell* **13:** 617-625.

Wataya-Kaneda M, Kaneda Y, Hino O, Adachi H, Hirayama Y, Seyama K *et al* (2001). Cells derived from tuberous sclerosis show a prolonged S phase of the cell cycle and increased apoptosis. *Arch Dermatol Res* **293:** 460-469.

Way SW, McKenna J, 3rd, Mietzsch U, Reith RM, Wu HC, Gambello MJ (2009). Loss of Tsc2 in radial glia models the brain pathology of tuberous sclerosis complex in the mouse. *Hum Mol Genet* **18:** 1252-1265.

Widjaja E, Simao G, Mahmoodabadi SZ, Ochi A, Snead OC, Rutka J *et al* (2010). Diffusion tensor imaging identifies changes in normal-appearing white matter within the epileptogenic zone in tuberous sclerosis complex. *Epilepsy Res* **89:** 246-253.

Wu Y, Li Y, Zhang H, Huang Y, Zhao P, Tang Y *et al* (2015). Autophagy and mTORC1 regulate the stochastic phase of somatic cell reprogramming. *Nat Cell Biol* **17:** 715-725.

Xu L, Sterner C, Maheshwar MM, Wilson PJ, Nellist M, Short PM *et al* (1995). Alternative splicing of the tuberous sclerosis 2 (TSC2) gene in human and mouse tissues. *Genomics* **27:** 475-480.

Yeung RS, Xiao GH, Jin F, Lee WC, Testa JR, Knudson AG (1994). Predisposition to renal carcinoma in the Eker rat is determined by germ-line mutation of the tuberous sclerosis 2 (TSC2) gene. *Proc Natl Acad Sci U S A* **91:** 11413-11416.

Yu K, Toral-Barza L, Shi C, Zhang WG, Lucas J, Shor B *et al* (2009). Biochemical, cellular, and in vivo activity of novel ATP-competitive and selective inhibitors of the mammalian target of rapamycin. *Cancer Res* **69:** 6232-6240.

Zhang D, Chen HP, Duan HF, Gao LH, Shao Y, Chen KY *et al* (2016). Aggregation of Ribosomal Protein S6 at Nucleolus Is Cell Cycle-Controlled and Its Function in Pre-rRNA Processing Is Phosphorylation Dependent. *J Cell Biochem* **117:** 1649-1657.

Zhang H, Cicchetti G, Onda H, Koon HB, Asrican K, Bajraszewski N *et al* (2003). Loss of Tsc1/Tsc2 activates mTOR and disrupts PI3K-Akt signaling through downregulation of PDGFR. *J Clin Invest* **112:** 1223-1233.

Zhou J, Su P, Wang L, Chen J, Zimmermann M, Genbacev O *et al* (2009). mTOR supports long-term self-renewal and suppresses mesoderm and endoderm activities of human embryonic stem cells. *Proc Natl Acad Sci U S A* **106:** 7840-7845.